1-1-2017

Neuropharmacological Investigation Of Stress And Nicotine Self-Administration Among Current Cigarette Smokers

Eric Woodcock
Wayne State University,

NEUROPHARMACOLOGICAL INVESTIGATION OF STRESS AND NICOTINE SELF-ADMINISTRATION AMONG CURRENT CIGARETTE SMOKERS

by

ERIC ANDREW WOODCOCK

DISSERTATION

Submitted to the Graduate School

of Wayne State University,

Detroit, Michigan

in partial fulfillment of the requirements

for the degree of

DOCTOR OF PHILOSOPHY

2017

MAJOR: NEUROSCIENCE (Translational)

Approved By:

_____

Adviser Date

_____

_____

_____

_____

DEDICATION

This work is dedicated to my parents. My parents cultivated my scientific curiosity and encouraged my intellectual pursuits. My upbringing was rich with creative, athletic, and scholarly activities. Without these experiences and their unwavering love and support, it is unlikely I would have pursued graduate training.

This is for you, mom and dad.

ACKNOWLEDGMENTS

Throughout my life, many academic and research mentors have influenced my scientific trajectory: Jeremy Argo, Lafe Purvis, Nicholas Salsman, PhD, Blair Beadnell, PhD, and Linda Dimeff, PhD. However, no single person influenced my thesis project or approach to biomedical research more than my primary research mentor, Dr. Mark Greenwald. Without Dr. Greenwald, this project literally would not be possible. In addition, Drs. Jeffrey Stanley and Vaibhav Diwadkar provided a rigorous and robust neuroimaging training experience. Collectively, my graduate mentor triad cultivated my scientific growth, fostered my productivity, and improved this project. Finally – my beautiful, supportive, and patient wife. To merely 'acknowledge' Lauren would be an egregious injustice. Without her, I would be a shell of myself – outwardly whole, but unquestionably incomplete. Lauren has supported my career goals from the beginning: despite years of long hours, small paychecks, and a seemingly omnipresent laptop. Any career successes are as much mine, as they are hers.

TABLE OF CONTENTS

LIST OF TABLES

LIST OF FIGURES

CHAPTER 1 NICOTINE USE DISORDER

1.1 Public Health Significance

Tobacco use, especially cigarette smoking, is a significant public health problem. Tobacco use is the leading cause of preventable death in the United States (US; 480,000+ deaths per year) (U.S. Department of Health and Human Services, 2014). Approximately one of every five deaths in the US each year are associated with tobacco use (U.S. Department of Health and Human Services, 2014). In addition to severe health consequences, cigarette smoking costs the US economy $300+ billion per year in lost productivity and medical expenses (U.S. Department of Health and Human Services, 2014). Approximately 57 million people (aged 12+ yrs) in the US currently smoke cigarettes (SAMHSA, 2011). However, encouragingly, ~70% of current smokers report a desire to quit (SAMHSA, 2011).

1.2 Pharmacotherapy

The most efficacious Food and Drug Administration (FDA)-indicated pharmacotherapies for smoking cessation are: nicotine replacement products (e.g. nicotine gum, lozenges, and transdermal patches), varenicline ($\alpha_4\beta_2$ nicotinic acetylcholine receptor partial agonist), and bupropion (aminoketone antidepressant) (Eisenberg et al., 2008; Etter & Stapleton, 2006; Gonzales et al., 2006; Jorenby et al., 1999; Lancaster, Stead, Silagy, & Sowden, 2000; Mills et al., 2012; Silagy, Lancaster, Stead, Mant, & Fowler, 2005; Ucar et al., 2014). These medications attenuated cigarette craving and nicotine withdrawal symptoms, and improved short-term abstinence rates, relative to placebo (Eisenberg et al., 2008; Etter & Stapleton, 2006; Gonzales et al., 2006; Jorenby et al., 1999; Lancaster et al., 2000; Mills et al., 2012;

Silagy et al., 2005; Ucar et al., 2014). However, meta-analyses of treatment studies indicated smoking abstinence rates at 6- and 12-month follow-ups were unacceptably low (14-36% and 13-28%, respectively) (Eisenberg et al., 2008; Etter & Stapleton, 2006; Gonzales et al., 2006; Jorenby et al., 1999; Nides et al., 2008; Silagy et al., 2005; Ucar et al., 2014). Despite effective attenuation of nicotine craving and withdrawal symptoms, the majority of smokers relapsed within the first year of treatment on these medications. This begs the question: what other factors precipitate smoking relapse, and are not attenuated by these medications? One such factor is stress. Historically, stress has been defined as physiological responses to demands placed upon the body (Selye, 1936, 1973). In this study, stress is defined by the acute physiological responses (e.g. elevated heart rate, blood pressure, breathing rate etc.) that are typically associated with stressful events (for a more complete description see below).

1.3 Stress and Smoking Relapse

Treatment research studies indicated stress was among the most commonly cited precipitants to smoking relapse (M. al'Absi, 2006; Heishman, 1999; Hymowitz, Sexton, Ockene, & Grandits, 1991; Matheny & Weatherman, 1998). One study found that more than 60% of cigarette smokers attributed their relapse to stress (Hughes, 2009). Moreover, individuals who reported high stress levels during abstinence were more likely to relapse (Brewer, Catalano, Haggerty, Gainey, & Fleming, 1998; S. Cohen & Lichtenstein, 1990).

Stressful events activate the Autonomic Nervous System (ANS) and Hypothalamus-Pituitary-Adrenal (HPA) axis which can increase heart rate, blood pressure, breathing rate, and levels of circulating noradrenaline and cortisol (among

other physiological effects) (Mustafa al'Absi, 2006; G. F. Koob, 2008; Pocock, Richards, & Richards, 2013; Sinha, Garcia, Paliwal, Kreek, & Rounsaville, 2006). Activation of the sympathetic branch of the ANS (associated with noradrenaline release) prepares an individual for immediate action (so-called 'fight or flight' response) (Pocock et al., 2013). The HPA axis response (associated with cortisol release) is slower and less predictable, but has important biological effects (Dickerson & Kemeny, 2004). Acute nicotine administration can activate, and chronic nicotine administration can dysregulate, ANS and HPA axis responses (Picciotto, Brunzell, & Caldarone, 2002). Nicotine is a central nervous system stimulant; acute administration is associated with increased blood pressure, heart rate, and plasma noradrenaline and corticosteroid levels (Brazell, Mitchell, & Gray, 1991; Cryer, Haymond, Santiago, & Shah, 1976; Picciotto et al., 2002). Chronic nicotine exposure was associated with elevated levels of noradrenaline and cortisol during active use and acute abstinence, and dysregulated physiological reactivity to experimental stress-induction (Andersson, Eneroth, Fuxe, Mascagni, & Agnati, 1985; Childs & De Wit, 2009; C Kirschbaum, Wüst, & Strasburger, 1992; G. F. Koob, 2008; George F. Koob & Moal, 1997; Kreek & Koob, 1998; Picciotto et al., 2002; Tsuda, Steptoe, West, Fieldman, & Kirschbaum, 1996; Wilkins et al., 1982). Thus, long-term cigarette smoking may dysregulate the stress system, which in turn, may increase the likelihood of relapse.

FDA-indicated pharmacotherapies were not designed to, and do not, attenuate stress-induced biobehavioral reactions. Ray et al. (2013) demonstrated that varenicline decreased basal cigarette craving and blocked cigarette cue-induced craving, but not cue- *plus* stress-induced cigarette craving (Ray et al., 2013). During acute smoking

abstinence, bupropion was associated with increased physiological indices of stress reactivity at rest and following an experimental stress-induction task (Kotlyar et al., 2006). Acute nicotine administration (e.g. nicotine replacement products) among chronic smokers can attenuate HPA axis response to experimental stress-induction (Childs & De Wit, 2009; Rohleder & Kirschbaum, 2006), but may increase cardiovascular output (heart rate and blood pressure) (Perkins, Epstein, Jennings, & Stiller, 1986). Moreover, chronic nicotine use is associated with overactive HPA axis and ANS systems (Andersson et al., 1985; G. F. Koob, 2008; George F Koob & Le Moal, 1997).

1.4 Adjunctive Medications

The effectiveness of existing pharmacotherapies may be enhanced by adjunctive medications that attenuate an individual's physiological response to stress. In a preclinical study, prazosin (α_1-adrenoreceptor antagonist) attenuated the effects of pharmacological stress-induction on alcohol seeking behavior (A. Le et al., 2011). In humans, prazosin blunted the effects of psychosocial stress-induction on blood pressure, alcohol craving, anxiety, and negative emotion among alcohol dependent individuals during outpatient treatment (Helen C Fox et al., 2012). Similarly, guanfacine (α_2-adrenoreceptor agonist) attenuated stress- and drug cue-induced craving and anxiety among cocaine-dependent individuals (H. C. Fox et al., 2012). These preliminary studies suggest that supplementing existing FDA-indicating pharmacotherapies with stress-blunting medications may improve smoking cessation rates. Indeed, an ongoing clinical trial is investigating the efficacy of combined varenicline + prazosin on smoking cessation (results not yet available).

1.5 Summary

The goal of this section was to briefly introduce the public health problem and research focus of this study. A review of all smoking cessation treatments (e.g. cognitive and behavioral interventions) was beyond the scope of this section and would not further clarify the concepts presented herein.

In summary, nicotine use, especially chronic cigarette smoking, is a significant public health problem. FDA-indicated pharmacotherapies for smoking cessation are associated with dismal long-term abstinence rates. One plausible explanation is that existing pharmacotherapies do not attenuate the deleterious effects of acute stress. There is ample non-experimental evidence linking stress to smoking relapse. In the next chapter, I will review the evidence that acute experimental stress potentiated substance use and reinstatement (model of relapse). In addition, I will review the literature on brain regions associated with substance use disorders and the impact of acute experimental stress on brain function. Finally, I will describe the dissertation study design, aims, and hypotheses.

CHAPTER 2 EXPERIMENTAL STRESS EFFECTS

2.1 Preclinical Models of Substance Use Relapse

The reinstatement model of preclinical substance use relapse is widely used and has good criterion and construct validity (Epstein, Preston, Stewart, & Shaham, 2006). The specific parameters of the reinstatement model vary across studies, but generally include the following: acquisition (initial drug self-administration), maintenance (regular drug self-administration), extinction (protracted abstinence), experimental challenge, and reinstatement (relapse) (Shaham, Shalev, Lu, de Wit, & Stewart, 2003). During the acquisition phase, the animal is able to earn units of drug via behavioral responding. Drug-seeking behavior is operationalized as behavioral responding (e.g. nose poke, pressing a lever) that resulted in drug administration. Drug-seeking behavior is a direct behavioral measure of appetitive drug motivation with translational validity in human experimental research. During the maintenance phase, the animal is able to earn units of drug via behavioral responding during predefined time periods until drug taking reaches a plateau and has stabilized. This phase is a proxy of chronic substance use. During the extinction phase, behavioral responding no longer results in receipt of drug (e.g. saline is substituted). Behavioral responding will gradually decrease until cessation (i.e. drug-seeking behavior was extinguished). Finally, the animal is challenged with an experimental manipulation (e.g. stress, drug-paired cue, or drug priming dose). If the animal exhibits behavioral responding on the drug-associated option, drug-seeking behavior has been reinstated (i.e. the animal is said to have relapsed).

2.2 Preclinical Experimental Stress Manipulation

A variety of preclinical experimental stress manipulations exist, including: predator scent, foot shock, restraint, and pharmacological agents. Pharmacological agents have methodological advantages over other approaches: neurochemical specificity, methodological control, and translational potential. Preclinical models of relapse demonstrated that pharmacological stress agents (that mimic ANS and HPA axis responses) reinstated drug-seeking and self-administration across drugs of abuse (Epstein et al., 2006; Feltenstein, Ghee, & See, 2012; Le, Harding, Juzytsch, Funk, & Shaham, 2005; Mantsch & Katz, 2007; Mantsch et al., 2014; Mantsch et al., 2010; Shaham, Erb, & Stewart, 2000; Shaham et al., 2003; Shaham & Stewart, 1995). Yohimbine (YOH) is an α_2-adrenoreceptor antagonist that increases noradrenergic levels (i.e. sympathetic ANS response to stressful events) by blocking the presynaptic autoreceptor (Doxey, Lane, Roach, & Virdce, 1984; Goldberg & Robertson, 1983). Acute YOH administration reinstated behavioral responding (i.e. YOH precipitated relapse) for cocaine, methamphetamine, alcohol, and nicotine in rodents (Ahmed & Koob, 1997; Buczek, Le, Wang, Stewart, & Shaham, 1999; Erb et al., 2000; Erb, Shaham, & Stewart, 1996; Gass & Olive, 2007; Le et al., 2005; Mantsch & Katz, 2007; Mantsch et al., 2014; Mantsch et al., 2010; Shepard, Bossert, Liu, & Shaham, 2004). YOH reliably produced anxiogenic effects in rodents and humans (Charney, Heninger, & Redmond Jr, 1983; A. D. Le et al., 2011; Pellow, Johnston, & File, 1987; Stine et al., 2002). YOH increased biomarkers of a physiological stress response: systolic and diastolic blood pressure and saliva α-amylase (Ehlert, Erni, Hebisch, & Nater, 2006; Greenwald, Lundahl, & Steinmiller, 2013; Murburg, Villacres, Ko, & Veith, 1991; Stine et

al., 2002). Glucocorticoid and mineralocorticoid receptor agonists (corticosterone [rodents] and cortisol [humans]) modulated the effect of YOH on drug-seeking behavior (de Jong, Steenbergen, & de Kloet, 2009; Deroche, Marinelli, Le Moal, & Piazza, 1997; Graf et al., 2013; Mantsch & Katz, 2007; Mantsch et al., 2014). In combination, they simulate a robust physiological stress response (both ANS and HPA axis) and reliably reinstate drug-seeking behavior in preclinical models of substance use relapse.

2.3 Human Experimental Stress Manipulation

Human experimental studies often use psychosocial stress-induction techniques, including: guided imagery, mental arithmetic, or public speaking (Dedovic, D'Aguiar, & Pruessner, 2009; Dickerson & Kemeny, 2004). Psychosocial stress-induction manipulations have non-trivial limitations, including: lack of placebo-control (possible expectancy effects); no dose manipulation (inability to control stressor intensity); and unreliable and brief physiological stress response (<30min) (Dickerson & Kemeny, 2004; Greenwald et al., 2013).

Pharmacological stress-induction has methodological advantages over psychosocial approaches and reverse-translational validity with preclinical studies. Pharmacological agents that mimic the endogenous HPA axis and ANS stress response (e.g. YOH in combination with a glucocorticoid and mineralocorticoid receptor agonist) provide a powerful model of acute experimental stress-induction. Hydrocortisone (HYD) is a glucocorticoid and mineralocorticoid receptor agonist with good bioavailability that reliably increases plasma and saliva cortisol levels in humans (Meikle & Tyler, 1977). Together, YOH+HYD: a) mimic ANS- and HPA axis-mediated stress responses (increase the primary stress hormones: noradrenaline and cortisol);

b) produce reliable, sustained, and dose-dependent physiological stress responses; and c) enable double-blind, placebo-controlled administration (de Jong et al., 2009; Deroche et al., 1997; Graf et al., 2013; Mantsch & Katz, 2007; Mantsch et al., 2014).

Our laboratory recently investigated the effects of oral pretreatment of YOH alone and YOH+HYD in non-treatment-seeking, opioid-dependent volunteers. The primary outcome variable was opioid-seeking behavior. Human experimental stress studies often measure proxies of substance use (e.g. craving) or infer statistical relationships to future substance use. In contrast to those approaches, drug-seeking behavior is a direct measure of appetitive drug motivation that results in drug administration. Participants in our recent lab study were able to earn (via computer 'mouse' clicking) units of hydromorphone (μ opioid receptor agonist) or money on a choice progressive ratio task. Response requirements (number of mouse clicks) increased with each successive unit earned (independently for both drug and money). Immediately after the task, earned units of hydromorphone were administered (intramuscular injection). Thus, appetitive opioid motivation (number of opioid units earned) was measured in the absence of acute drug effects (e.g. disinhibition or satiation). Findings indicated YOH alone (Greenwald et al., 2013) and YOH+HYD (Greenwald et al., in preparation) increased opioid (hydromorphone) seeking behavior in sublingual buprenorphine-maintained (8mg/day) heroin-dependent individuals. In addition, oral pretreatment with YOH 54mg + HYD 20mg (similar to doses proposed in this study) produced statistically-significant, but clinically-safe, increases in blood pressure (both systolic and diastolic) and saliva cortisol that lasted for approximately three hours. These findings demonstrated that oral pretreatment with YOH+HYD is a

robust pharmacological stress-induction technique that potentiated drug-seeking behavior among opioid-dependent individuals. Together with the preclinical literature, there is substantial evidence that experimental stress-induction reliably increases drug-seeking behavior. However, the neurobiological pathways through which stress potentiates drug-seeking behavior remain unclear.

2.4 Substance Use and Brain Function

2.4.1 Top-down vs. Bottom-up

Neuroimaging studies provide insight into brain regions and networks associated with substance use. Broadly speaking, brain regions associated with drug cue appraisal, appetitive motivation, and decision making can be divided into two networks: top-down and bottom-up (Bechara, 2005; Nestor, McCabe, Jones, Clancy, & Garavan, 2011). The top-down network is often conceptualized as the 'brake pedal' to the bottom-up 'gas pedal'. Bottom-up signals are associated with appetitive drug motivation, craving, and withdrawal/negative affect. Top-down network structures modulate bottom-up signals, and are associated with executive function, planning, and goal-directed behaviors. Substance use-related decision making (e.g. whether or not to use a drug at a particular moment) is thought to arise from these competing signals (Rangel, Camerer, & Montague, 2008).

2.4.2 Bottom-up Network

Dopaminergic signaling in the ventral striatum (including the nucleus accumbens [NAcc]) mediates acute drug reinforcement (Di Chiara & Imperato, 1988). Following repeated substance use, drug-paired visual cues become conditioned stimuli and elicit dopamine release in the NAcc (in the absence of substance administration), consistent

with appetitive craving (N. Volkow, Fowler, Wang, Baler, & Telang, 2009; N. D. Volkow et al., 2006, 2008). Substance use disorders are associated with enhanced salience attribution to drug-related visual cues (Rita Z Goldstein & Volkow, 2002; R. Z. Goldstein & Volkow, 2011). Visual drug cue evoked blood oxygen level-dependent (BOLD) activation measured via functional magnetic resonance imaging (fMRI) is often robust, but patterns vary across studies and are influenced by several methodological factors (Jasinska, Stein, Kaiser, Naumer, & Yalachkov, 2014), such as *treatment status* (out-of-treatment individuals show more robust activation), *time since last cigarette* (acute abstinence enhanced cue reactivity), and *temporal delay until next smoking opportunity* (immediate smoking opportunities are associated with more robust activation) (Jasinska et al., 2014; Wilson, Sayette, Delgado, & Fiez, 2005). Meta-analyses of fMRI studies indicated that consistently activated regions included: the medial orbitofrontal cortex (mOFC), medial prefrontal cortex (mPFC), ventral striatum (including NAcc), and dorsal striatum (Chase, Eickhoff, Laird, & Hogarth, 2011; Engelmann et al., 2012; Kühn & Gallinat, 2011; Wilson, Sayette, & Fiez, 2004)). BOLD activation in the mPFC and mOFC is thought to reflect drug cue appraisal and/or salience (Chase et al., 2011; Hayashi, Ko, Strafella, & Dagher, 2013; Wilson et al., 2004). The two most consistently activated regions are the amygdala and the ventral striatum (e.g. NAcc) (Chase et al., 2011; Engelmann et al., 2012; Kühn & Gallinat, 2011; Wilson et al., 2004). Activation in the amygdala may reflect the emotional salience of the visual drug cue presented (Chase et al., 2011; Engelmann et al., 2012; Kühn & Gallinat, 2011; Wilson et al., 2004). The ventral striatum is associated with craving and appetitive motivation, and is part of the 'final common pathway' of addiction (Rita Z Goldstein & Volkow, 2002; P. W.

Kalivas, Volkow, & Seamans, 2005; G. F. Koob & Volkow, 2010; N. Volkow et al., 2009). Collectively, activation in bottom-up 'reward' network structures is associated with drug cue salience, craving, and appetitive motivation.

2.4.3 Top-down Network

Top-down (frontal-to-striatal) network function is important for many cognitive processes, including: attention, decision making, and goal-directed behavior (Rita Z Goldstein & Volkow, 2002; R. Z. Goldstein & Volkow, 2011; Rangel et al., 2008). Top-down network function emanates from the dorsolateral prefrontal cortex (dlPFC) (Rita Z Goldstein & Volkow, 2002; R. Z. Goldstein & Volkow, 2011). Substance abuse is associated with structural and functional changes. Relative to matched controls, cigarette smokers exhibited reduced gray matter volume in dlPFC and ventrolateral PFC (vlPFC) (Brody et al., 2004). Chronic substance use is associated with impaired dlPFC-dependent non-drug-specific cognitive processes (attentional control, decision making, and impulse inhibition) (Banich, 2009; R. Z. Goldstein & Volkow, 2011). In addition, the dlPFC is involved in drug use-related cognitive processes: self-control, delayed gratification, drug cue reactivity, and response inhibition (Hare, Camerer, & Rangel, 2009; Hare, Hakimi, & Rangel, 2014; Nestor et al., 2011; Wilson et al., 2004). Smoking cue appraisal was associated with attenuated dlPFC, and exaggerated striatal, activation in current smokers, compared to ex-smokers (Nestor et al., 2011). Moreover, response inhibition (associated with PFC activation (Aron & Poldrack, 2006; Chikazoe et al., 2009)) was impaired in cigarette smokers, relative to controls (Luijten, Littel, & Franken, 2011; Powell, Dawkins, & Davis, 2002). Activation in the dlPFC was positively correlated with selection of delayed monetary rewards (delayed gratification) (Figner et al., 2010; Hare et al., 2014; Luo, Ainslie, Pollini, Giragosian, & Monterosso,

2012; McClure, Ericson, Laibson, Loewenstein, & Cohen, 2007; McClure, Laibson, Loewenstein, & Cohen, 2004). Repetitive transcranial magnetic stimulation (rTMS) is a non-invasive technique capable of temporally potentiating (pulse frequency ≥ 5Hz) or inhibiting (< 1Hz) neural activity (Leo & Latif, 2007). rTMS delivers a series of magnetic pulses that pass through the skull and modulate electrical potential in the brain (usually not deeper than the cortex) (Leo & Latif, 2007). rTMS-induced temporary 'functional lesions' indicated that left (and not right) dlPFC function was associated with selection of delayed rewards (Figner et al., 2010). Moreover, rTMS-induced 'functional lesion' of the left dlPFC attenuated the potentiating effect of an immediate (vs. delayed) smoking opportunity on cigarette craving (Hayashi et al., 2013). Collectively, these studies illustrated the critical role of the dlPFC (and top-down executive control) in cognitive processes (e.g. self-control, delayed gratification, and drug cue appraisal) associated with substance use. Further, impaired dlPFC function (and associated cognitive processes) may be an important factor that (temporally) precedes substance use relapse.

2.5 Stress, Drugs, and Brain Function

2.5.1 Stress and Brain Function

The effects of acute experimental stress on brain function have been widely studied in the learning and memory literature (more so than the substance use literature). Review of this literature was useful for identifying the neural substrates of experimental stress-induction. The specific effects of experimental stress on memory vary depending on the stress manipulation and the type of memory investigated. However, broadly speaking, experimental stress tends to impair prefrontal-dependent,

and enhance striatal-dependent, cognitive processes. It should be noted there is a rich literature of the effects of chronic stress on brain function, but discussion of those findings are beyond the scope of this dissertation study.

In a series of studies, Schwabe and colleagues examined the effects of pretreatment with pharmacological stress-inducing agents (self-administration of oral YOH and HYD) on instrumental learning behavior (L. Schwabe, Joels, Roozendaal, Wolf, & Oitzl, 2012; L. Schwabe, Tegenthoff, Hoffken, & Wolf, 2010, 2012; L. Schwabe & Wolf, 2011; Lars Schwabe & Wolf, 2013)). Results demonstrated that YOH+HYD, but not YOH or HYD alone, rendered participant behavior insensitive to outcome devaluation (L. Schwabe et al., 2010; L. Schwabe, Tegenthoff, et al., 2012; L. Schwabe & Wolf, 2011). The authors interpreted these data to indicate that participants responded habitually and YOH+HYD impaired 'goal-directed' behavior during the task. Preclinical lesion and human neuroimaging studies indicated that goal-directed behavior is dlPFC-dependent (Bernard W Balleine & Dickinson, 1998; B. W. Balleine & O'Doherty, 2010; Corbit & Balleine, 2003; Valentin, Dickinson, & O'Doherty, 2007) whereas habit-directed responding is associated with the dorsal striatum (Tricomi, Balleine, & O'Doherty, 2009; Yin & Knowlton, 2006; Yin, Knowlton, & Balleine, 2004; Yin, Ostlund, Knowlton, & Balleine, 2005). YOH+HYD reduced the sensitivity of mOFC/mPFC to changes in outcome value, whereas the dorsal striatum was unaffected (L. Schwabe et al., 2010; L. Schwabe, Tegenthoff, et al., 2012; L. Schwabe & Wolf, 2011). Thus, during YOH+HYD, the outcome devaluation signal (encoded by mOFC/mPFC) failed to shift behavior (i.e. to goal-directed responding; dlPFC) during task performance (L. Schwabe et al., 2010; L. Schwabe, Tegenthoff, et al., 2012; L.

Schwabe & Wolf, 2011). In the context of substance use, acute stress may shift an individual's behavior from goal-directed (e.g. maintaining abstinence) to habit-directed (stimulus-response; e.g. cue elicited smoking relapse). Acute stress may increase the likelihood of substance use relapse via impaired dlPFC function. As described above, dlPFC function is associated with cognitive processes essential for maintenance of substance use abstinence (e.g. self-control, delayed gratification, and goal-directed behavior).

A widely studied cognitive function associated with the dlPFC function is working memory. Working memory is the active maintenance and neural representation of information over a brief delay period (typically 2-10 sec) prior to recall. A meta-analysis of fMRI studies indicated that working memory task performance (N-back; described in Section 3.2.8) was consistently associated with dlPFC and vlPFC activation (Owen, McMillan, Laird, & Bullmore, 2005). Importantly, the N-back working memory task is versatile and can be administered with or without drug-related stimuli (e.g. smoking images). One study found that psychosocial stress-induction attenuated dlPFC activation during a neutral N-back task performance and impaired response accuracy in healthy control subjects (Qin, Hermans, van Marle, Luo, & Fernández, 2009).

In non-human primates, spatial working memory has been studied. Primates were trained to retain the spatial location of a visual cue and respond via saccade (eye movement) following a brief delay period (typically 2-10 sec) (Goldman-Rakic, 1995). Electrodes implanted in the primate dlPFC indicated that spiking frequency increased during the delay period (time period between stimulus presentation and recall). Researchers concluded that feedforward microcircuits in the dlPFC (cortical layer III)

maintained a neural representation of the cue during the delay period, such that the primate was able to respond accurately (A. F. Arnsten, Wang, & Paspalas, 2012; Goldman-Rakic, 1995; Wang et al., 2013). Follow-up studies indicated that local, and systemic, administration of NMDA receptor antagonists attenuated neural spiking activity in the dlPFC and impaired response accuracy (Honey et al., 2004; Krystal et al., 2005; Wang et al., 2013). These well-controlled studies provided compelling evidence that working memory performance was mediated via neural spiking activity – specifically, glutamatergic neurotransmission binding post-synaptic NMDA receptors – in the dlPFC.

Non-human primate working memory performance (using the same experimental paradigm) exhibited an inverted "U" relationship with noradrenaline levels (A. F. Arnsten, 2009). Abnormally low (e.g. fatigue) (A. Arnsten & Goldman-Rakic, 1985) and high levels of noradrenaline (e.g. stress or YOH dose) (A. F. Arnsten, Mathew, Ubriani, Taylor, & Li, 1999; S. Birnbaum, Gobeske, Auerbach, Taylor, & Arnsten, 1999; S. G. Birnbaum et al., 2004; Doxey et al., 1984; Ramos et al., 2005) impaired working memory task performance (A. F. Arnsten, 2009). Optimal working memory performance (during alert and non-stressed conditions) was associated with moderate noradrenaline levels, and predominantly, α_{2A}-adrenoreceptor stimulation (A. Arnsten & Goldman-Rakic, 1985; Li & Mei, 1994). High levels of noradrenaline stimulated the lower affinity α_1- and β_1-adrenoreceptors (S. Birnbaum et al., 1999; Ramos et al., 2005), suppressed dlPFC neuronal spiking activity (Li, Mao, Wang, & Mei, 1999; Wang et al., 2007), and impaired response accuracy (A. F. Arnsten et al., 1999; S. G. Birnbaum et al., 2004).

In summary, a widely studied dlPFC-dependent cognitive process is working memory. Experimental stress (or administration of its neurochemical substrates: i.e. noradrenaline) attenuated dlPFC working memory task engagement (BOLD and neural spiking frequency) and impaired response accuracy. In addition, pharmacological stress-induction was associated with impaired 'goal-directed' behavior (dlPFC-dependent). Collectively, these studies provide support for the hypothesis that acute stress may increase the likelihood of substance use relapse via attenuated dlPFC engagement and impaired function.

2.5.2 Stress, Drugs, and Brain Function

The effects of acute experimental stress on substance use-related cognitive processes are not well understood. Research in this area has been limited by the experimental approaches used. As described above, with few exceptions, prior research studies used psychosocial stress manipulations. Psychosocial stress manipulations are associated with unreliable and short-lived (<30min) physiological stress responses that hinder their utility in neuroimaging investigations. Perhaps most limiting, psychosocial stressors are inherently dependent on cognitive processing to induce a physiological stress response. The BOLD response associated with the stress-inducing task will confound network activation changes associated with the physiological stress response (i.e. elevated cortisol and noradrenaline). These limitations and varied psychosocial stress-induction methodology have contributed to an inconsistent, and sometimes conflicting, neuroimaging literature (Dedovic et al., 2009). Despite these limitations, several effects have been reliably observed across studies and are described below.

Experimental stress-induction (in the absence of drug cues or drug administration) reliably increased dopaminergic neurotransmission in the NAcc in preclinical and clinical studies (Abercrombie, Keefe, DiFrischia, & Zigmond, 1989; Imperato, Angelucci, Casolini, Zocchi, & Puglisi-Allegra, 1992; Pruessner, Champagne, Meaney, & Dagher, 2004; Rougé-Pont, Piazza, Kharouby, Le Moal, & Simon, 1993). As described above, increased dopaminergic signaling in the NAcc is consistent with the reinforcing effects of acute drug administration (G. F. Koob & Volkow, 2010). Thus, acute stress may elicit appetitive craving in absence of drug cues or administration (i.e. stress may amplify 'bottom-up' signals). In addition, fMRI studies indicated that acute psychosocial stressors altered neural network activation and increased drug craving in the absence of drug cues (Sinha, 2001; Sinha, 2009; Sinha et al., 2006; Sinha & Li, 2007). Despite similar levels of subjective distress during a guided imagery stress-inducing technique, cocaine-dependent individuals exhibited greater BOLD activation in the caudate and dorsal striatum, and less activation in the parahippocampal gyrus, hippocampus, fusiform and anterior cingulate, compared to drug-naive controls (Sinha et al., 2005). In a related study (using the same stress-induction technique), increased BOLD activation in the mPFC during stress predicted shorter time to relapse during a 90-day post-treatment follow-up period (Sinha & Li, 2007).

To date, no clinical neuroimaging studies (to the knowledge of the author) have examined the potentially additive effects of concurrent experimental stress-induction and drug cue appraisal. Two studies examined the effects of sequential stress-induction and visual drug cue exposure during BOLD fMRI (Dagher, Tannenbaum, Hayashi, Pruessner, & McBride, 2009; Potenza et al., 2012). However, both studies used

psychosocial stress-induction techniques that may have confounded the physiological stress effects on visual drug cue appraisal and resultant BOLD activation. Moreover, physiological stress response biomarkers were not consistently measured. One study did not measure cortisol or noradrenaline levels (Potenza et al., 2012), whereas the other reported non-significant stress effects on saliva cortisol (Dagher et al., 2009). Moreover, neither study measured blood pressure (Dagher et al., 2009; Potenza et al., 2012). Thus, it remains unclear whether experimental stress-induction alters neural network response to visual drug cues.

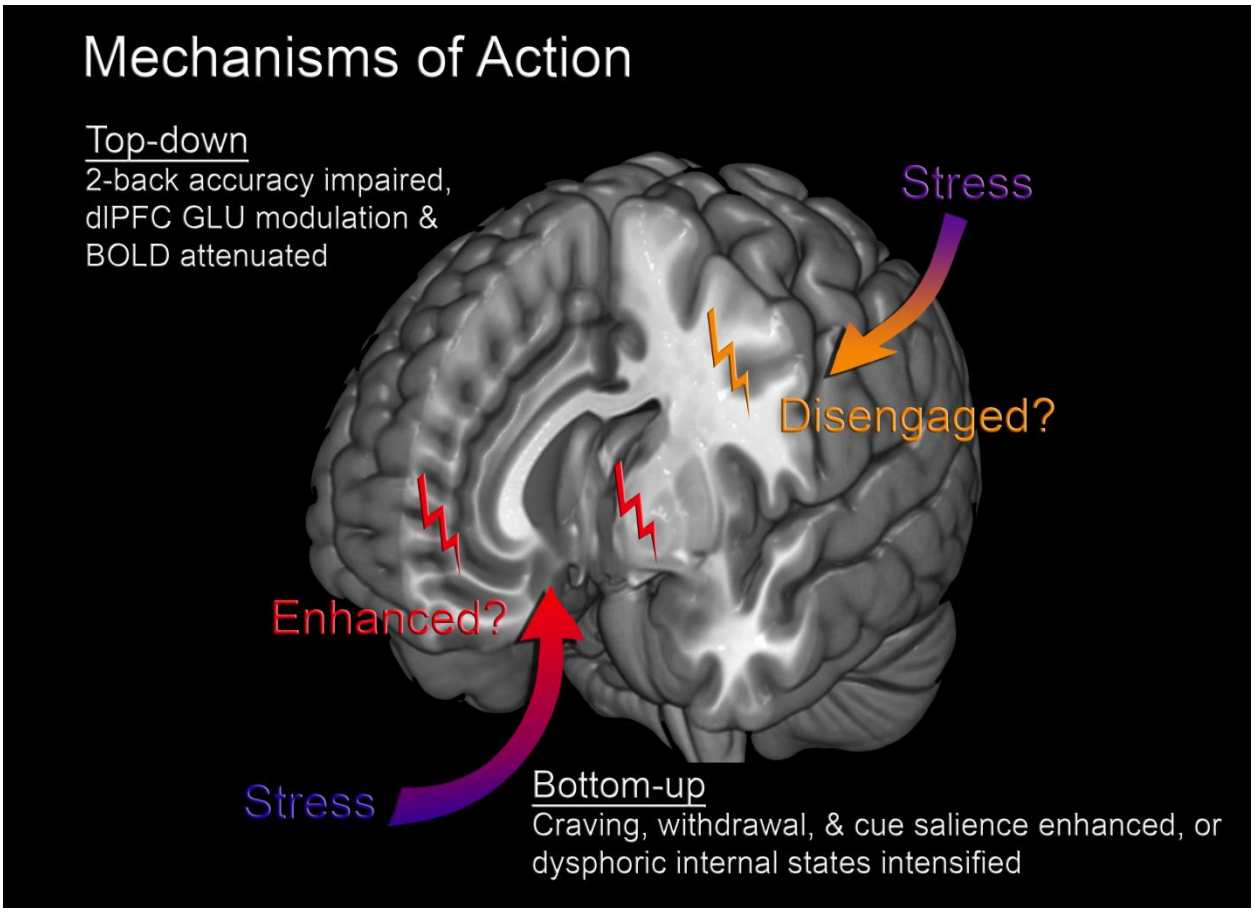

Figure 1.1: Proposed Mechanisms of Action. The conceptual guiding hypothesis and proposed mechanisms of action are illustrated. Acute stress may potentiate drug-seeking behavior via impaired top-down executive function (specifically, dlPFC function) and/or enhanced bottom-up signals (aversive internal states, cue salience, drug craving, or withdrawal symptoms).

2.6 Study Aims and Hypotheses

2.6.1 Conceptual Overview

Conceptually, the guiding hypothesis of this project is that *stress potentiates drug-seeking and self-administration by altering frontostriatal network function (with the dlPFC acting as a fulcrum) to:* 1) disrupt homeostasis; 2) mediate aversive internal states; 3) enhance smoking cue salience and appetitive motivation; and 4) attenuate dlPFC task engagement and impair dlPFC function (Figure 1.1). Our approach aligns with Goldstein & Volkow's conceptualization of substance use disorders (impaired response inhibition and salience attribution; iRISA), and with Koob's theory that chronic substance use causes neural counter-adaptations that dysregulate motivation and induce sensitization to stressors (Rita Z Goldstein & Volkow, 2002; R. Z. Goldstein & Volkow, 2011; G. F. Koob, 2008, 2009, 2010; George F. Koob & Moal, 1997).

2.6.2 Neurobiological Mechanism

The central aim of this study was to investigate a plausible neurobiological mechanism for stress-potentiated drug-seeking behavior. This study used a pharmacological stress-induction approach (oral pretreatment with YOH 54mg + HYD 10mg). Combined oral pretreatment with YOH+HYD offers a powerful stress-induction approach that activates both HPA and ANS stress systems. We hypothesized that acute experimental stress would attenuate dlPFC engagement and impair response accuracy on a dlPFC-dependent cognitive task. Impaired dlPFC function is a plausible neurobiological mechanism through which acute stress may potentiate nicotine self-administration. A multimodal neuroimaging approach (*in vivo* functional proton magnetic resonance spectroscopy [^{1}H fMRS] and BOLD fMRI) was used to examine dlPFC

engagement and function during letter N-back task performance. There is widespread support indicating this neurobiological mechanism is plausible (described in detail above), but has not been directly tested in any published studies (known to the author).

2.6.3 Study Aims and Hypotheses

Brief study overview. Chronic, regular cigarette smokers were recruited locally and screened for participation. Participants completed two identical experimental sessions under double-blind, placebo-controlled and within-subject randomized cross-over oral-dosing conditions: active (YOH 54mg + HYD 10mg) and placebo (YOH 0mg + HYD 0mg) stress. Throughout each session, subjective and physiological stress effects were assessed periodically. Participants completed a 60min MRI scan (which included ^{1}H fMRS and BOLD fMRI). Finally, nicotine-seeking and self-administration behavior was measured via a choice, progressive ratio task. Nicotine-seeking and self-administration directly measure nicotine motivation. This experimental design isolated the effects of pharmacological stress-induction on stress response biomarkers, subjective internal states, dlPFC function and task engagement, and nicotine-seeking and self-administration among non-treatment-seeking cigarette smokers.

Aim 1: Assess the effects of YOH+HYD on physiologic stress response biomarkers and subjective internal states. Hypotheses: 1a) Relative to placebo (0mg + 0mg), oral pretreatment with YOH+HYD (54mg + 10mg) will significantly increase blood pressure (systolic and diastolic), saliva cortisol and α-amylase. Prior research in our laboratory indicated that comparable oral pretreatment doses of YOH+HYD elicited a robust physiological stress response among buprenorphine-maintained, opioid-dependent individuals (Greenwald et al., in preparation). 1b) Relative to placebo,

YOH+HYD will significantly increase self-reported anxiety, negative affect, nicotine withdrawal symptom severity, and relief-motivated nicotine craving, but will not alter positive affect or appetitive craving. Prior research indicated that acute stressors can induce aversive internal states (M. al'Absi, 2006; al'Absi, Hatsukami, & Davis, 2005; Kalman, 2002; Swan, Ward, & Jack, 1996). Exploratory hypothesis: 1c) Relative to placebo, YOH+HYD will produce a physiologic stress response (e.g. heart rate, blood pressure, and saliva cortisol) comparable in magnitude to robust psychosocial stressors (i.e. qualitative comparison of effect sizes from the literature).

Aim 2: Investigate the effect of YOH+HYD on nicotine-seeking and self-administration among non-treatment-seeking current cigarette smokers. Hypotheses: 2a) Relative to placebo, YOH+HYD will potentiate nicotine-seeking and self-administration behavior (more cigarette puffs earned during the choice progressive ratio task and smoked during the self-administration phase). Prior research in our laboratory (Section 3.2.10) demonstrated that oral pretreatment with YOH+HYD increased opioid-seeking among buprenorphine-maintained, opioid-dependent individuals (Greenwald et al., in preparation). Exploratory hypothesis: 2b) YOH+HYD will not alter nicotine consumption rate (i.e. inter-puff intervals).

Aim 3: Investigate ^{1}H fMRS glutamate (GLU) modulation in the dlPFC during working memory task performance. Hypotheses: 3a) Relative to fixation cross rest, 2-back task performance will be associated with higher GLU levels during placebo. Prior research indicated that 2-back task performance was associated with robust BOLD activation bilaterally in the dlPFC (Owen et al., 2005) and fMRI BOLD activation was co-located with elevated GLU levels (measured via ^{1}H fMRS) (Mangia et al., 2006;

Schaller, Mekle, Xin, Kunz, & Gruetter, 2013; Schaller, Xin, O'Brien, Magill, & Gruetter, 2014). GLU modulation is an *in* vivo biomarker of neural activation (or task-engagement) that may reflect increased metabolic activity (Mangia et al., 2006; Schaller et al., 2013; Schaller et al., 2014). Importantly, GLU modulation is not confounded by vasoactive pharmaceutical agents (e.g. YOH). 3b) During YOH+HYD, 2-back GLU levels will not differ from fixation cross rest GLU levels. 3c) 2-back response accuracy will be higher during placebo, relative to YOH+HYD. Prior research in working memory task performance indicated that acute stress (e.g. YOH+HYD) attenuated dlPFC engagement (BOLD and neural spiking frequency) and impaired response accuracy (A. F. Arnsten, 2009; Qin et al., 2009).

Aim 4: Investigate BOLD activation changes associated with YOH+HYD during smoking (> neutral) cued N-back fMRI task. Hypotheses: 4a) Relative to placebo, YOH+HYD will enhance BOLD activation in the mPFC, mOFC, ventral and dorsal striatum during smoking cue (> neutral) images across N-back task levels (0-, 1-, and 2-back). These hypotheses are consistent with published literature; YOH+HYD will increase mOFC/mPFC activation (consistent with (Sinha & Li, 2007)), and decrease activation of the Amg (consistent with (Dagher et al., 2009)) and dlPFC (consistent with (Qin et al., 2009)). 4b) During 2-back task performance, smoking cued images will be associated with higher response accuracy, relative to neutral images, during both experimental sessions. Consistent with the iRISA theory (Rita Z Goldstein & Volkow, 2002; R. Z. Goldstein & Volkow, 2011), attentional bias toward drug-related stimuli will facilitate more accurate responding for smoking cued images, relative to neutral

images. 4c) Response accuracy will not differ by image type during 0- or 1-back task performance during either experimental session (ceiling effect anticipated).

CHAPTER 3 MATERIALS AND METHODS

3.1 ^{1}H fMRS Pilot Study

3.1.1 Study Overview

Prior ^{1}H fMRS research has demonstrated significant GLU modulation in the occipital cortex (during visual stimulation) (Mangia et al., 2006; Schaller et al., 2013) and motor cortex (during a finger tapping task) (Schaller et al., 2014). Our group recently extended this approach to cognitive task performance and replicated this effect in the hippocampus (during hippocampal-dependent cognitive task performance) (Jeffrey A Stanley et al., 2017). However, ^{1}H fMRS measurement of *in vivo* GLU modulation in the dlPFC during working memory task performance is novel. Therefore, a pilot study was conducted to develop a ^{1}H fMRS working memory task paradigm and evaluate the effect of task performance on GLU levels in the dlPFC.

3.1.2 Participant Recruitment

The Wayne State University Institutional Review Board (WSU IRB) approved all study procedures, which were conducted in accordance with the Declaration of Helsinki (1964). Healthy right-hand dominant male and female volunteers (aged 18-30 years) who reported no MRI contraindications, psychiatric diagnoses, or psychoactive medications were recruited from the Detroit metropolitan area. Interested individuals completed a brief screening procedure to verify eligibility. Participants deemed eligible provided informed consent and were compensated $50 for their time.

3.1.3 Experimental Protocol

Participants (N = 16) completed self-report measures (medication history, demographic questionnaire, and contact information), a comprehensive MRI safety

screen with an MRI technologist (~5 min), and a MRI scan (~60 min) during a single experimental session. Each participant received verbal instructions and completed several practice runs of the letter 2-back task outside of the magnet (until deemed proficient by the experimenter), prior to the MRI scan. Experimental tasks were programmed using Presentation software (version 18.1) and displayed on-screen inside the MRI scanner via projection system. Participants were able to communicate with the MR technologist via speaker/microphone system inside the scanner.

Each MRI scan consisted of a structural image, left dlPFC B_0-field shimming, voxel placement, and two ^{1}H fMRS experimental tasks (Figure 3.1): continuous fixation-cross rest and letter 2-back. Participants were verbally instructed to relax, focus their gaze on the fixation-cross, and let their thoughts drift during continuous fixation-cross rest. On screen, participants were prompted to “Rest” (2s) followed by a static, continuous fixation-cross (238s; centered on screen). The letter 2-back working memory task consisted of two phases: flashing grayscale checkerboard (3Hz; 208s) and seven blocks of alternating periods of fixation-cross rest (32s) and letter 2-back (64s). Prior research in our laboratory demonstrated that the flashing checkerboard minimized the variability in the GLU signal prior to investigation of task-related modulation (Lynn et al., in preparation). Participants were instructed to relax, focus their gaze on screen, and let their thoughts drift during the flashing checkerboard and interleaved fixation-cross rest. Every period of interleaved fixation-cross rest was prompted on screen with “Rest” (2s) prior to static fixation-cross (30s). Similarly, every letter 2-back task block was prompted with “2-back” (4s) followed by serial presentation of 20 capitalized letters (3s/letter; 6 target letters; letters displayed for 500ms followed

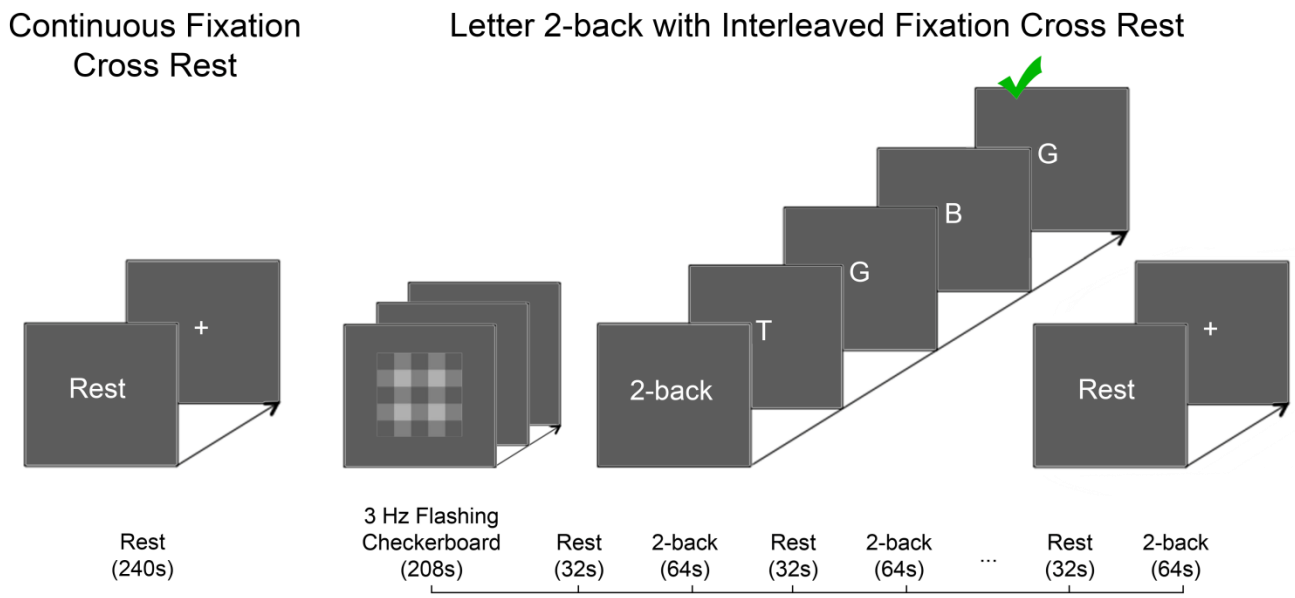

Figure 3.1: ^{1}H fMRS Pilot Study Experimental Paradigm. The continuous fixation cross rest (left) consisted of instructions ('Rest,' 2s) followed by continuous, static fixation cross (238s). The letter 2-back task (right) consisted of two phases: flashing checkerboard (3Hz, 208s) and seven repetitions of letter 2-back (64s; instructions '2-back' [4s], 20 letters [3s/letter; 60s]) with interleaved fixation cross rest (instructions 'Rest' [2s] and static fixation cross rest by 2500ms of blank screen). Subjects indicated (via button press) if the letter on screen matched the letter presented two previously. Participants were not provided feedback about response accuracy. Response accuracy was quantified as a percentage of correct responses for each task block.

3.1.4 Neuroimaging Parameters

All imaging was conducted on a 3 Tesla Siemens Verio system with 32-channel receive-only head coil. All participant scans were completed in the morning between 9:00-11:30am. High resolution T_1-weighted structural scans were collected using the 3D Magnetization Prepared Rapid Gradient Echo (MPRAGE) sequence with the following parameters: TR = 2.2s, TE = 3ms, TI = 799ms, flip angle = 13°, Field-of-View (FOV) = 256 x 256 x 160mm, 256 x 1mm thick axial slices, matrix = 176 x 256. Prior to ^{1}H fMRS acquisition, a region of the left dlPFC (2.5 x 2.5 x 2.5cm) larger than ^{1}H fMRS voxel was

shimmed to improve B_0-field homogeneity (FASTESTMAP). ^{1}H fMRS spectra were continuously acquired every 16s (PRESS with OVS and VAPOR, TE = 23ms, TR = 4.0s, 4 averages/spectrum, bandwidth = 2 kHz, 2048 data points, no apodization) during the continuous fixation-cross task (15 spectra, 240s) and letter 2-back (55 spectra, 880s). ^{1}H fMRS spectra were acquired without water suppression immediately after each task (TE = 23ms, TR = 10s, 2 averages/spectrum, bandwidth = 2 kHz, 2048 data points, no apodization). Unsuppressed water levels were used to scale metabolite levels to absolute concentration values (mmol/kg wet weight).

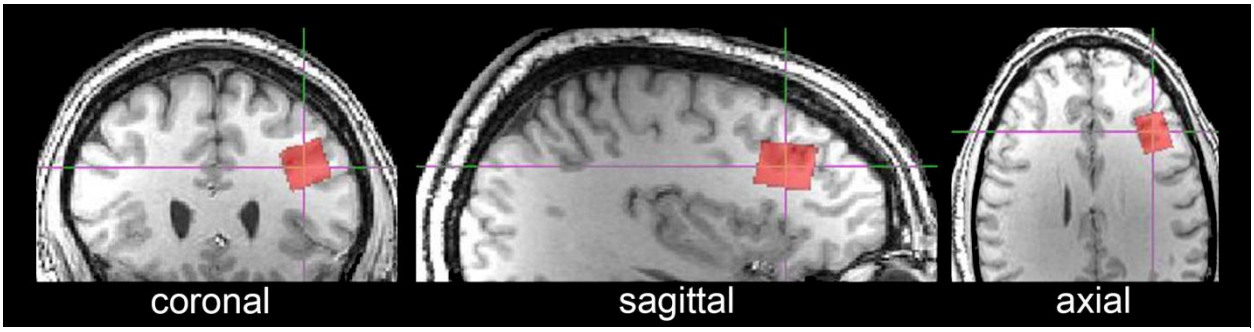

Figure 3.2: ^{1}H fMRS Pilot Study Voxel Placement. The ^{1}H fMRS Pilot Study voxel (1.5 x 2.0 1.5 cm; 4.5 cm^3) was located in the left dlPFC (Brodmann Areas 45 and 46).

3.1.5 Voxel Placement

^{1}H fMRS spectra were acquired from the left dlPFC (15 x 20 x 15 mm; 4.5 cm^3; Brodmann Areas 45 and 46; Figure 3.2). The voxel location was selected to encompass regions consistently associated with significant BOLD activation in the dlPFC during letter 2-back task performance (fMRI meta-analysis) (Owen et al., 2005). The automated voxel placement (AVP) method (Woodcock, Arshad, Khatib, & Stanley, 2017) was used to prescribe 15 of 16 participant's voxel locations (AVP not used for one subject; experimenter error).

3.1.6 Automated Voxel Placement (AVP)

Single voxel MRS research studies often manually prescribe a voxel based on a 2D image of the current subject's anatomy. Despite its widespread use, manual voxel placement is time-consuming, challenging, and unreliable. This is especially problematic for research studies, whose goal is often to investigate neurochemistry as a function of psychiatric diagnosis (i.e. between-group research study) or treatment (i.e. longitudinal study). Metabolite levels are known to vary across brain regions and by voxel tissue composition (gray matter vs white matter vs cerebrospinal fluid). Therefore, to avoid Type I or II error, voxel placement must be accurate and reliable across research subjects and/or within a research subject across scans. AVP was developed in response to the lack of reliable automated approaches for single voxel prescription.

The AVP suite consisted of three Linux- and Matlab-based scripts (Woodcock et al., 2017). The first script, avp_create, facilitated creation of a library of template voxel locations that were retained for future subject scans. The second script, avp_coregister, facilitated accurate coregistration and prescription of a template voxel to each research subject at the scanner (~2 min computer processing time) based on that subject's T_1-weighted image (i.e. subject head position in the scanner). Figure 3.3 illustrates the processing logic used in avp_create and avp_coregister. The third and final script, avp_overlap, gathered information stored in the subject's .rda file (ASCII file created during MRS measurements), recreated the prescribed voxel, coregistered the voxel to the template brain, and calculated 3D geometric voxel overlap accuracy and reliability across subject scans. The AVP suite is available for download free-of-charge (Woodcock et al., 2017).

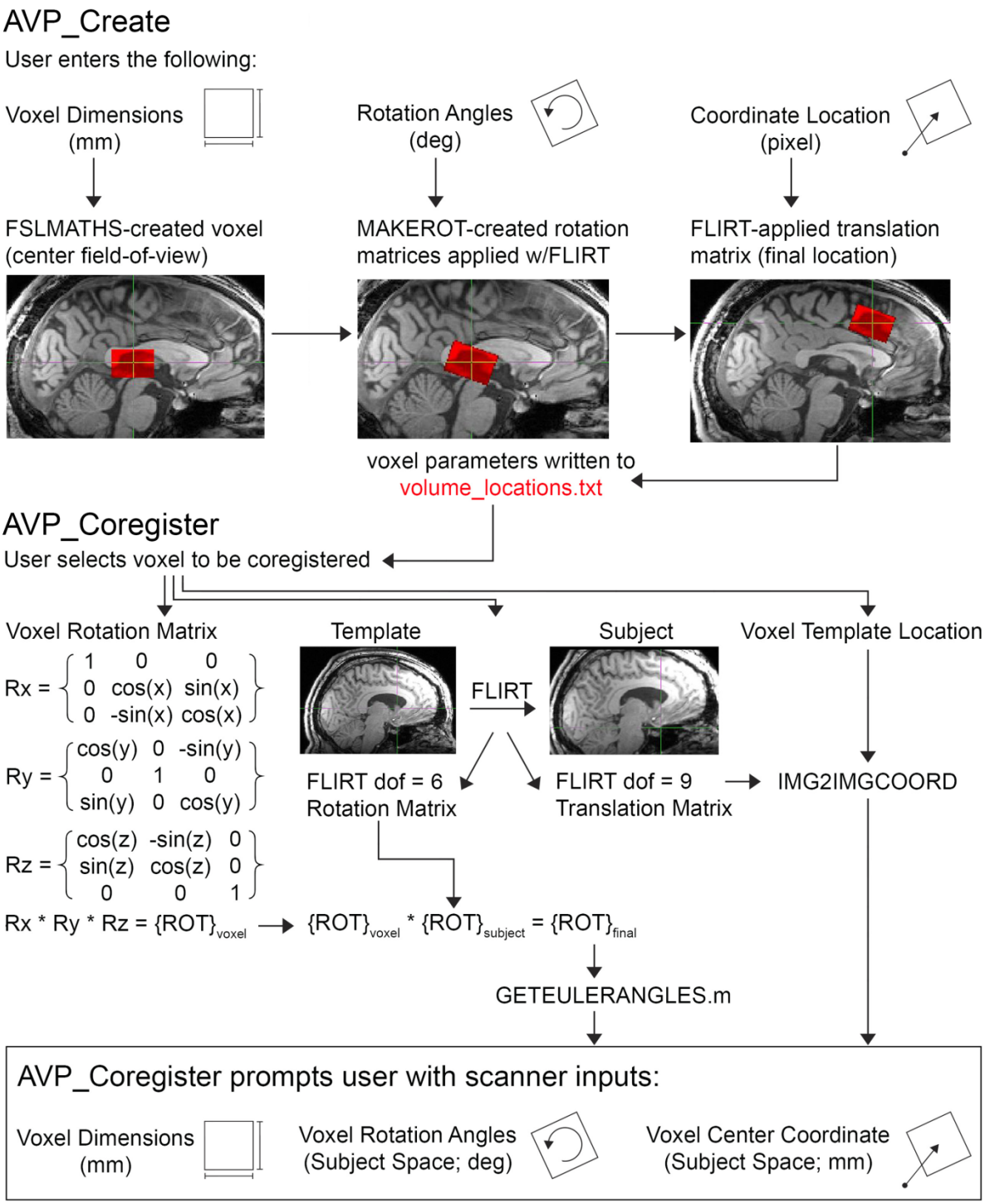

Figure 3.3: AVP Processing Logic. First, the user selects a template brain and enters voxel parameters (dimensions, center coordinate, and rotation angles; 'avp_create'). The generated voxel is retained for future coregistration. Second, the user selects a template voxel for coregistration to the current subject ('avp_coregister'). The subject's structural image is coregistered to the template brain and two inversion matrices are generated (DOF = 6 and 9). These matrices facilitate calculation of rotation angles and voxel center coordinate (respectively) in subject space for voxel prescription.

3.1.7 Analysis Strategy

^{1}H fMRS Analyses. ^{1}H fMRS spectra were analyzed using LCModel version 6.3 (Provencher, 2008). Post-processing and metabolite quantification steps were 100% automated. Eddy current effects were corrected using the unsuppressed water signal (Klose, 1990). T_1-weighted structural images were B_1-field corrected, the brain image extracted, and segmented into partial volume maps of CSF, grey and white matter using FreeSurfer and FSL tools (e.g. FLIRT, NU_CORRECT, BET and FAST) (Dale, Fischl, & Sereno, 1999; Smith et al., 2004). Finally, tissue composition within the MRS voxel and appropriate correction factors (e.g. T_1 and T_2 relaxation) were used to calculate absolute GLU concentration (mmol/kg wet weight) (J. A. Stanley, Drost, Williamson, & Thompson, 1995). Raw spectra were phase- and shift-corrected prior to quantification. Consecutive raw spectra (4 averages, 16s, no apodization or zero-filling) were averaged which resulted in 32s temporal resolution (8 averages). GLU levels during the first 32s and final 32s of 2-back task performance (2-back A and B, respectively) were contrasted with fixation-cross rest GLU levels (continuous and interleaved fixation-cross considered separately).

Shapiro-Wilk test of normality and skewness and kurtosis statistics were used to evaluate variable distributions prior to outcome analyses. Whenever necessary, extreme values were winsorized (extreme value replaced with nearest value) to normalize distributions prior to outcome analyses. Repeated measures analyses of variance (rmANOVA) were used to analyze behavioral and neurochemical data. Follow-up paired t-tests were used to clarify significant main effects. Mean metabolite levels during 2-back task were contrasted with rest levels. The metabolite of interest for this

study was GLU. However, other metabolites (NAA, Myo-Inositol, GPC+PC, and PCr+Cr) were analyzed to determine the neurochemical specificity of working memory task modulation. Voxel overlap was quantified using the avp_overlap script (included in the AVP suite) (Woodcock et al., 2017). 3D geometric voxel overlap percentage was calculated between each subject's voxel and the template voxel (i.e. accuracy), and voxel overlap across all subjects (i.e. reliability). Descriptive statistics are presented as mean ± one standard deviation (M ± 1 SD) unless otherwise noted. In all figures, error bars represent ± one standard error of the mean (SEM).

3.2 Dissertation Study

3.2.1 Participant Recruitment

The WSU IRB approved all study procedures, which were conducted in accordance with the Declaration of Helsinki (1964). Participants were recruited from the Detroit metropolitan area via Craigslist advertisements. Interested individuals (> 500) completed a brief (20min) standardized phone screen to rule out obvious study contraindications. At the end of the phone screen, eligible individuals were provided an overview of experimental procedures, including a description of pharmacological agents (and possible side effects), MRI scan, and urine drug screen (UDS) procedure. Interested individuals (105) were scheduled for a thorough in-person screen (2hr) at the Human Pharmacology Laboratory (Tolan Park Medical Building, Suite 2A).

Upon arrival to the in-person screening appointment, participant sobriety was verified (expired breath alcohol concentration: <.002%). Prior to obtaining participant informed consent, a research assistant described the in-person interview procedures in detail. Participants who provided written informed consent were eligible to complete the remainder of the in-person screen which included: self-report measures (described in the Self-Report Measures section below), brief (~20min) computerized psychiatric interview, expired breath carbon monoxide measurement (CO; biomarker of recent cigarette smoking), UDS (tested for substance use and pregnancy), electrocardiogram (ECG), vital signs measurement (resting blood pressure, heart rate, blood oxygen saturation), and MRI contraindications screen (self-report). A licensed cardiologist evaluated the ECG. A complete description of inclusion and exclusion criteria is listed below. Participants were compensated $20 for completion of the in-person screening visit (independent of eligibility).

3.2.2 Inclusion and Exclusion Criteria

Inclusion criteria:

1) Current smoker: expired breath CO ≥ 5ppm, self-reported 10+ cigarettes/day, Fagerstrom Test of Nicotine Dependence (FTND) score ≥ 4
2) Aged 21-35 years: date of birth verification (driver's license)
3) Sober at screening: negligible expired breath alcohol (<.002%)
4) Cardiovascular health: normal resting blood pressure (systolic: 80-160mmHg; diastolic: 50-90mmHg), heart rate (50-90bpm), and ECG
5) Normal or corrected-normal vision
6) Cognitively Intact: Shipley Institute of Living Scale (Zachary, 1991) verbal intelligence score ≥ 80

Exclusion criteria:

1) Urinalysis: positive for illicit substance use (opioids, methadone, cocaine metabolites, benzodiazepines, barbiturates [≥300ng/ml], or amphetamines [≥1000ng/ml]) or pregnancy (females only)
2) Recent substance use: 15+ days of marijuana and/or alcohol use in past month
3) Psychiatric evaluation: met criteria for current Axis I disorder (MINI-6)
4) Medical contraindications: diabetes, steroid-based contraceptives
5) MRI contraindications: pacemaker, ferrous implants, metal fragments
6) Current motivation to reduce, or seek treatment for, their nicotine use
7) Lactose intolerance (placebo dose)

Individuals (N = 27) who satisfied inclusion and exclusion criteria were deemed eligible and invited to participate in the research study. Participants provided written

informed consent to all experimental study procedures prior to the first experimental session. Participants were scheduled for experimental sessions on non-consecutive weekdays (M-F). Whenever possible, experimental sessions were scheduled within the same week. Eligible female participants were scheduled for both experimental sessions during their luteal phase (self-reported final 14 days of the menstrual cycle) to minimize stress reactivity variability (Clemens Kirschbaum, Kudielka, Gaab, Schommer, & Hellhammer, 1999; Kumsta, Entringer, Hellhammer, & Wüst, 2007). Participants who completed both experimental sessions (N = 21) were included in outcome analyses.

3.2.3 Power Analyses

Power analyses for this study were based on the effect sizes observed in a related study using similar experimental procedures. Prior research in our laboratory (Greenwald et al., in preparation) demonstrated that similar pharmacological doses, YOH 54mg + [HYD 0mg vs. 20mg], were associated with moderate effects on opioid drug-seeking behavior (Cohen's *d* = 0.62 and 0.68, respectively) in opioid-dependent, buprenorphine-maintained volunteers. The pharmacological doses (YOH 54mg + HYD 10mg) used in the present study were assumed to be associated with similar effect sizes (Cohen's *d* = 0.64) on the primary outcome variable: nicotine-seeking and self-administration behavior (see Choice Task section below). G*Power version 3.1 (Dusseldorf, Germany) indicated that a sample of 21 subjects would afford sufficient statistical power to reliably detect a main effect for a two-tailed paired t-test, power = .80, and $\alpha < .05$ (J. Cohen, 1992).

3.2.4 Experimental Procedures

Participants completed two experimental sessions (active vs. placebo stress; random order) using a double-blind, placebo-controlled, and within-subject crossover design. Participants were allowed to smoke cigarettes *ad libitum* prior to each experimental session. Upon arrival at our laboratory (11:00am), participants were tested for sobriety (expired breath alcohol < .002%). At 11:20am, a saliva sample was collected, vital signs (resting blood pressure and heart rate) and expired breath CO (see Physiological Measures section below) were measured, and the periodic battery of self-report measures (see Periodic Self-Report Battery below) was completed (see Table 3.1 for complete experimental procedures). The periodic battery of self-report measures was collected five times throughout each experimental visit and included: Minnesota Nicotine Withdrawal Scale (MNWS), Brief Questionnaire of Smoking Urges (QSU), State-Trait Anxiety Inventory (STAI; state version), and Positive and Negative Affect Scale (PANAS). At 11:30am, participants completed the paced puff procedure. Participants smoked one puff (1-2sec inhale; video-verified) of their preferred brand of cigarette every minute for five minutes (6 total puffs; stopwatch timed; experimental control of recent nicotine exposure; experimental room ventilated). At 11:40am, participants were moved to a new experimental room that was not used for cigarette smoking and was devoid of smoking/cigarette cues. A saliva sample was collected, and vital signs and expired breath CO were measured. At 11:45am, participants self-administered the oral YOH dose (54mg or 0mg). Prior research in our laboratory (Greenwald et al., in preparation) indicated that an oral 54mg YOH dose elevated resting blood pressure (relative to placebo; consistent with a physiological stress

response) approximately 75min after dose and remained elevated for 2+ hours. For this study, YOH was self-administered 75min prior to the onset of the MRI scan. Participants completed another repetition of the self-report measure battery, as well as the Timeline Follow-Back Questionnaire. At 12:15pm, participants self-administered the oral HYD dose (10mg or 0mg). Prior research in our laboratory (Greenwald et al., in preparation) demonstrated that oral HYD dose elevated saliva cortisol levels (relative to placebo; consistent with a physiological stress response) approximately 45min after dose and remained elevated for 2+ hours. Participants received detailed instructions about the MRI scan procedure and experimental tasks, and completed practice runs of the letter 2-back (until proficient). At 12:40am, periodic self-report questionnaires were completed, vital signs were measured, and a saliva sample collected. Participants were escorted to the MRI center (~8min walk) and upon arrival allowed to rest briefly (~3-4min), while the MRI room was prepared. Participants completed the MRI safety screen with the MR technologist (Dalal Khatib) prior to the scan (1-2pm; see Neuroimaging

Time	Procedure / Measure
11:00am	Participant arrival at Tolan Park Medical Building
11:20am	Vital signs, saliva, breath CO, periodic self-report measures
11:30am	Paced puff procedure
11:39am	Change experimental rooms
11:40am	Vital signs, saliva, breath CO
11:45am	YOH dose (54mg vs. 0mg)
11:46am	Periodic self-report measures, TLFB
12:15pm	HYD dose (10mg vs. 0mg)
12:40pm	Vital signs, saliva, periodic self-report measures
12:50pm	Escort to MRI center
1:00pm	MRI scan
2:00pm	Escort back to Tolan Park Medical Building
2:20pm	Vital signs, saliva, periodic self-report measures
2:30pm	Puffs vs. Money Choice Task
3:00pm	Vital signs, saliva, periodic self-report measures
3:05pm	Nicotine self-administration
4:00pm	Participant discharge

Table 3.1: Experimental Timeline. Experimental timeline was identical for both experimental sessions (active and placebo stress).

Experimental Tasks and Neuroimaging Parameters sections below). After being escorted back to the Tolan Park Medical building (~8min walk) and following a brief rest (~5min), a saliva sample was collected, vital signs were measured, and periodic self-report measures were completed (2:20pm). At 2:28pm, participants were provided verbal instructions that described the cigarette puff vs. money choice progressive ratio task. From 2:30-3pm, participants completed the 30min choice task (see Choice Task section below). At 3:00pm, vital signs were measured, a saliva sample was collected, and the periodic self-report battery was completed. At 3:05pm, participants were escorted to the cigarette-smoking experimental room (ventilated) and self-administered the cigarette puffs earned on the choice task. Participants were instructed to smoke exactly the number of earned puffs (not more and not fewer; 1-2sec inhale; video-verified) at a comfortable pace of their choosing. Inter-puff interval (s) was measured via video monitor unbeknownst to the participant. Participants remained on site until 4pm for monitoring. Participants were not able to smoke *ad libitum* until after 4pm. Each experimental session lasted 5 hours. Participants were compensated $70 at the end of each experimental session and a bonus of $40 for completing both sessions (total compensation for study completion: $200). Any money earned during the choice task was added to the participant's study payment.

Participant safety. Participant safety was paramount. Previous research in our laboratory using comparable and higher YOH and HYD oral dose combinations were not associated with adverse events. However, personnel and safety procedures were established prior to participant enrollment to ensure participant safety throughout the study. Medical staff (licensed physicians and nurses), clinical psychologists, trained

masters-level clinical students, and research staff were onsite throughout each experimental session. Medications were onsite and available to counteract YOH and HYD if necessary [e.g. clonidine and/or diazepam; (Charney et al., 1983; Charney, Woods, Krystal, Nagy, & Heninger, 1992; Mattila, Seppala, & Mattila, 1988)].

3.2.5 Physiological Measures

Vital signs: Resting heart rate and systolic and diastolic blood pressure were measured during the in-person screening visit (index of cardiovascular health) and periodically throughout each experimental session (biomarker of physiological stress response) via Welch-Allyn vital signs monitor. In addition, heart rate and blood pressure were monitored to ensure participant cardiovascular safety throughout the study (safety thresholds; resting heart rate ≤ 100 beats/min and blood pressure ≤ 160 / 100 mmHg [systolic / diastolic]).

Saliva measures: Saliva was collected via oral swab (SalivaBio Oral Swab; Salimetrics®, State College, PA) which was placed under the participant's tongue for ~2 minutes. After saliva collection, swabs were returned to the individual storage tube. At the end of each experimental session, samples were spun down via centrifuge (3386 RPMs) for 15 minutes and stored upright at -80ºC until analysis and quantification. *Saliva α-amylase* is a digestive enzyme and indirect biomarker of sympathetic ANS activity (Nater & Rohleder, 2009). Saliva α-amylase responds to β-adrenergic receptor stimulation, but prior research indicated α-amylase reflected indirect stimulation by YOH (Ehlert et al., 2006). Saliva α-amylase was quantified (units: U/mL) via enzymatic reaction with 2-chloro-p-nitrophenol and the change in spectrophotometric absorption at 405nm (sensitivity threshold: 0.4 U/mL). *Salivary cortisol* is a well-validated correlate of

plasma cortisol levels and HPA axis activity (Kahn, Rubinow, Davis, Kling, & Post, 1988). HYD reliably and dose-dependently increases cortisol levels (van Stegeren, Roozendaal, Kindt, Wolf, & Joëls, 2010). Saliva cortisol was quantified (units: ug/dL) via ELISA assay and reaction with horseradish peroxidase enzyme, followed by measurement of optical density at 450nm (sensitivity threshold: <0.007 ug/dL).

3.2.6 Self-Report Measures

The following self-report measures were administered during the in-person screening visit only (unless otherwise noted). Drug History and Use Questionnaire: The DHUQ was developed in-house as a comprehensive assessment of substance use history (across drugs of abuse), including age at onset, use frequency, and substance use consequences. This measure was used to determine participant eligibility (e.g. past-month cigarette smoking and alcohol use frequency). Medical History Questionnaire: The MHQ was developed in-house as a comprehensive self-report assessment of participant medical history, including lifetime and current medical diagnoses, reproductive status, current medication and contraceptive use. This measure was used to determine participant eligibility (e.g. cardiovascular conditions, medication allergies). Distress Tolerance Scale: This 15-item 5-point Likert scale (1 = 'strongly agree' to 5 = 'strongly disagree') measured an individual's ability to tolerate distress. This scale demonstrated good construct validity and reliability (Simons & Gaher, 2005). Barratt Impulsivity Scale (BIS-11): This widely-used 30-item 4-point Likert scale (0 = 'rarely/never' to 4 = 'almost always/always) measured trait impulsivity (e.g. 'I plan tasks carefully') along three dimensions: motor, attention, and non-planning impulsiveness (Patton & Stanford, 1995; Stanford et al., 2009). State-Trait Anxiety

Inventory (STAI; trait): The 20-item 4-point Likert scale (1 = 'not at all' to 4 = 'very much so') measured trait anxiety ('how you generally feel') via first-person statements (e.g. 'I feel secure') (Spielberger, 1983). The STAI has excellent psychometric properties (Spielberger, 1983, 2010). Stress Mindset Scale (SMS): This 8-item 5-point Likert scale (1 = 'strongly disagree' to 5 = 'strongly agree') measured an individual's subjective assessment (or experience) of how stress affected his/her performance, health, and learning ability (e.g. 'the effects of stress are negative and should be avoided') (Crum, Salovey, & Achor, 2013). Fagerstrom Test for Nicotine Dependence (FTND): The FTND is the gold standard self-report questionnaire for assessing nicotine dependence. The FTND consists of 6 items (e.g. 'do you smoke more frequently in the morning?' [yes=1, no=0]) that are summed for a total score (range: 0-10) of nicotine dependence severity (Heatherton, Kozlowski, Frecker, & Fagerstrom, 1991). Timeline Follow-Back Questionnaire (TLFB): Participants completed the TLFB questionnaire once during each experimental session. The TLFB assessed frequency of past week (7 days) nicotine use across products (cigarettes, e-cigarettes, cigars, and smokeless tobacco).

3.2.7 Periodic Self-Report Battery

Questionnaires described below were administered periodically throughout each experimental session (see Table 3.1). State-Trait Anxiety Inventory (STAI): The 20-item 4-point Likert scale (1 = 'not at all' to 4 = 'very much so') measured state anxiety ('right now, at this moment') via first-person statements (e.g. 'I feel calm') (Spielberger, 1983). Positive and Negative Affect Schedule (PANAS): The PANAS is a 20-item 5-point Likert scale (1 = 'not at all or very slightly' to 5 = 'extremely') that is a reliable and well-validated measure of state positive and negative affect (Watson, Clark, & Tellegen,

1988). Participants rated 20 adjectives (e.g. 'interested' or 'excited') 'at the present moment.' Items loaded onto one of two affect subscales: 'positive' or 'negative' (analyzed separately). Questionnaire of Smoking Urges (QSU; brief version): This 10-item 7-point Likert scale (1 = 'strongly disagree' to 7 = 'strongly agree') measured a participant's desire to smoke a cigarette (e.g. 'I have a desire for a cigarette right now') 'at this moment' (Cox, Tiffany, & Christen, 2001). Items loaded onto one of two craving subscales: 'appetitive' or 'relief-motivated' (analyzed separately). Minnesota Nicotine Withdrawal Scale (MNWS): The MNWS consisted of 15 adjectives (descriptions of possible nicotine withdrawal symptoms; e.g. 'restless' and 'impatient') rated on a 5-point Likert scale (0 = 'none' to 4 = 'severe') (Hughes & Hatsukami, 1986). The MNWS is a well-validated measure of nicotine withdrawal severity (Hughes, 1992; Hughes, Gust, Skoog, Keenan, & Fenwick, 1991; Hughes & Hatsukami, 1986; Shiffman, West, & Gilbert, 2004).

3.2.8 Neuroimaging Experimental Tasks

Participant scans were completed in the afternoon (1-2pm) for both experimental sessions. Prior to each scan, participants completed an MRI safety assessment (~3min) with the MR technologist (Dalal Khatib). All imaging was conducted on a 3 Tesla Siemens Verio system with 32-channel receive-only head coil. Experimental tasks were programmed using Presentation software version 18.1 and displayed on-screen inside the MRI scanner via projection system. Participants were able to communicate with the MR technologist via speaker/microphone system.

^{1}H fMRS Letter 2-back Task. The letter 2-back task paradigm (Figure 3.4) was a shortened version of the letter 2-back task paradigm used in the pilot study. The pilot

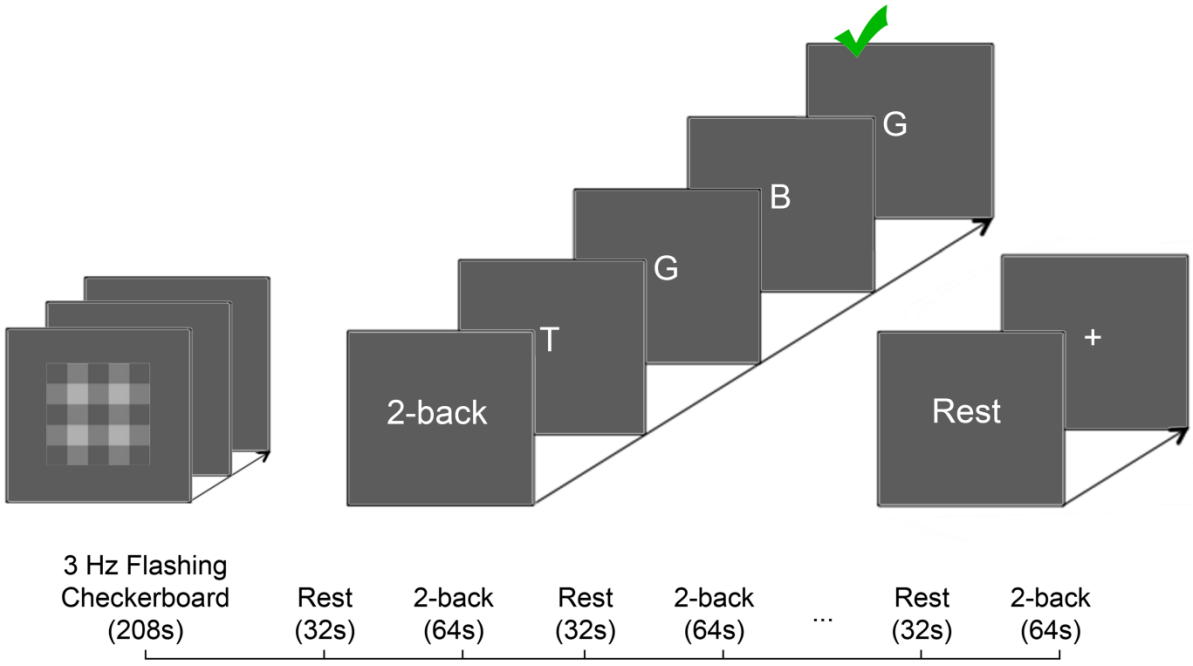

Figure 3.4: ^{1}H fMRS Dissertation Study Experimental Paradigm. The letter 2-back task (right) consisted of two phases: flashing checkerboard (3Hz, 208s) and five repetitions of letter 2-back (64s; instructions '2-back' [4s], 20 letters [3s/letter; 60s]) with interleaved fixation cross rest (instructions 'Rest' [2s] and static fixation cross rest [30s]).

study contained seven blocks of alternating letter 2-back and interleaved fixation-cross rest, while this version contained only five blocks. All other aspects of the task paradigm and instructions were identical. Briefly, the task consisted of two phases: flashing grayscale checkerboard (3Hz; 208s) and 5 blocks of alternating letter 2-back (64s; on-screen '2-back' instructions [4s] followed by 20 capitalized letters [3s/letter; 6 target letters; each letter [500ms] followed by blank screen [2500ms]) and interleaved fixation-cross rest (32s; 'Rest' instructions [2s], static fixation-cross [30s]). Participants indicated (via button press) if the letter on screen matched the letter presented two previously. Participants were not provided feedback about response accuracy. Response accuracy was quantified as a percentage of correct responses for each task block.

fMRI Letter 2-back Task. The fMRI version of the letter 2-back task consisted of two blocks of letter 2-back (64s; same parameters as ^{1}H fMRS version) and fixation-

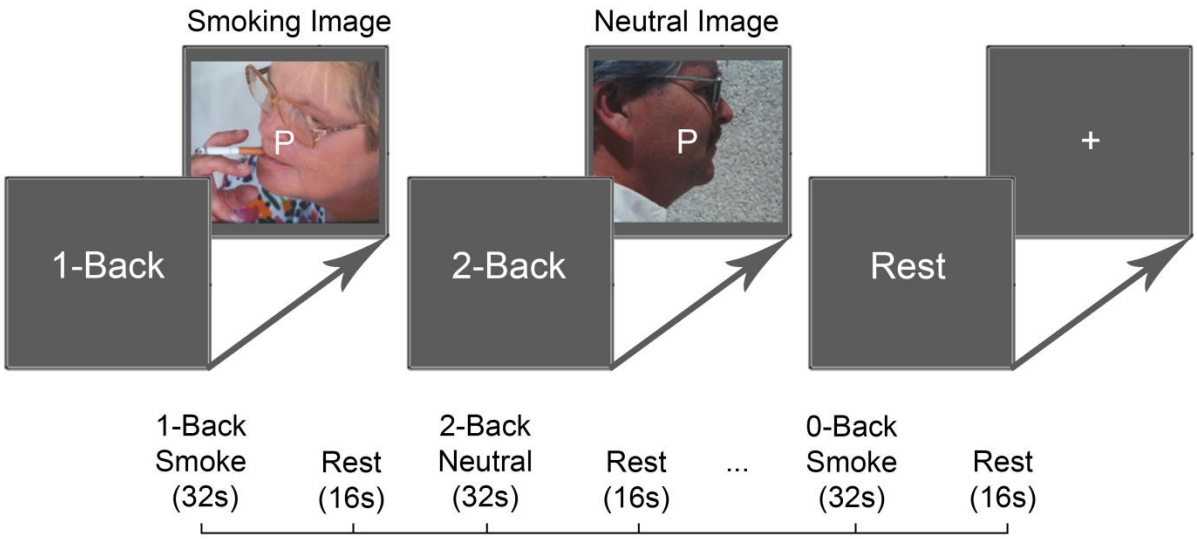

Figure 3.5: fMRI Smoking Cued N-back Paradigm. Participants completed two blocks of each task difficulty (0-, 1-, and 2-back) of letter N-back yoked with neutral or smoking-related images. Each block (32s) consisted of instructions (e.g. '1-Back'; 2s) and 10 letters (3s/letter) interleaved with fixation cross (16s).

cross rest (32s). The fMRI letter 2-back task blocks were mixed in among blocks of the smoking vs. neutral cued N-back task.

fMRI Smoking vs. Neutral Cued N-back Task. This task consisted of blocks of letter 0-, 1-, and 2-back overlaid in the center of either cigarette smoking-related images or neutral, non-smoking images (Figure 3.5; matched for image characteristics and content [e.g. image of a hand with and without a lit cigarette]). Two blocks of each N-back category (e.g. 0-back smoking cued, 1-back neutral cued, etc.) was displayed in pseudo-random order. Each block had an identical structure (32s; instructions [e.g. '1-back'; 2s], 10 letters [3s/letter; 750ms on-screen, 2250ms blank screen; 3 targets]) separated by fixation-cross rest (16s; not analyzed; minimize carry-over effects). Participants were instructed to focus on the letters in the center of screen (as they would during a letter N-back task) and indicate (via button press) when the current letter on screen matched the target letter (0-back), when the same letter was depicted sequentially (1-back), or when the current letter matched the letter presented two

previous (2-back). Participant performance (% correct and response latency [ms]) was analyzed separately for each N-back trial (0-, 1-, and 2-back) and image type (smoking vs. neutral).

Cerebrovascular Reactivity (CVR) Task. Following the fMRI N-back task, a subset of participants completed the CVR task. The task consisted of five blocks of unconstrained 'normal' breathing (22s), paced breathing (4 repetitions of breathing in [3s] and out [3s]), and breath-hold challenges (11s; following exhale). On-screen instructions guided participant breathing throughout the task (Figure 3.6). Prior research demonstrated that breath-hold challenge tasks were robust and reliable measures of CVR (Bright & Murphy, 2013; Lipp, Murphy, Caseras, & Wise, 2015; Magon et al., 2009; Murphy, Harris, & Wise, 2011; Sousa, Vilela, & Figueiredo, 2014). Carbon dioxide is a powerful vasodilator. As carbon dioxide accumulates in blood vessels during breath hold, cerebral blood flow will increase substantially. The ratio of

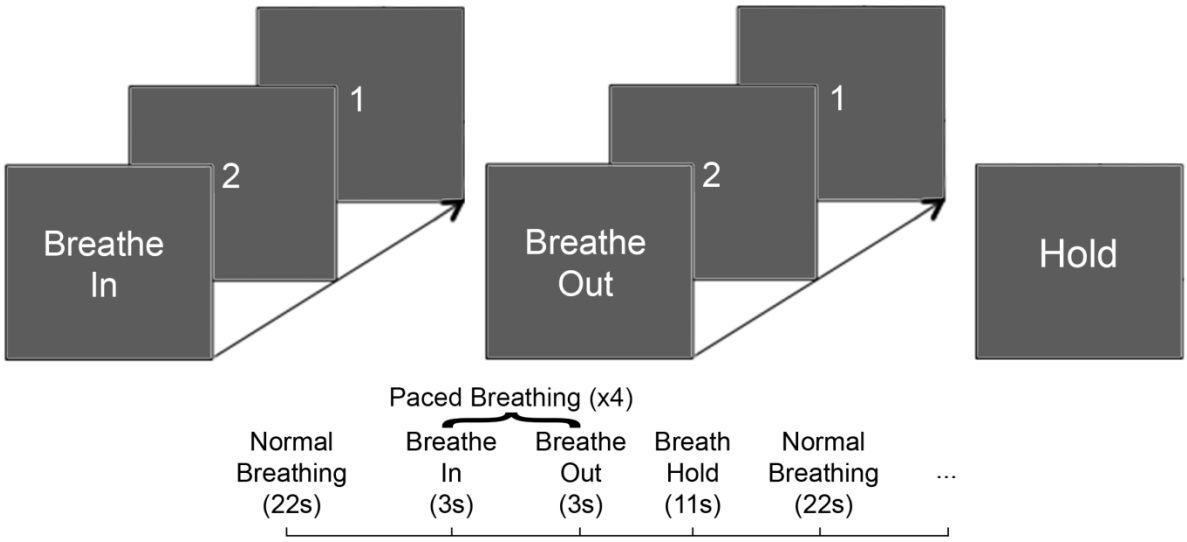

Figure 3.6: Cerebrovascular Reactivity Paradigm. Participants were instructed to alter their breathing to match the instructions on screen. Three phases were completed sequentially across five repetitions: normal (uncontrolled; 22s), paced breathing (3s in/ 3s out; four repetitions), and breath hold (11s).

oxygenated hemoglobin to deoxygenated hemoglobin will increase which will alter local T_2* decay, resulting in a robust BOLD signal (relative to periods of paced breathing). The source of the CVR BOLD signal is vascular (i.e. non-neuronal). Thus, this task facilitated identification of clusters throughout the brain that differed as a function of active vs. placebo stress. Clusters identified on this task were subtracted from between-session contrasts of interest (see Analysis Strategy section below for a detailed explanation).

3.2.9 Neuroimaging Parameters

All imaging was conducted on a 3 Tesla Siemens Verio system with 32-channel receive-only head coil. High-resolution T_1-weighted structural scans were collected using the 3D MPRAGE sequence with the following parameters: TR = 2.2s, TE = 3ms, TI = 799ms, flip angle = 13°, FOV = 256x256x160mm, 256 x 1mm thick axial slices, matrix = 176 x 256. Prior to ^{1}H fMRS acquisition, a region of the left dlPFC (2.5 x 2.5 x 2.5cm) larger than ^{1}H fMRS voxel was shimmed to improve B_0-field homogeneity (FASTESTMAP). ^{1}H fMRS spectra were continuously acquired every 16s (PRESS with OVS and VAPOR, TE = 23ms, TR = 4.0s, 4 averages/spectrum, bandwidth = 2 kHz, 2048 data points, no apodization) during the letter 2-back task (42 spectra, 672s). ^{1}H fMRS spectra were acquired without water suppression immediately after the task (TE = 23ms, TR = 10s, 2 averages/spectrum, bandwidth = 2 kHz, 2048 data points, no apodization). Unsuppressed water levels were used to scale metabolite levels to absolute concentration values during each task (mmol/kg wet weight). BOLD fMRI data were collected continuously throughout the N-back and CVR tasks using a gradient

echo planar imaging sequence with the following acquisition parameters: TE = 36ms, TR = 2.83s, matrix = 80x80, 40 interleaved slices, voxel size = 2.9mm isotropic.

3.2.10 Choice Task

The choice progressive ratio task was the only opportunity for participants to smoke cigarette puffs (after the 11:30am paced puff procedure) during either experimental session (until after the 4pm discharge). During this task, participants were seated at a computer and could earn (via computer 'mouse' clicking) one puff of their preferred brand of cigarette or a money alternative ($0.25 [amount based on prior study] (Tidey, Higgins, Bickel, & Steingard, 1999)) on 11 independent choice trials. On each trial, the participant was able to earn a cigarette puff, money, or do nothing (not punished). Once an option (cigarette puff vs. money) was selected on each trial, the participant had to satisfy each trial's response requirement (escalating number of mouse clicks for each subsequent trial [progressive ratio schedule]; i.e., 5, 12, 33, 100, 180, 340, 540, 835, 1220, 1660 and 2275 clicks) to earn that unit of the option selected. Participants could earn any combination of cigarette puffs or money that summed to a total of 11 units. After the 30min task, participants were presented with the earned units (money was added to their study payment). Participants were instructed to smoke the exact number of puffs earned (not more or less) at the pace of their choosing. Participants were instructed to inhale 1-2s for each cigarette puff and were video-monitored to verify compliance. Number of puffs earned and smoked during each experimental session is a direct measure of appetitive nicotine motivation and will be referred to as 'nicotine-seeking and self-administration' hereafter. Unbeknownst the participant, the amount of time between cigarette puffs was timed via stopwatch and

mean inter-puff interval (s) was calculated for each experimental session. Inter-puff interval was a direct measure of nicotine consumption rate. Nicotine-seeking and self-administration (appetitive phase) was analyzed separately from nicotine consumption rate (consumptive phase).

3.2.11 Analysis Strategy

^{1}H fMRS Analyses. ^{1}H fMRS spectra were analyzed using LCModel version 6.3 (Provencher, 2008). Post-processing and metabolite quantification steps were 100% automated. Eddy current effects were corrected using the unsuppressed water signal (Klose, 1990). T_1-weighted structural images were B_1 field corrected, the brain image extracted, and segmented into partial volume maps of CSF, grey and white matter using FreeSurfer and FSL tools (e.g. FLIRT, BET, and FAST) (Dale et al., 1999; Smith et al., 2004). Finally, tissue composition within the MRS voxel and appropriate correction factors (e.g. T_1 and T_2 relaxation) were used to calculate the absolute glutamate (GLU) concentration (mmol/kg wet weight) (J. A. Stanley et al., 1995). Two outcome analysis strategies were employed in this study. First, raw spectra were phase- and shift-corrected. Consecutive raw spectra (4 averages, 16s, no apodization or zero-filling) were averaged which resulted in 32s (8 averages) temporal resolution. LCModel fit characteristics demonstrated that this temporal resolution was at the lower limit of reliable GLU quantification. Therefore, a second analysis strategy was used: 64s temporal resolution moving average. 32s resolution spectra from the first approach were averaged across consecutive task blocks (moving average: 64s resolution) to improve signal-to-noise (SNR) and fit reliability. Therefore, spectra collected during first 32s of letter 2-back task block 1 (2-back A) were averaged with spectra collected during

first 32s of letter 2-back task block 2 (2-back A; and so on for 2-back B and rest). Mean metabolite levels during 2-back task were contrasted with interleaved fixation-cross rest. The metabolite of interest for this study was GLU. However, other metabolites (NAA, Myo-Inositol, GPC+PC, and PCr+Cr) were also analyzed to determine the neurochemical specificity of working memory task modulation.

^{1}H fMRS voxel overlap was quantified using the avp_overlap script (Woodcock et al., 2017). 3D Geometric voxel overlap percentage was calculated between each subject's voxel and the template voxel (i.e. accuracy), and across all subjects (i.e. reliability).

fMRI Analyses. Statistical Parametric Mapping (SPM) version 8 software was used to process the raw fMRI data. Raw data were slice time-corrected, motion-corrected, high-pass filtered (128Hz), coregistered to the Montreal Neurologic Institute (MNI) template space, spatially-smoothed (6mm Gaussian kernel), and resliced (2mm isotropic) prior to outcome analyses. First-level contrast maps (e.g. 1-back smoking cued > 1-back neutral cued; within-subject) were submitted to group-level, random-effects analyses (FTND included as a covariate) and cluster-level corrected (AFNI 3dClustSim; $p < .05$). FTND was included as a covariate for three reasons: 1) chronic cigarette smoking has known vascular effects and thus could alter the BOLD signal, 2) chronic cigarette smoking could alter smoking cue salience and thus BOLD response, and 3) to be consistent with the analysis strategy used for other variables. Regions of interest included: ventrolateral [vl] PFC (Brodmann areas 44 and 45), dlPFC (Brodmann Area 46), dPFC (Brodmann area 9), dorsal anterior cingulate (dACC), mOFC, mPFC, striatum, insula and amygdala. Within an experimental session, clusters

that survived cluster-level correction were considered significant and interpreted. For comparisons between experimental sessions (active vs. placebo stress), an additional analysis step was implemented. First-level CVR contrast maps (breath hold > paced breathing) were submitted to group-level, random-effects analyses. Between-session CVR contrasts (active > placebo stress and placebo > active stress) were saved as thresholded maps (voxel-level; $p < .05$). Using ImCalc in SPM8, CVR between-session difference maps were subtracted from cluster-level corrected between-session contrasts of interest (e.g. active > placebo stress: 1-back smoking image > 1-back neutral image) to remove regions that exhibited vascular reactivity differences as a function of active vs. placebo stress. This approach reduced the likelihood of false positive clusters (i.e. removed clusters attributed to vascular effects [non-neuronal] of the stress manipulation) for between-session contrasts of interest.

^{1}H fMRS vs. fMRI comparison. Parameters for the ^{1}H fMRS and fMRI letter 2-back tasks were identical which enabled an exploratory comparison of ^{1}H fMRS GLU levels and fMRI BOLD response. First, each subject's ^{1}H fMRS voxel was recreated in subject space then coregistered to the SPM template brain. Next, the ^{1}H fMRS voxel was used as a mask for first-level BOLD contrasts (letter 2-back > fix cross rest) at the same temporal resolution as ^{1}H fMRS (32s; 2-back A and B). Z scores (peak activation) and peak cluster extents were extracted for each subject and correlated with GLU levels during letter 2-back task performance. fMRI metrics (Z score and cluster extents) were compared with ^{1}H fMRS GLU levels for 2-back A and B for each task repetition (first ^{1}H fMRS task block was excluded; practice effects) using bivariate Pearson correlations. The analysis space consisted of a correlation matrix with 32 cells (4 fMRI

2-back blocks X 8 ^{1}H fMRS 2-back blocks) for both Z scores and cluster extents for each of the placebo and stress sessions. For this exploratory analysis only, the statistical threshold was $p \leq .10$.

All self-report, behavioral, physiological and neurochemical data were evaluated for missing data, extreme values, and normality (Shapiro-Wilk test of normality; skewness and kurtosis statistics > 1.5) (West, Finch, & Curran, 1995). Ordinal and continuous variable distributions were normalized with statistical transformations ($\log_{10}$) or winsorization (extreme values) prior to outcome analyses. Ordinal or continuous variables measured at only one time point were evaluated using one-way ANOVA, Pearson bivariate correlations, or linear regression. Ordinal or continuous variables collected repeatedly across multiple time points (e.g. physiological, periodic self-report, N-back behavioral data, and neurochemistry) were evaluated using rmANOVA. Follow-up paired t-tests evaluated differences for any significant rmANOVA main effects. Sphericity was verified (Mauchly's test of sphericity) prior to rmANOVA analyses. Categorical variables were evaluated using Chi-Square test of independence. FTND score was evaluated as a covariate for all outcome variables (only included in analytic models when significant). Descriptive statistics are presented as mean ± one standard deviation (M ± 1 SD) unless otherwise noted. In figures, error bars represent ± one standard error of the mean (SEM) unless otherwise noted. The threshold for statistical significance was $p \leq .05$.

CHAPTER 4 RESULTS

4.1 ^{1}H fMRS Pilot Study

4.1.1 Sample Characteristics

The modal participant was a 24 year old (± 3.4 yrs; range: 19-30 yrs) Caucasian or Asian (50% each) male (56.3%). The sample consisted of cognitively-normal and psychiatrically-healthy college-educated participants not currently taking psychoactive medications. All participants were right hand dominant.

4.1.2 Voxel Overlap

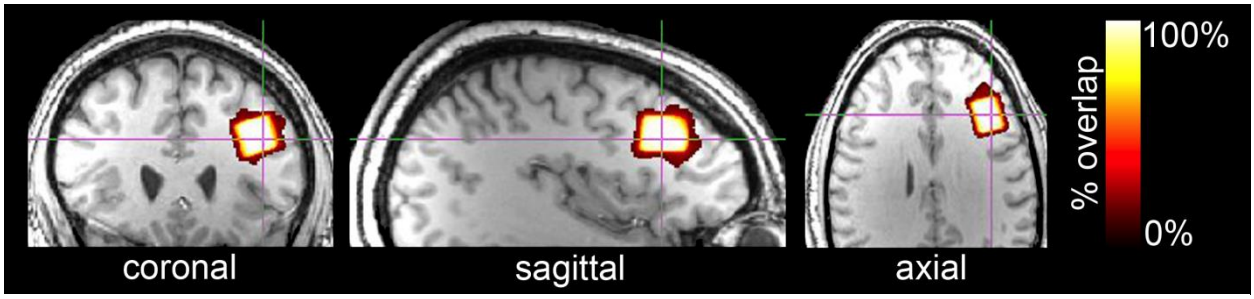

Figure 4.1: ^{1}H fMRS Pilot Study Voxel Overlap. Participant voxel placement (N=16) was coregistered to template space and orthonormal views depict geometric voxel overlap. Percentage of geometric voxel overlap is indicated by color: white indicates voxel space with complete overlap, yellow/red indicate incomplete overlap, across all subjects.

AVP was used to prescribe each participant's voxel location (less one subject due to experimenter error; manual placement). Voxel placement was highly accurate (mean percent geometric overlap with the template voxel = 92.3 ± 4.7%) and reliable (mean percent geometric overlap across all participants = 89.9%) across all participants (Figure 4.1) (Woodcock et al., 2017). Mean (± one SD) voxel tissue composition was 36.8 ± 3.8% gray and 60.8 ± 4.5% white matter. Voxel placement was less accurate for the one subject without AVP (manual placement: 77.7% vs. AVP: 86.2-96.9%).

4.1.3 Behavioral Data

Behavioral data demonstrated task compliance (mean correct: 94.8% ± 10.7%; mean reaction time: 644 ± 171ms). rmANOVA indicated that task performance increased across blocks (Time effect; $F(6,90) = 2.39$, $p < .05$, from 88.5% in block 1 to 96.9% in block 7; Figure 4.2). Reaction time non-significantly decreased across blocks ($F(6,90) = 1.90$, $p = .09$, from 697ms in block 1 to 638ms in block 7; Figure 4.3).

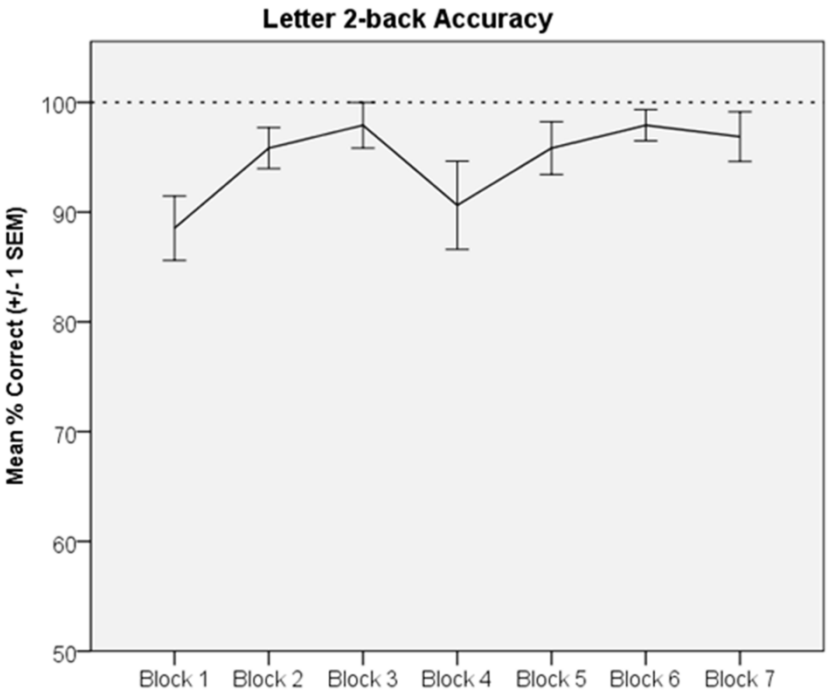

Figure 4.2: Letter 2-back Response Accuracy. Mean response accuracy (% correct) is depicted across task blocks (± 1 SEM).

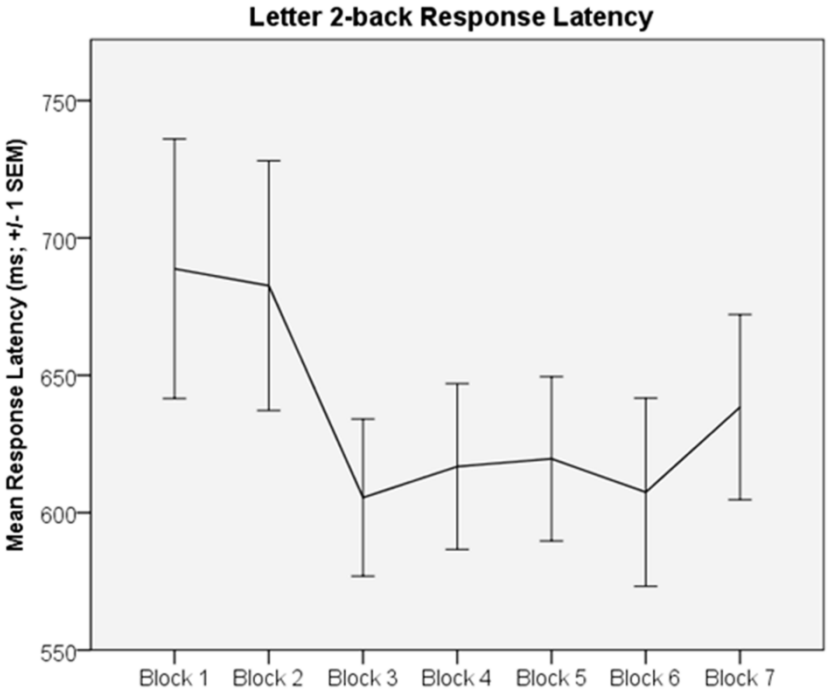

Figure 4.3: Letter 2-back Response Latency. Mean response latency (s) is depicted across task blocks (± 1 SEM).

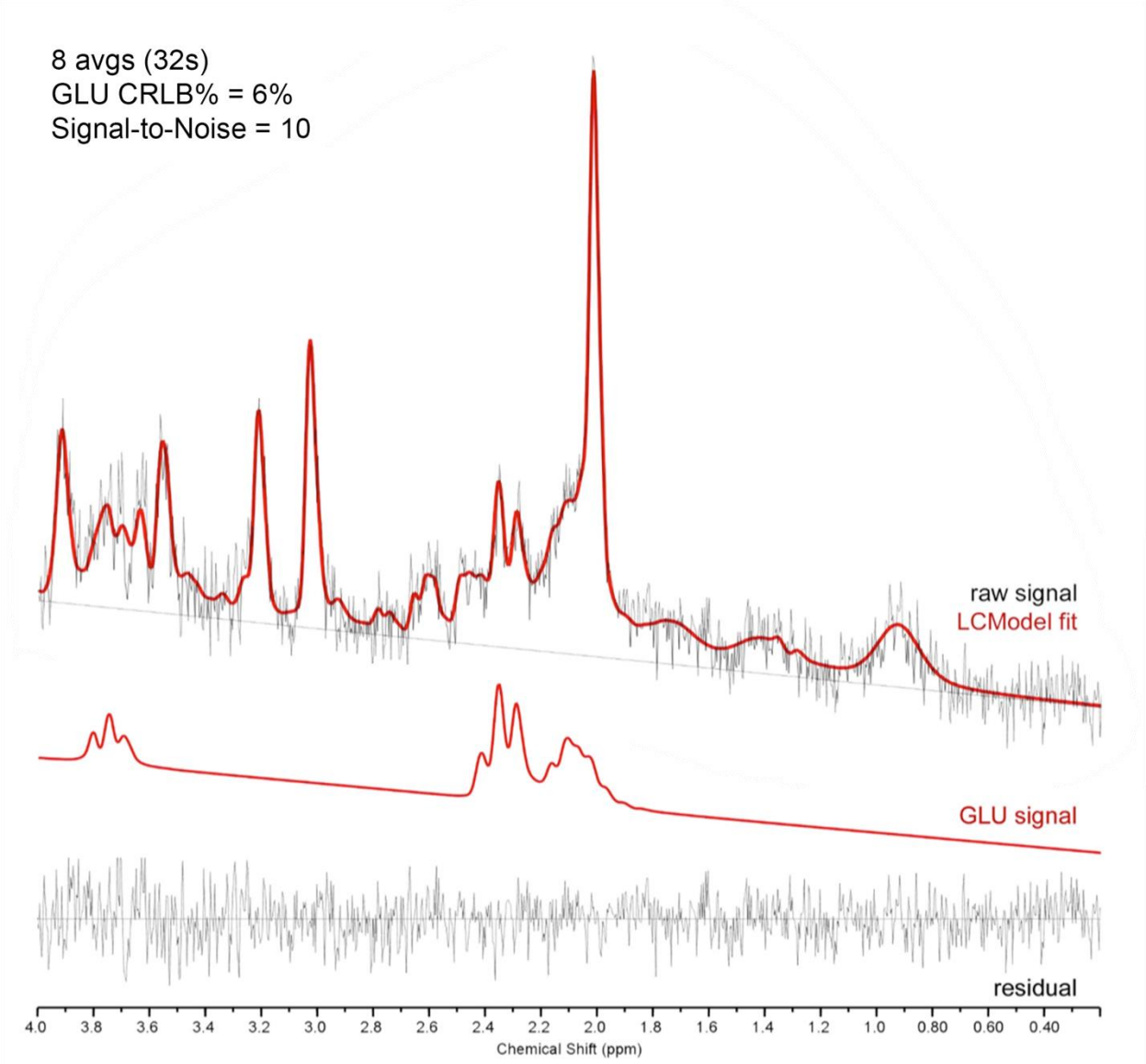

Figure 4.4: LCModel Fit of Representative Spectrum. A representative quality ^{1}H fMRS spectrum (32s temporal resolution; 8 avgs) is depicted. The raw (black line) and LCModel fit (red line) signal are displayed above the estimated spectral peaks for GLU (red line). At the bottom of the figure, the residual signal (black line; i.e. noise) and chemical shift (ppm) are displayed.

4.1.4 LCModel Fit Characteristics

LCModel fit reliability was evaluated for continuous fixation-cross rest, letter 2-back A (first 32s of each task block), letter 2-back B (final 32s of each task block), and interleaved fixation-cross rests (between 2-back task blocks). Importantly, LCModel fit characteristics did not differ as a function of 2-back vs. rest (Time and Task X Time

LCModel Fit Characteristic	2-back A	2-back B	Interleaved Rest	Continuous Rest	2-back vs. Rest (*p*)
GLU CRLB %	6.8 ± 0.9	6.9 ± 0.9	6.8 ± 0.7	7.1 ± 0.9	> .19
GLN CRLB %	23.3 ± 4.1	23.4 ± 3.7	22.9 ± 3.0	23.2 ± 4.0	> .50
FWHM Hz	4.9 ± 1.0	4.9 ± 1.0	5.0 ± 1.0	4.9 ± 0.9	> .10
SNR	12.0 ± 1.9	12.1 ± 2.0	11.8 ± 1.7	11.7 ± 1.9	> .13

Table 4.1: LCModel Fit Characteristics. Mean (± 1 SD) LCModel fit characteristics are presented by task phase. GLU = glutamate; GLN = glutamine; FWHM = full-width half-maximum; SNR = signal-to-noise; CRLB = Cramer Rao Lower Bound.

effects examined; *p*s > .10; see Table 4.1). A representative spectrum and LCModel estimation of GLU levels are depicted in Figure 4.4.

4.1.5 GLU Modulation

Flashing checkerboard reduced GLU level fluctuation (mean coefficient of variation percentage = 4.6%) prior to 2-back (vs. rest) modulation.

2-back A vs. rest. GLU levels during 2-back A (first 32s of task performance across task blocks) were compared to continuous and interleaved fixation-cross rest (Figure 4.5). Overall, GLU levels during 2-back A were significantly higher (3.4%) than continuous fixation-cross rest ($F(1,111) = 6.26$, $p < .05$, partial $\eta^2 = 0.05$ [small-to-moderate effect size]; 12.07 ± 0.85 vs. 11.75 ± 1.00, respectively). Overall 2-back A GLU levels did

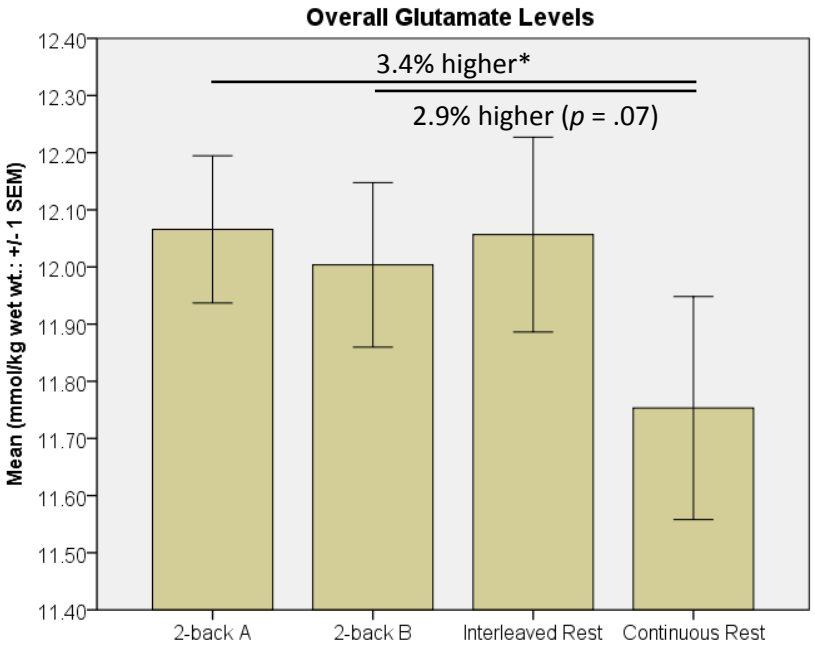

Figure 4.5: Overall GLU Levels. Mean (± 1 SEM) GLU levels for each task phase are depicted. Paired t-test: *$p < .05$

not differ from interleaved fixation-cross rest (p = .92; 12.07 ± 0.85 vs. 12.06 ± 1.04, respectively).

Relative to continuous fixation-cross rest, rmANOVA indicated a significant Time effect ($F(6,90)$ = 3.35, p < .01, partial η^2 = 0.18 [moderate-to-large effect size]) as GLU levels increased across task blocks (Figure 4.6). Task (2-back A vs. rest) and Time X Task interaction effects were non-significant (ps > .20).

Relative to interleaved fixation-

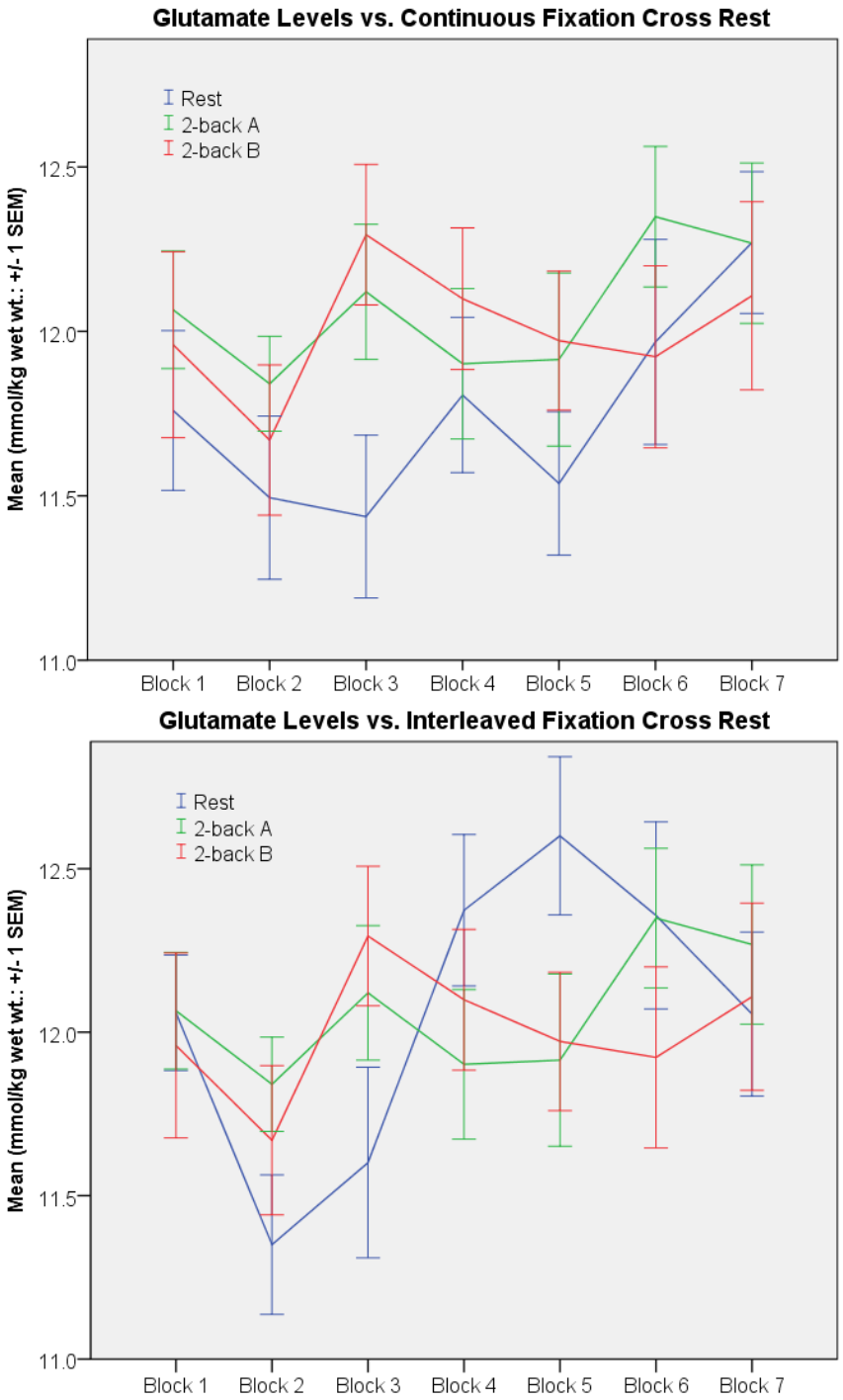

Figure 4.6 & 4.7: GLU Levels across Task Blocks. Mean (± 1 SEM) 2-back GLU levels vs. continuous fixation-cross (upper panel) and interleaved fixation-cross (lower panel) are depicted across task blocks.

cross rest, rmANOVA indicated significant Time ($F(6,90) = 2.78$, $p < .05$, partial $\eta^2 = 0.16$ [moderate-to-large effect size]) and Time X Task interaction effects ($F(6,90) = 2.95$, $p < .05$, partial $\eta^2 = 0.16$ [moderate-to-large effect size]; Figure 4.7). The Task effect was not significant ($p = .52$). The Time effect indicated that GLU levels increased across task blocks. The Time X Task interaction confirmed that GLU levels were significantly higher (4.4%) than interleaved rest during task blocks 2 and 3 ($F(1,31) = 8.49$, $p < .01$,

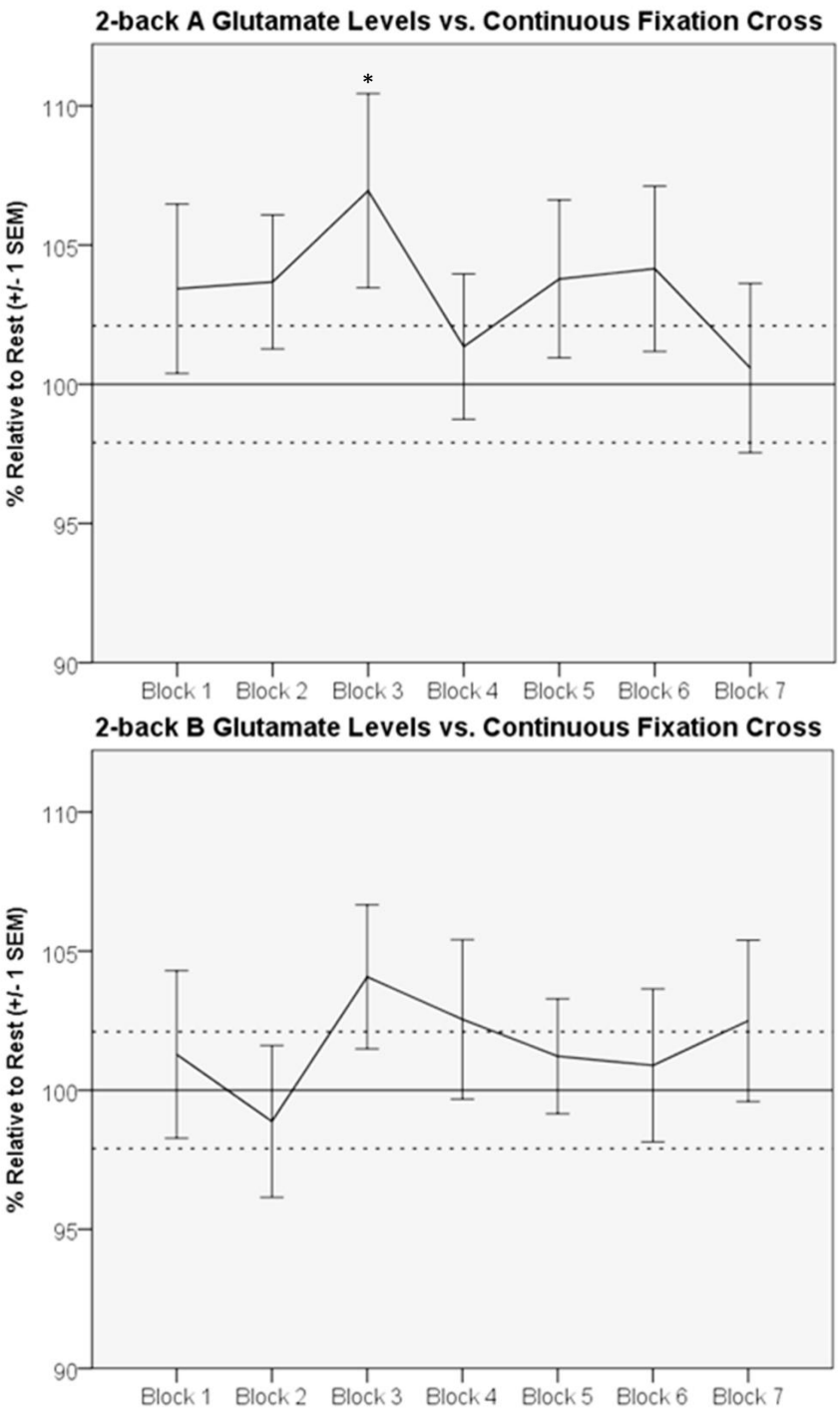

Figure 4.8 & 4.9: 2-back A & B GLU Levels vs. Continuous Fixation Cross. Mean (± 1 SEM) 2-back A (upper panel) and B (lower panel) GLU levels (% relative to continuous fixation cross) are depicted across task blocks. Paired t-test: *$p < .05$, **$p < .01$

partial η^2 = 0.22 [moderate-to-large effect size]; 11.98 ± 0.71 vs. 11.48 ± 1.01, respectively; Figure 4.10), and significantly lower (4.8%) during task blocks 4 and 5 ($F(1,31) = 12.39$, $p < .001$, partial $\eta^2 = 0.29$ [large effect size]; 11.91 ± 0.97 vs. 12.49 ± 0.94, respectively).

2-back B vs. rest. Overall GLU levels during 2-back B (final 32s of task performance across task blocks) were non-significantly higher (2.9%) than continuous fixation-cross rest ($F(1,111) = 3.28$, $p = .07$, partial $\eta^2 = 0.03$ [small-to-moderate effect size]; 12.00 ± 0.98

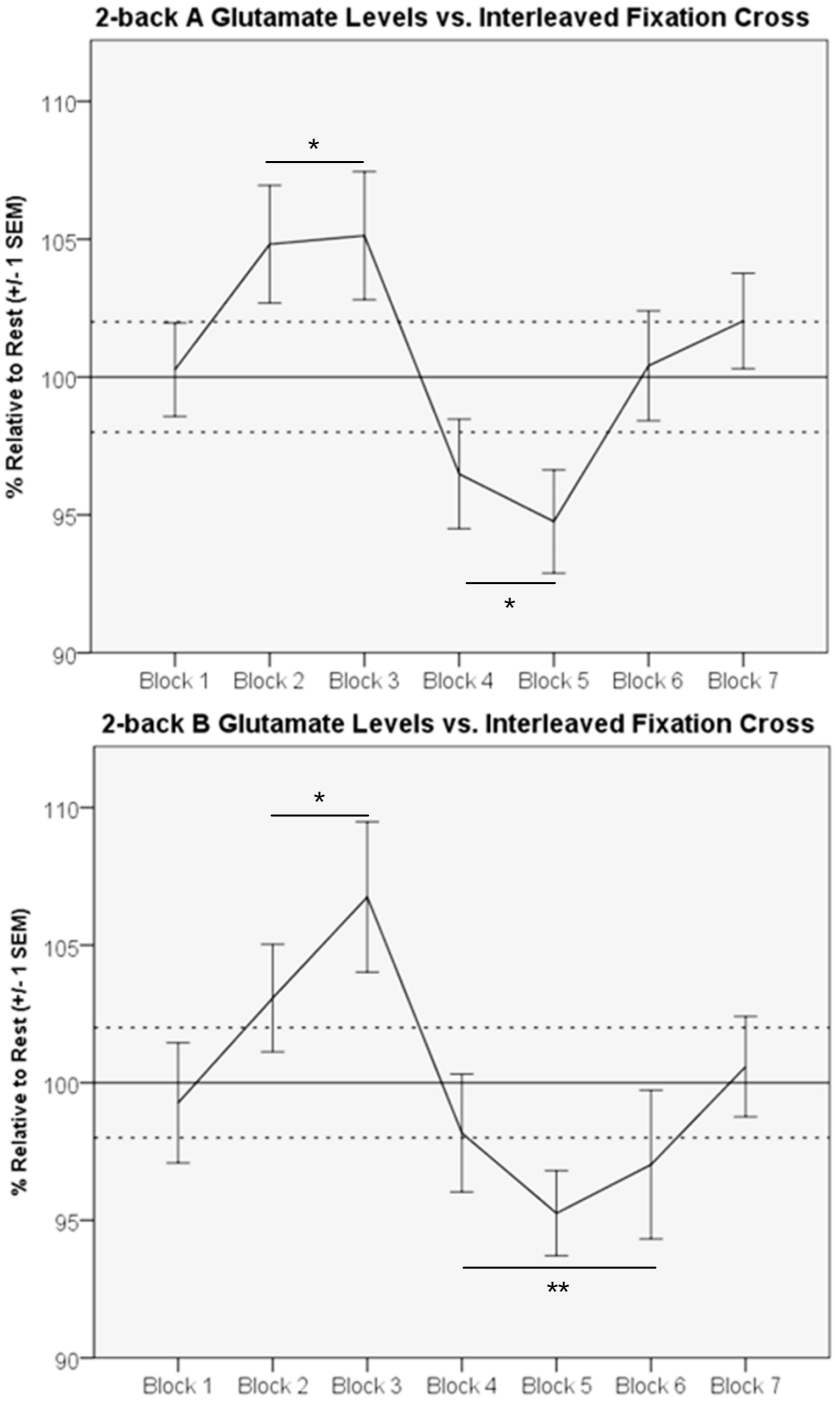

Figure 4.10 & 4.11: 2-back A & B GLU Levels vs. Interleaved Fixation Cross. Mean (± 1 SEM) 2-back A (upper panel) and B (lower panel) GLU levels (% relative to interleaved fixation cross) are depicted across task blocks. Paired t-test: *$p < .05$, **$p < .01$

vs. 11.75 ± 1.00, respectively; Figure 4.5). Overall GLU levels during 2-back B did not differ from interleaved fixation-cross rest (p = .61; 12.00 ± 0.98 vs. 12.06 ± 1.04, respectively).

Relative to continuous fixation-cross rest, rmANOVA indicated a non-significant Time effect ($F(6,165) = 2.08$, p = .06; partial $\eta^2 = 0.12$ [moderate-to-large effect size]) as GLU levels increased across task blocks (Figure 4.6). Task (2-back B vs. rest) and Time X Task interaction effects were non-significant (ps > .20).

Relative to interleaved fixation-cross rest, rmANOVA indicated significant Time ($F(6,90) = 3.14$, $p < .01$, partial $\eta^2 = 0.17$ [moderate-to-large effect size]) and Time X Task interaction effects ($F(6,90) = 3.71$, $p < .01$, partial $\eta^2 = 0.20$ [moderate-to-large effect size]; Figure 4.10). The Task effect was not significant (p = .91). The Time effect indicated that GLU levels increased across task blocks (Figure 4.7). The Time X Task interaction indicated that GLU levels were significantly higher (4.4%) than interleaved rest during task blocks 2 and 3 ($F(1,31) = 7.28$, $p < .05$, partial $\eta^2 = 0.19$ [moderate-to-large effect size]; 11.98 ± 0.93 vs. 11.48 ± 1.01, respectively; Figure 4.11), and significantly lower (3.6%) during task blocks 4, 5, and 6 ($F(1,47) = 8.74$, $p < .01$, partial $\eta^2 = 0.16$ [moderate-to-large effect size]; 12.00 ± 0.93 vs. 12.44 ± 1.00, respectively).

4.1.6 BOLD Effect

Prior ^{1}H fMRS studies found a significant BOLD effect as a function of task vs. rest (Mangia et al., 2006; Schaller et al., 2013; Schaller et al., 2014). Increased concentration of oxygenated blood in task-active brain regions (i.e. BOLD effect) can reduce spectral linewidth (FWHM). Relative to continuous fixation-cross rest, rmANOVA revealed FWHM did not significantly differ as a function of 2-back A or B (Task ps > .80;

Time X Task interaction *p*s > .07). Relative to interleaved fixation-cross rest, rmANOVA indicated that FWHM did not significantly differ as a function of 2-back A or B (Task *p*s > .10; Time X Task interaction *p*s > .40).

4.1.7 Neurochemical Specificity

Metabolites other than GLU (Myo-Inositol, GPC+PC, PCr+Cr, and NAA) were examined as a function of experimental task. During 2-back A, no metabolites (other than GLU) differed as a function of task. However, during 2-back B, rmANOVA indicated Time X Task interaction effects for Myo-Inositol and NAA ($F(6,90) = 2.57$, $p < .05$ and $F(6,90) = 2.28$, $p < .05$, respectively). Myo-Inositol and NAA levels were higher during 2-back B than interleaved fixation-cross rest in the first few task blocks, but converged in later task blocks. GPC+PC and PCr+Cr did not differ significantly as a function of task during 2-back A or B (*p*s > .05).

4.2 Dissertation Study

4.2.1 Sample Characteristics

The modal participant was 28 (± 3.9) years old (range: 21-34 years), male (85.7%), and African-American (71.4%). Participants (N = 21) reported smoking 17.2 ± 5.9 cigarettes/day and were moderately nicotine dependent (FTND = 6.1 ± 2.0). Sample characteristics are described in detail in Table 4.2.

Sample Characteristics	M ± 1 SD or %
Smoking (cigarettes/day)	17.2 ± 5.9
Age at first cigarette	16.5 ± 3.5
Menthol cigarette (%)	85.7%
FTND	6.1 ± 2.0
Age (yrs)	28.0 ± 3.9
Gender (% Male)	85.7%
Race (% African-American)	66.7%
Body Weight (lbs)	193.2 ± 42.6
Education (yrs)	13.1 ± 2.4
Employed (%)	76.2%
Alcohol use (days/month)	3.8 ± 4.9
Marijuana use (days/month)	4.3 ± 5.4
BIS Total (range: 0-90)	29.3 ± 11.4
Distress Tolerance (range: 1-5)	3.9 ± 0.5
Trait Anxiety (range: 20-80)	33.4 ± 5.7
Stress Mindset (range: 0-4)	2.0 ± 0.5

Table 4.2: Dissertation Sample Characteristics.

4.2.2 Physiological Effects

Physiological and periodic self-report measurements from the first time point of each session (11:20am; prior to experimental nicotine exposure control [paced puff procedure]) were excluded from analyses for the following reasons. Participant data were highly variable at the initial time point, which suggested external factors influenced participant physiology and self-report

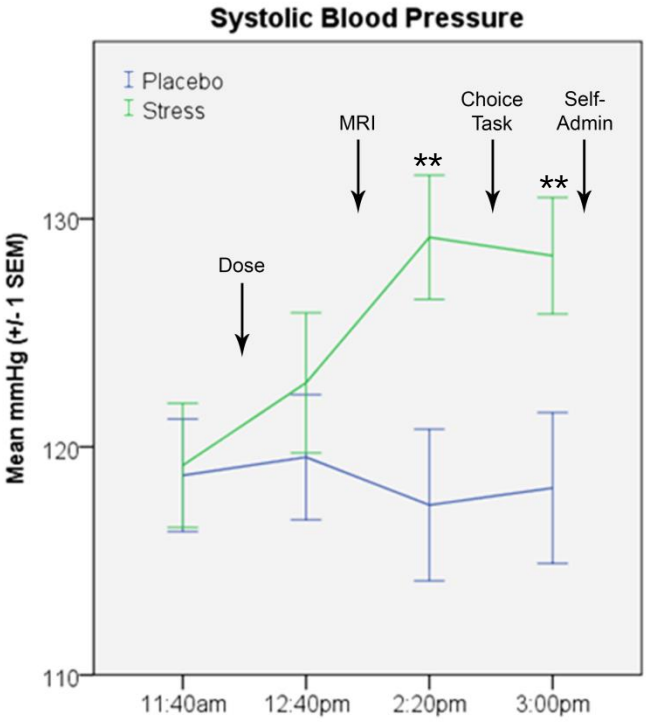

Figure 4.12: Systolic Blood Pressure. Mean (± 1 SEM) systolic blood pressure (mmHg) is depicted for active (green line) and placebo stress sessions (blue line). Approximate experimental procedure timing is noted with arrows. Paired t-test: *$p \leq .05$; **$p < .01$

responses. Moreover, several participants reported they did not have access to cigarettes in the morning before the start of the experimental session (and were in mild nicotine withdrawal). Acclimation to the experimental setting and experimental control for recent nicotine exposure established a more stable baseline measurement. Therefore, only the final four time points for physiological indices and the periodic self-report battery were included in outcome analyses.

Blood pressure. As a function of time point and experimental condition (active vs. placebo stress), rmANOVA indicated that systolic BP (mmHg) exhibited significant Time ($F(3,57) = 4.14$, $p < .01$; partial $\eta^2 = 0.18$ [moderate-to-large effect size]), Dose ($F(1,19) = 10.31$, $p < .01$; partial $\eta^2 = 0.35$ [large effect size]), and Time X Dose interaction effects ($F(3,57) = 8.33$, $p < .001$; partial $\eta^2 = 0.31$ [large effect size]; Figure 4.12). YOH+HYD significantly increased systolic BP for 2+ hours throughout the remainder of the stress session. At peak YOH+HYD effects, systolic BP was ~11.5 mmHg higher during active vs. placebo stress (128.8 mmHg vs. 117.5 mmHg). FTND was not significantly related to systolic BP (*p*s > .20).

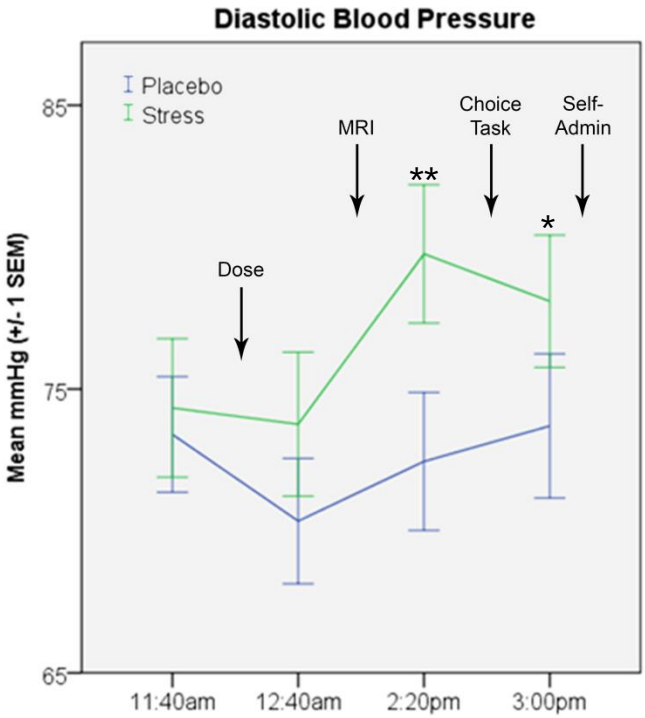

Figure 4.13: Diastolic Blood Pressure. Mean (± 1 SEM) diastolic blood pressure (mmHg) is depicted for the active stress (green line) and placebo sessions (blue line). The approximate timing of each experimental procedure is noted with arrows. Paired t-test: *$p \leq .05$; **$p < .01$

rmANOVA indicated that diastolic BP (mmHg) exhibited significant Time ($F(3,57) = 5.88$, $p < .001$; partial $\eta^2 = 0.24$ [large effect size]), Dose ($F(1,19) = 6.65$, $p < .05$; partial $\eta^2 = 0.26$ [large effect size]), and Time X Dose interaction effects ($F(3,57) = 2.98$, $p < .05$; partial $\eta^2 = 0.14$ [moderate-to-large effect size]) as a function of time point and experimental condition (Figure 4.13). YOH+HYD significantly increased diastolic BP for 2+ hours throughout the remainder of the stress session. At peak effects, diastolic BP was ~7 mmHg higher during active vs. placebo stress (79.6 mmHg vs. 72.5 mmHg). FTND was not significantly related to diastolic BP (*p*s > .25).

Heart rate. rmANOVA indicated that HR (bpm) exhibited non-significant Time ($F(3,57) = 2.58$, $p = .06$; partial $\eta^2 = 0.12$ [moderate-to-large effect size]) and Dose effects ($p = .42$), but there was a significant Time X Dose interaction ($F(3,57) = 3.38$, $p < .05$; partial $\eta^2 = 0.15$ [moderate-to-large effect size]; Figure 4.14). HR decreased significantly over time during the placebo session ($F(3,57) = 3.92$, $p < .01$; partial $\eta^2 = 0.09$ [moderate effect size]), but not the active stress session ($p = .55$). At peak YOH+HYD effects, HR was ~4 bpm faster during active vs. placebo stress (77.8 bpm

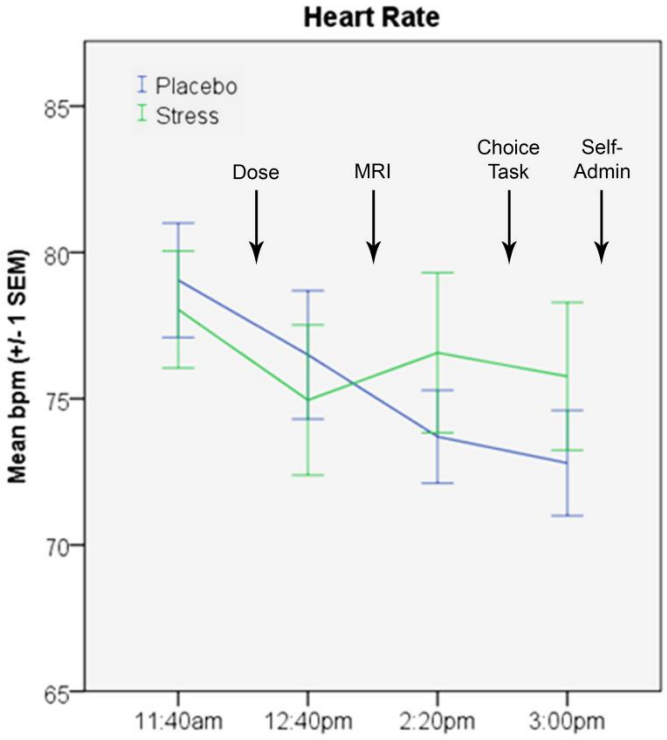

Figure 4.14: Heart Rate. Mean (± 1 SEM) heart rate (bpm) is depicted for the active stress (green line) and placebo sessions (blue line). The approximate timing of each experimental procedure is noted with arrows.

vs. 73.7 bpm). FTND was not significantly related to HR (*p*s > .35).

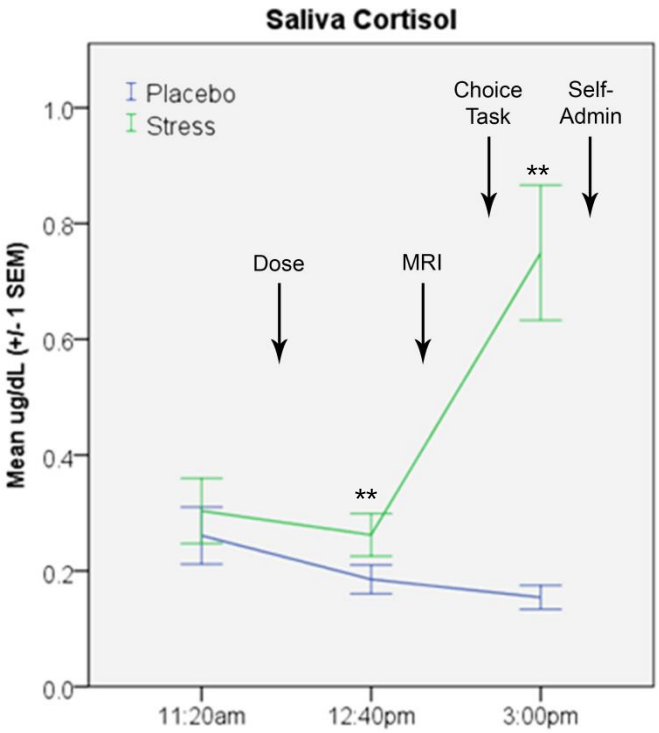

Figure 4.15: Saliva Cortisol. Mean (± 1 SEM) saliva cortisol (ug/dL) is depicted for the active stress (green line) and placebo sessions (blue line). The approximate timing of each experimental procedure is noted with arrows. Paired t-test: *$p \leq .05$; **$p < .01$

Saliva cortisol. Due to budget restrictions, saliva biomarker data (cortisol and α-amylase) were only analyzed at three time points (baseline, after YOH+HYD dosing but prior to the MRI scan, and after the puff/money choice task but prior to earned nicotine self-administration). rmANOVA indicated that saliva cortisol (ug/dL; log_{10}-transformed) exhibited significant Time ($F(2,38) = 13.59$, $p < .001$; partial $\eta^2 = 0.42$ [very large effect size]), Dose ($F(1,19) = 29.14$, $p < .001$; partial $\eta^2 = 0.61$ [very large effect size]), and Time X Dose interaction effects ($F(2,38) = 25.13$, $p < .001$; partial $\eta^2 = 0.57$ [very large effect size]; Figure 4.15). YOH+HYD significantly increased saliva cortisol levels for 2+ hours throughout the remainder of the stress session. At peak YOH+HYD effects, saliva cortisol level was ~4x higher during active vs. placebo stress session. FTND was not significantly related to saliva cortisol level (*p*s > .40).

Saliva α-amylase. rmANOVA indicated that saliva α-amylase (U/mL) exhibited a significant Time effect ($F(2,38) = 4.50$, $p < .05$; partial $\eta^2 = 0.19$ [moderate-to-large effect size]), but non-significant Dose ($p = .57$) and Time X Dose interaction effects (p =

.13; Figure 4.16). Saliva α-amylase levels increased significantly over time during the active stress session ($F(2,38) = 5.02$, $p < .05$; partial $\eta^2 = 0.21$ [moderate-to-large effect size]), but not the placebo session ($p = .25$). At peak YOH+HYD effects, saliva α-amylase level was 28.7% higher during active vs. placebo stress session. FTND was not significantly related to saliva α-amylase level (*p*s > .20).

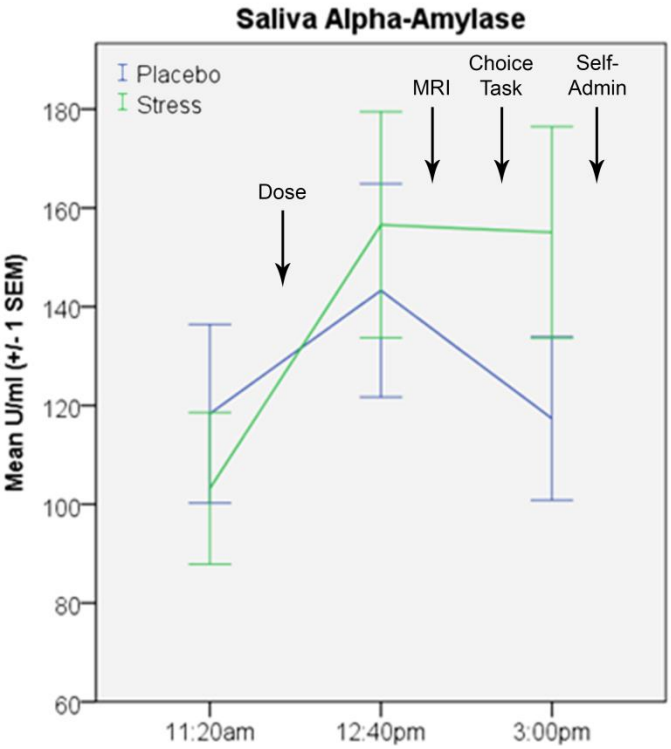

Figure 4.16: Saliva α-Amylase. Mean (± 1 SEM) saliva α-amylase (U/ml) is depicted for the active stress (green line) and placebo sessions (blue line). The approximate timing of each experimental procedure is noted with arrows.

4.2.3 Magnitude of Stress Manipulation

The magnitude of the physiological stress response was an important experimental design consideration. If the YOH and HYD doses induced physiological responses beyond a naturalistic level, the generalizability of study findings might be limited. Thus, to provide context for the magnitude of the physiological effects described above, the observed pharmacological stress data were qualitatively compared with published studies that used psychosocial stress manipulations.

With regard to saliva cortisol (biomarker of HPA axis response), a meta-analysis of psychosocial stress manipulations and saliva cortisol response was examined (Dickerson & Kemeny, 2004). A robust psychosocial stress manipulation (public

speaking + cognitive tasks) used in 23 different studies conducted in the afternoon (consistent with the present study; an important consideration because of the diurnal rhythm of cortisol) was associated with a large effect on saliva cortisol (Cohen's *d* = 1.09). Similarly, peak saliva cortisol response to YOH+HYD was also a large effect (Cohen's *d* = 1.61). With regard to cardiovascular biomarkers, a recent study of 102 cigarette smokers was selected for comparison (Ginty et al., 2014). A similar psychosocial stress manipulation (public speaking + cognitive tasks) exhibited large effects on systolic BP and HR (Cohen's *d* = 1.18 and 1.53, respectively) (Ginty et al., 2014). In the present study, YOH+HYD was associated with a comparable peak effect on systolic BP (Cohen's *d* = 1.17; range = 0.96-1.37) and smaller effect on HR (Cohen's *d* = 0.26; range = 0.19-0.32). Collectively, these qualitative comparisons demonstrated the magnitude of physiological stress response induced by oral pretreatment with 54mg YOH and 10mg HYD was comparable to a robust psychosocial stress manipulation.

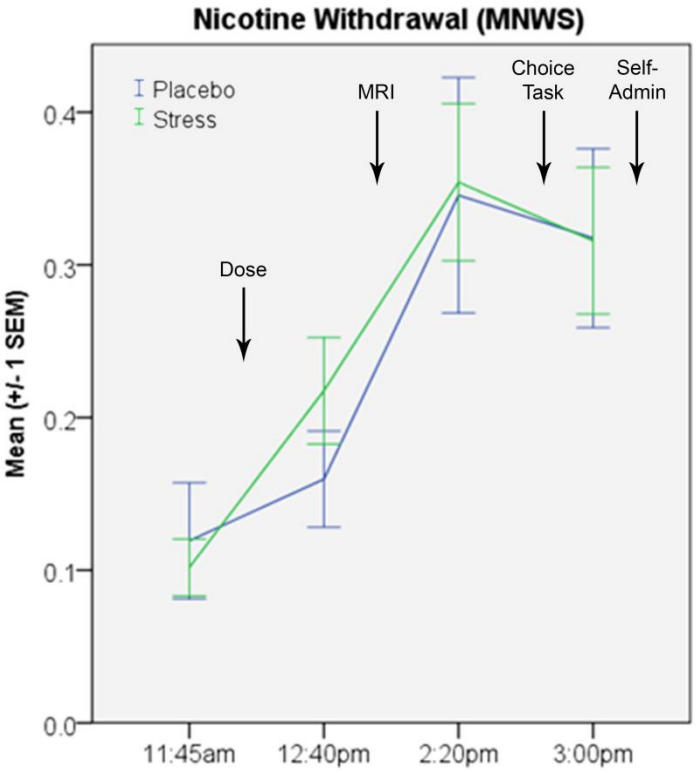

Figure 4.17: Nicotine Withdrawal. Mean (± 1 SEM) self-reported nicotine withdrawal symptom severity is depicted for the active stress (green line) and placebo sessions (blue line). The approximate timing of each experimental procedure is noted with arrows.

4.2.4 Subjective Effects

Nicotine withdrawal. Nicotine withdrawal symptoms were

measured via self-report (MNWS) as part of the periodic self-report battery. rmANOVA indicated that nicotine withdrawal exhibited a significant Time effect ($F(3,54) = 18.15$, $p < .001$; partial $\eta^2 = 0.50$ [very large effect size]), but non-significant Dose ($p = .83$) and Time X Dose interaction effects ($p = .67$; Figure 4.17). Nicotine withdrawal symptoms increased significantly throughout each experimental session, but did not differ as a function of active vs. placebo stress. Mean nicotine withdrawal severity was 'slight' or 'mild' at peak levels. FTND was not significantly related to nicotine withdrawal (*p*s > .06).

Appetitive cigarette craving. Appetitive craving was measured via self-report (QSU) as part of the periodic self-report battery.

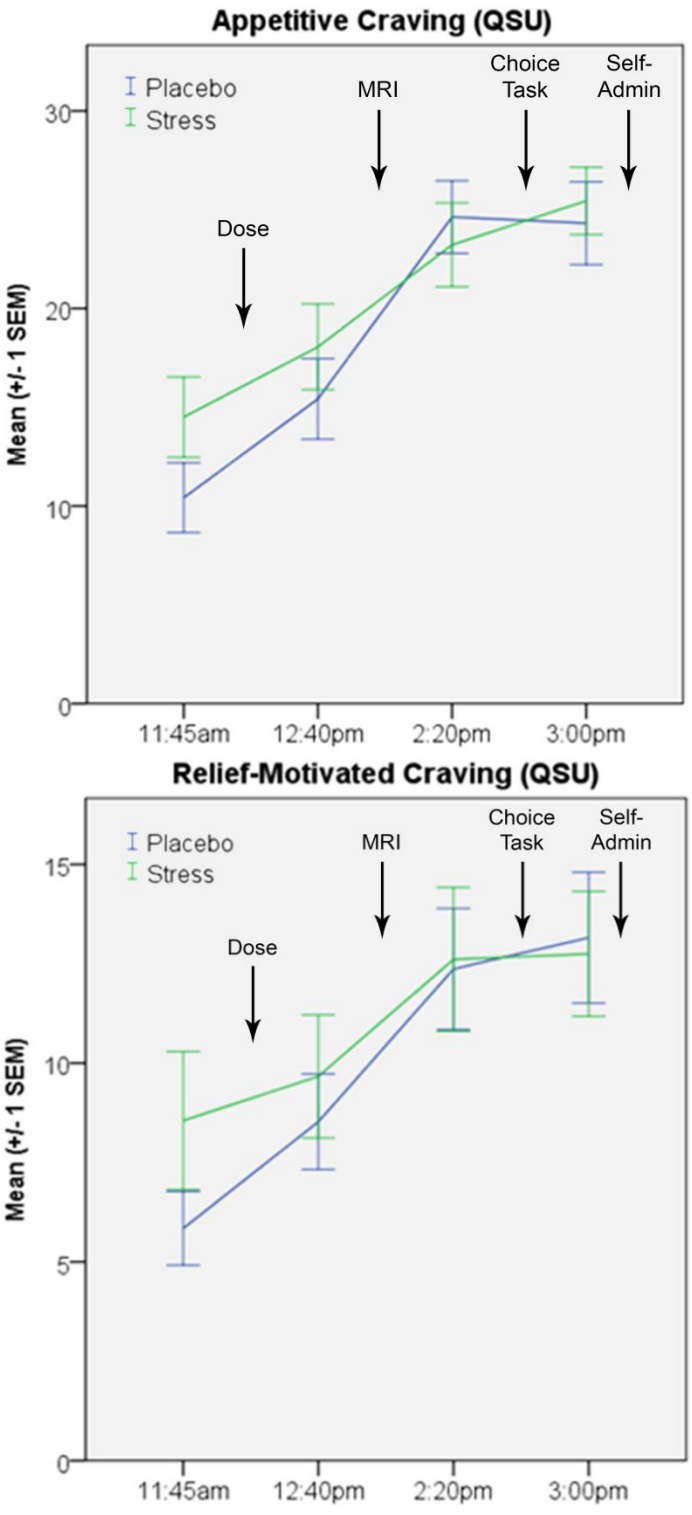

Figures 4.18 & 4.19: Appetitive and Relief-Motivated Cigarette Craving. Mean (± 1 SEM) self-reported appetitive (upper panel) and relief-motivated (lower panel) cigarette craving is depicted for the stress (green line) and placebo sessions (blue line). The approximate timing of each experimental procedure is noted with arrows.

rmANOVA indicated that appetitive craving exhibited a significant Time effect ($F(3,51) = 34.02$, $p < .001$; partial $\eta^2 = 0.67$ [very large effect size]), but non-significant Dose ($p = .62$) and Time X Dose interaction effects ($p = .12$; Figure 4.18). Appetitive cigarette craving increased significantly throughout each experimental session, but did not differ as a function of active vs. placebo stress. At peak levels, appetitive cigarette craving was 'moderate' to 'substantial.' FTND was not significantly related to appetitive craving (ps > .20).

Relief-motivated cigarette craving. Relief-motivated craving was measured via self-report (QSU) as part of the periodic self-report battery. rmANOVA indicated that relief-motivated craving ($\log_{10}$-transformed) exhibited a significant Time effect ($F(3,51) = 25.31$, $p < .001$; partial $\eta^2 = 0.60$ [very large effect size]), but non-significant Dose ($p = .77$) and Time X Dose interaction effects ($p = .18$; Figure 4.19). Relief-motivated cigarette craving increased significantly throughout each experimental session, but did not differ as a function of active vs. placebo stress. At peak levels, relief-motivated cigarette craving was 'moderate' to 'substantial.' FTND was not significantly related to relief-motivated craving (ps > .30).

Anxiety. Anxiety levels were measured via self-report (STAI; state version) as part of the periodic self-report battery. rmANOVA indicated that anxiety exhibited a significant Time effect ($F(3,54) = 8.61$, $p < .001$; partial $\eta^2 = 0.32$ [large effect size]), but non-significant Dose ($p = .49$) and Time X Dose interaction effects ($p = .81$; Figure 4.20). Anxiety levels decreased significantly throughout each experimental session, but did not differ as a function of active vs. placebo stress. At peak levels (baseline),

participants reported they were 'somewhat' anxious. FTND was not significantly related to anxiety (*p*s > .15).

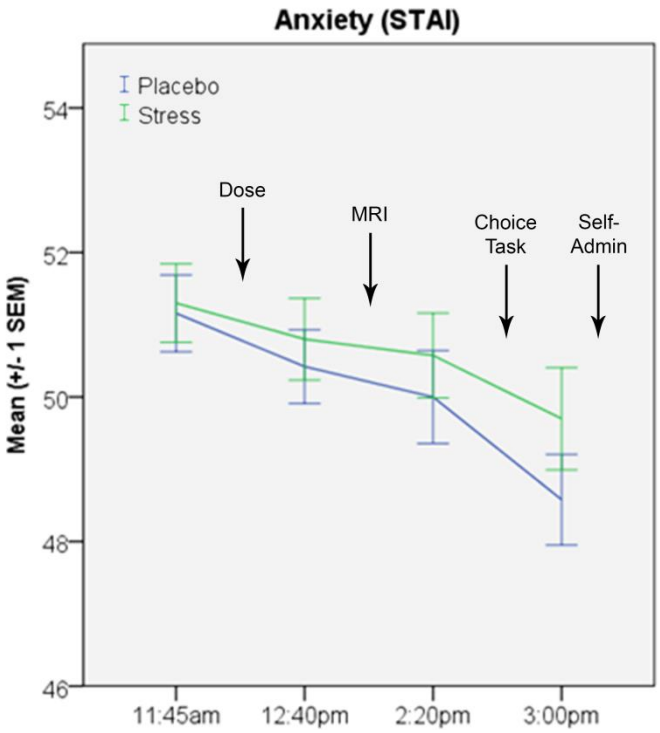

Figure 4.20: Anxiety. Mean (± 1 SEM) self-reported anxiety level is depicted for the active stress (green line) and placebo sessions (blue line). The approximate timing of each experimental procedure is noted with arrows.

Negative affect. Negative affect was measured via self-report (PANAS) as part of the periodic self-report battery. rmANOVA indicated that negative affect exhibited a significant Time effect ($F(3,54) = 3.81$, $p < .05$; partial $\eta^2 = 0.18$ [moderate-to-large effect size]), but non-significant Dose ($p = .47$) and Time X Dose interaction effects ($p = .34$; Figure 4.21). Negative affect increased significantly throughout each experimental session, but did not differ as a function of active vs. placebo stress. At peak levels, participants reported 'very slight' negative affect. FTND was not significantly related to negative affect (*p*s > .35).

Positive affect. Positive affect was measured via self-report (PANAS) as part of the periodic self-report battery. rmANOVA indicated that positive affect exhibited no significant effects: Time (p = .23), Dose (p = .91), or Time X Dose interaction (p = .73; Figure 4.22). FTND was significantly related to positive affect: the FTND X Time interaction was significant ($F(3,51)$ = 4.31, p < .01; partial η^2 = 0.20 [moderate-to-large effect size]). Controlling for FTND, positive affect decreased_ throughout each experimental session, but did not differ as a function of active vs. placebo stress (ps > .20). Participants reported 'moderate' positive affect at baseline (peak levels) and between 'moderate'

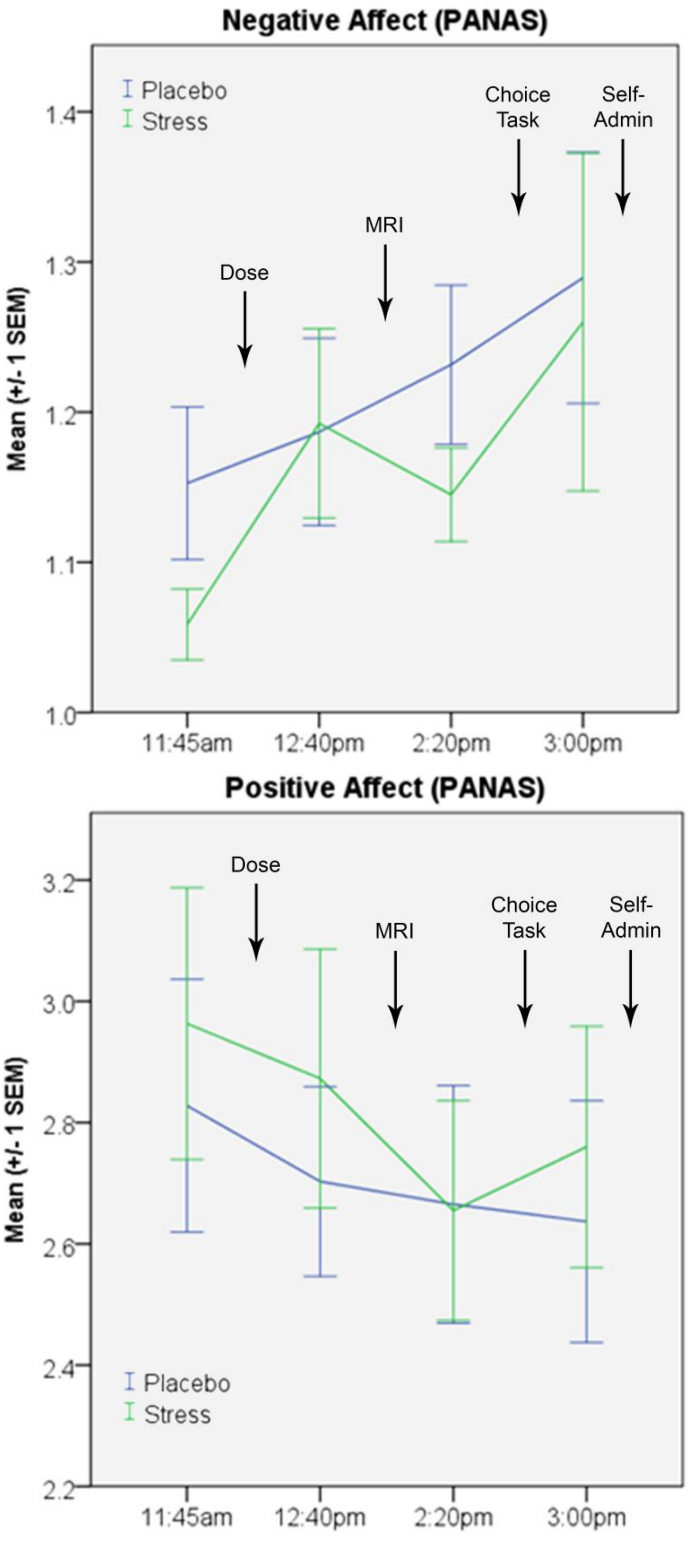

Figure 4.21: Negative Affect (upper panel).
Figure 4.22: Positive Affect (lower panel).
Mean (± 1 SEM) self-reported affect is depicted for the active stress (green line) and placebo sessions (blue line). The approximate timing of each experimental procedure is noted with arrows.

and ‘a little’ positive affect at their lowest levels.

4.2.5 Nicotine-seeking and Self-Administration

Nicotine-seeking and self-administration behavior. Nicotine-seeking was measured via the choice (puffs vs. money) progressive ratio task. Three participants were excluded from nicotine-seeking analyses for the following reasons. Task instructions were explained incorrectly to the first participant in the study (experimenter error). One participant reported a significant reduction in smoking frequency between study enrollment and the experimental sessions (below study inclusion thresholds; FTND < 4 and < 10 cigarettes/day). The third participant switched from paper cigarettes to e-cigarettes between study enrollment and experimental sessions. Thus, nicotine-seeking analyses included 18 participants. The initial rmANOVA indicated that

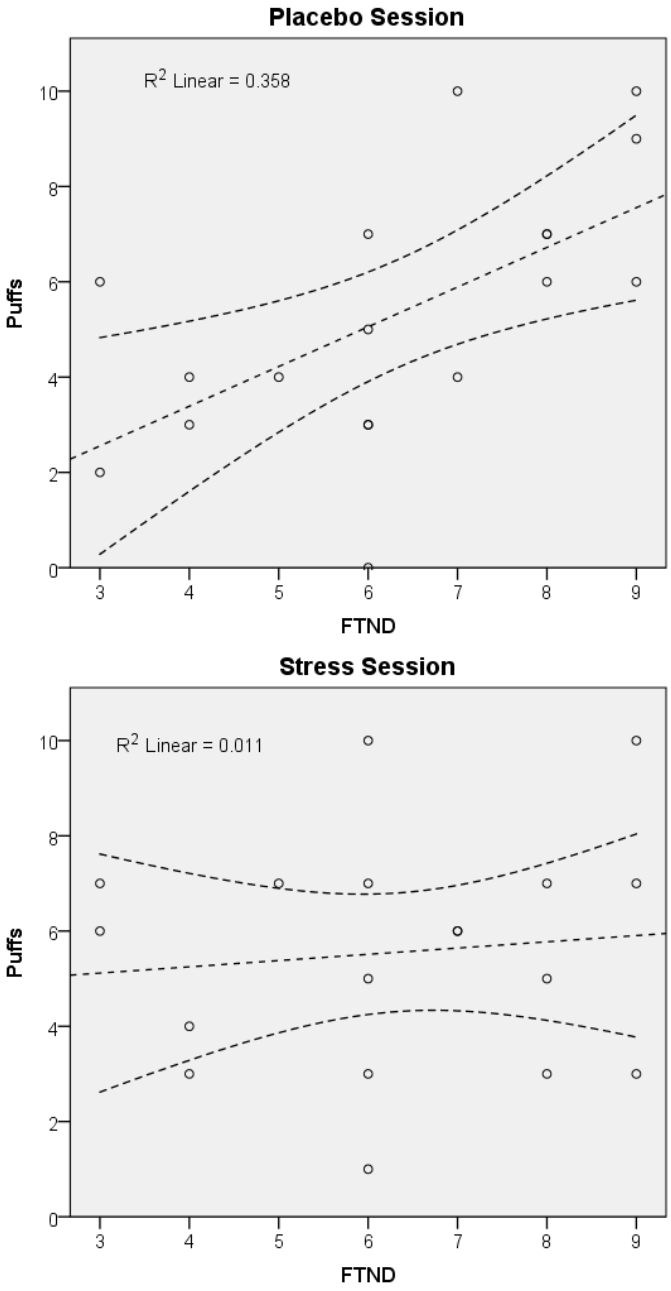

Figure 4.23 & 4.24: Placebo & Stress Puffs vs. FTND. Cigarette puffs earned/smoked during the placebo (upper panel) and stress (lower panel) session are depicted by FTND score.

nicotine-seeking did not differ as a function of active vs. placebo stress (p = .75; 5.3 ± 2.7 vs. 5.6 ± 2.4 puffs, respectively). However, FTND was significantly related to nicotine-seeking. FTND was positively correlated with nicotine-seeking during the placebo (Pearson = .60, p < .01; Figure 4.23), but not active stress session (Pearson = .11 p = .67; Figure 4.24). FTND was negatively correlated with the nicotine-seeking change score (puffs earned during the stress *minus* placebo session; Pearson = -.48, p < .05; Figure 4.25). Including FTND in the model, rmANOVA indicated significant Dose (F(1,16) = 4.93, p < .05; partial η^2 = 0.24 [large effect size]) and Dose X FTND interaction effects (F(1,16) = 4.83, p < .05; partial η^2 = 0.23 [large effect size]). Relative to placebo, nicotine-seeking

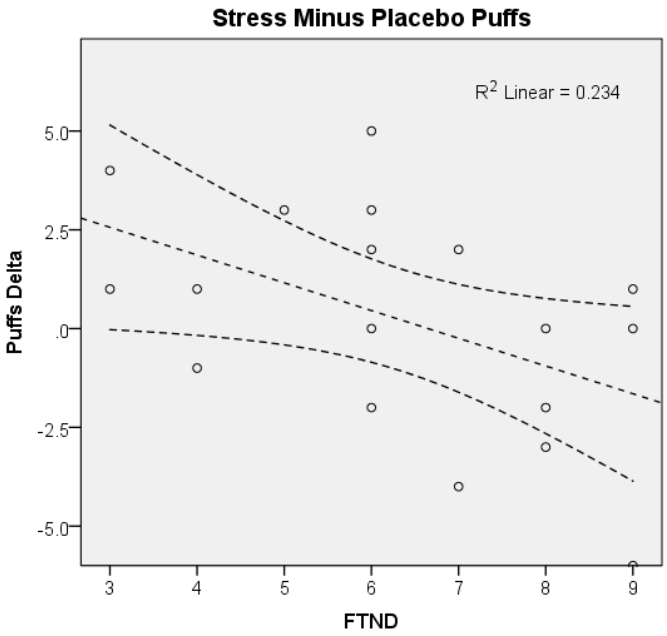

Figure 4.25: Puffs Delta vs. FTND. Cigarette puffs earned/smoked during the placebo *minus*

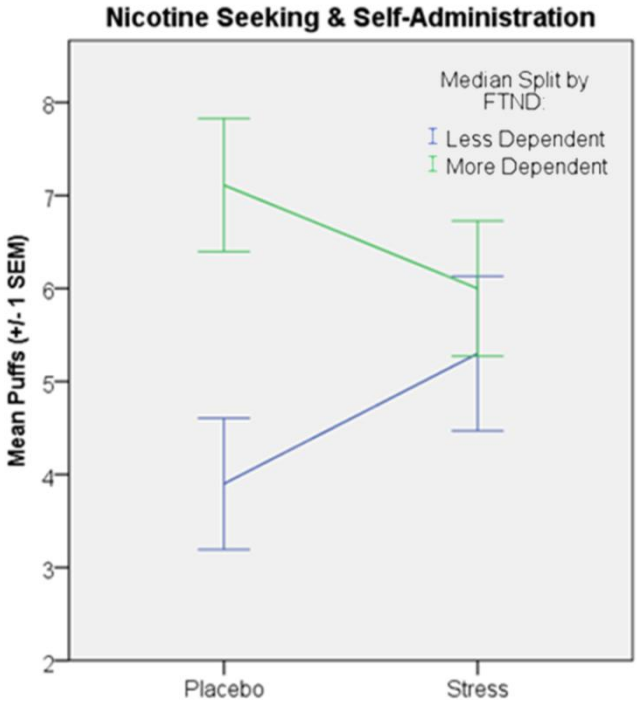

Figure 4.26: Nicotine-Seeking and Self-Administration. Mean (± 1 SEM) cigarette puffs earned and smoked for more (green line) and less (blue line) nicotine dependent participants (median split by FTND score) are depicted for each experimental session.

increased as a function of active stress, controlling for FTND. Moreover, median-split by FTND, nicotine-seeking exhibited a significant Dose X FTND interaction ($F(1,16) = 4.78$, $p < .05$; partial $\eta^2 = 0.23$ [large effect size]) as a function of experimental session (Figure 4.26). Relative to placebo, less dependent participants exhibited an increase in nicotine-seeking during active stress (~1.5 puffs), while more dependent exhibited a decrease in nicotine-seeking (~1.0 puff).

Nicotine consumption rate. Nicotine consumption rate was measured, unbeknownst the participant, as mean inter-puff interval (s) during nicotine self-administration following the nicotine-seeking task. Individuals with valid choice data and who earned (and smoked) at least two cigarette puffs (n = 16) were included in analyses. rmANOVA indicated that nicotine consumption rate (log_{10}-transformed) did not differ as a function of active vs. placebo stress ($p = .60$; 27.5 ± 20.8s vs. 26.4 ± 14.9s, respectively; Figure 4.27). FTND was not significantly related to nicotine consumption rate ($p > .15$).

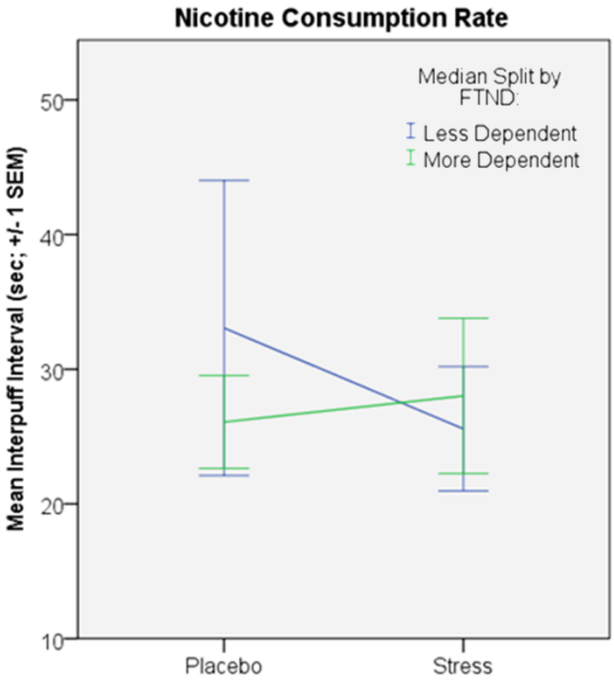

Figure 4.27: Nicotine Consumption Rate. Mean (± 1 SEM) inter-puff interval (s) for more (green line) and less (blue line) nicotine dependent participants (median split by FTND score) are depicted for each experimental session.

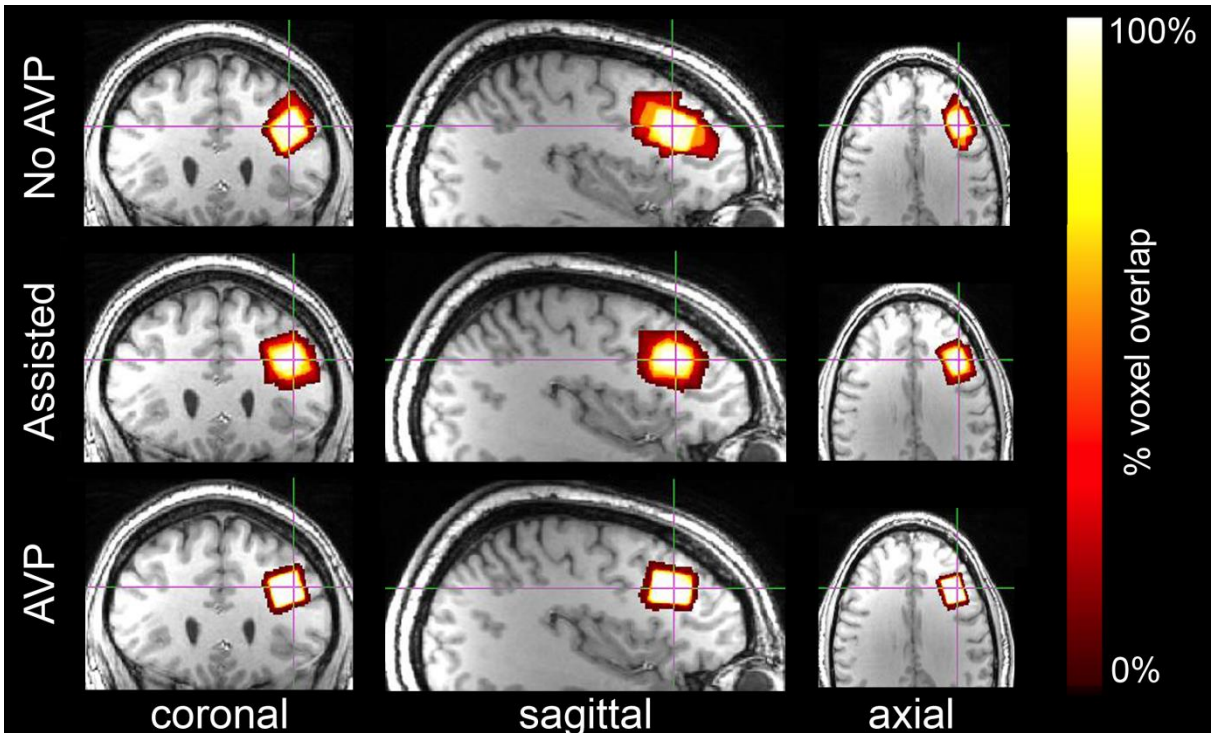

Figure 4.28: Geometric Voxel Overlap. Participant voxel placement was coregistered to template space and orthonormal views depict geometric voxel overlap separately for each voxel placement method. Percentage of geometric voxel overlap is indicated by color: white indicates voxel space with complete overlap, while yellow/red indicate incomplete overlap, across subjects.

4.2.6 Voxel Overlap

The voxel used in this study (location, dimensions, and rotation angles) was identical to the ^{1}H fMRS pilot study. AVP was used to prescribe voxel placement for a subset of participants (AVP was under development at the onset of this study) (Woodcock et al., 2017). Percentage of voxel overlap (with the template voxel) by voxel placement method is described in Table 4.3 and illustrated in Figure 4.28. Voxel overlap improved as AVP became functional. Within-subject voxel overlap across experimental

Placement Method	Scans (%)	Overlap (%)
No AVP (manual)	14.30%	61.8 ± 22.8%
AVP assisted	26.20%	74.8 ± 13.5%
AVP used	59.50%	96.0 ± 3.7%
Overall	**100.00%**	**85.6 ± 16.8%**

Table 4.3: Geometric Voxel Overlap. Mean percentage (± 1 SD) of geometric voxel overlap with the template voxel (i.e. placement accuracy) is depicted by voxel placement

sessions (active vs. placebo stress) was very good: 87.3 ± 15.1%. Voxel tissue composition was 31.8% gray and 66.0% white matter.

4.2.7 Letter 2-back Behavioral Data

Behavioral data were unintelligible and discarded for 10 scans (23.8%) due to data collection error. Behavioral data demonstrated task compliance for both the placebo (87.1 ± 13.3% correct; 674 ± 233ms response latency) and active stress (78.2 ± 15.1% correct; 715 ± 187ms response latency) sessions. As a function of experimental session and task block, rmANOVA indicated that accuracy exhibited a significant Time effect ($F(4,48) = 6.61$, $p < .001$; partial $\eta^2 = 0.36$ [large effect size]; Figure 4.29), generally improving across task

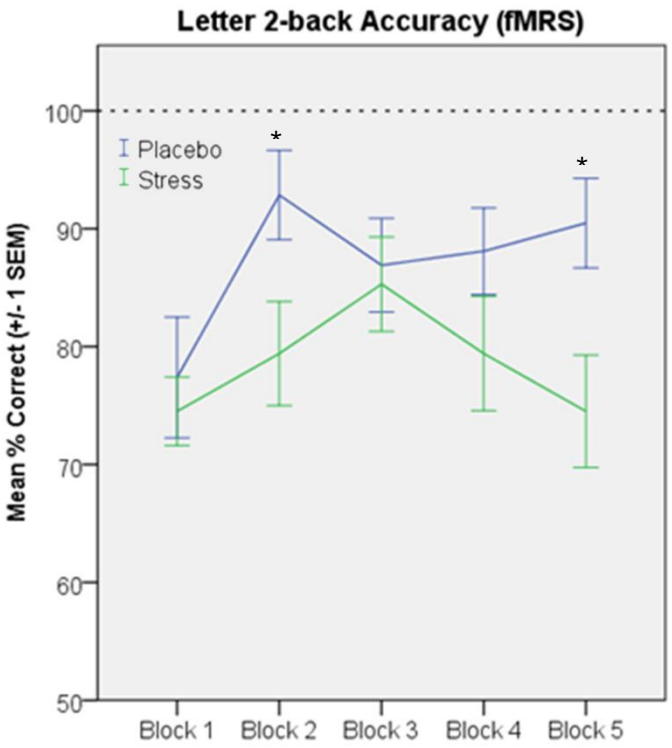

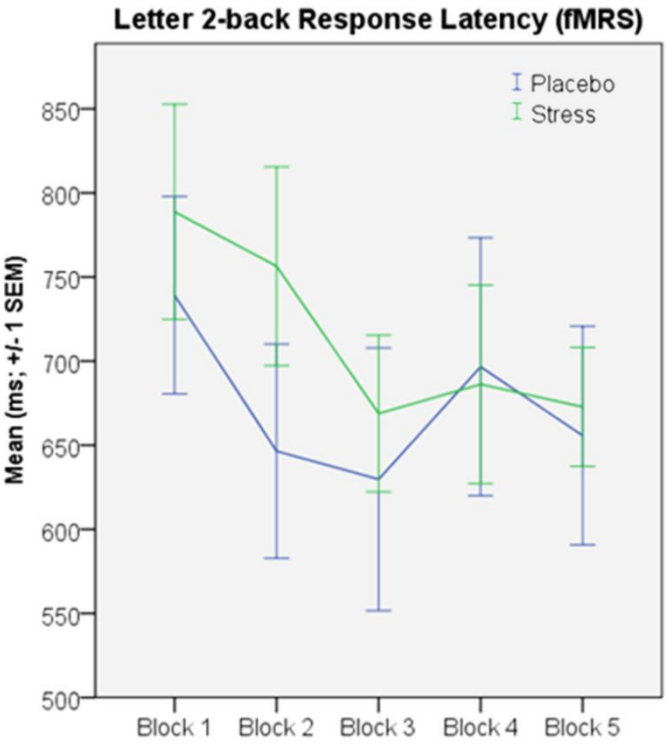

Figure 4.29: Letter 2-back Response Accuracy.

Figure 4.30: Letter 2-back Response Latency. Mean (± 1 SEM) response accuracy (% correct; upper panel) and latency (ms; lower panel) are depicted across task blocks separately for the active stress (green line) and placebo (blue line)

blocks during both experimental sessions (Placebo: Block 1 = 77.4 ± 19.2%, Block 5 = 90.5 ± 14.2%; Stress: Block 1 = 74.5 ± 12.0%, Block 5 = 74.5 ± 19.6%). Response accuracy exhibited a significant Dose effect ($F(1,12) = 6.35$, $p < .05$; partial $\eta^2 = 0.35$ [large effect size]), which indicated it was higher during placebo than active stress (87.1 ± 13.3% vs. 78.2 ± 15.1%). Finally, a significant Time X Dose interaction ($F(4,48) = 3.08$, $p < .05$; partial $\eta^2 = 0.20$ [moderate-to-large effect size]) indicated that response accuracy improved more across task blocks during the placebo, relative to the active stress session.

rmANOVA indicated that response latency exhibited a significant Time effect ($F(4,52) = 3.15$, $p < .05$; partial $\eta^2 = 0.20$ [moderate-to-large effect size]), but non-significant Dose ($p = .89$) and Time X Dose interaction effects ($p = .56$; Figure 4.30). The significant Time effect indicated response latency generally decreased across task blocks during both experimental sessions (Placebo: Block 1 = 739.2 ± 219.8ms, Block 5 = 655.7 ± 243.1ms; Stress: Block 1 = 788.8 ± 271.4ms, Block 5 = 672.8 ± 150.0ms).

Placebo Session				
Fit Characteristic	2-back A	2-back B	Interleaved Rest	Rest vs. Task (p)
GLU CRLB %	6.5 ± 0.9	6.6 ± 0.9	6.6 ± 0.9	> .16
GLN CRLB %	24.0 ± 4.7	23.2 ± 3.7	24.2 ± 4.8	> .30
FWHM Hz	5.0 ± 0.7	5.0 ± 0.9	5.1 ± 0.8	> .06
SNR	12.9 ± 2.0	13.1 ± 2.0	12.9 ± 2.0	> .14
Stress Session				
Fit Characteristic	2-back A	2-back B	Interleaved Rest	Rest vs. Task (p)
GLU CRLB %	6.7 ± 0.8	6.8 ± 0.6	6.7 ± 0.9	> .19
GLN CRLB %	24.6 ± 3.0	23.4 ± 3.1	24.6 ± 3.0	> .50
FWHM Hz	4.8 ± 0.5	4.8 ± 0.5	5.0 ± 0.5	< .05
SNR	12.4 ± 1.7	12.4 ± 1.7	12.1 ± 1.5	< .05

Table 4.4: LCModel Fit Characteristics (32s). Mean (± 1 SD) LCModel fit characteristics (32s; 8 avgs) are presented by task phase. GLU = glutamate; GLN = glutamine; FWHM = full-width half-maximum; SNR = signal-to-noise; CRLB = Cramer Rao Lower Bound.

FTND was not significantly related to task accuracy or response latency (*p*s > .10).

4.2.8 LCModel Fit Characteristics (32s Resolution)

LCModel fit reliability was evaluated for 2-back A, 2-back B, and interleaved fixation-cross rests for both experimental sessions. Four subjects were excluded from outcome analyses due to relatively poor LCModel fit quality (greater than two SDs worse SNR and GLU CRLB% relative to the group mean). Importantly, LCModel fit characteristics did not differ as a function of experimental task (Task and Task X Time interaction effects examined) during the placebo session (Table 4.4; upper panel). However, during the stress session, SNR and FWHM did differ as a function of experimental task (Table 4.4; lower panel). FWHM was lower during 2-back A relative to interleaved

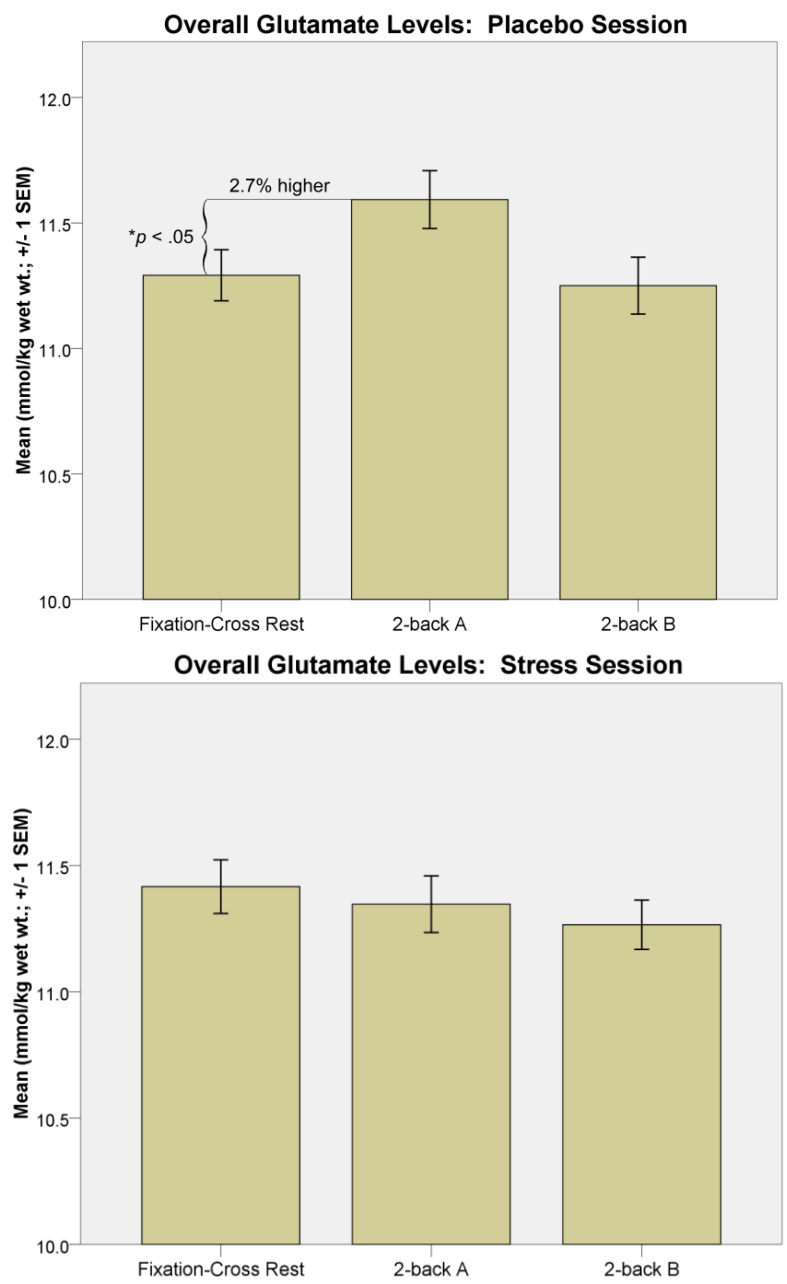

Figure 4.31 & 4.32: Overall GLU Levels. Mean (± 1 SEM) GLU levels during the placebo (upper panel) and stress (lower panel) session are depicted.

rest (Task effect; $p < .05$). SNR was higher during task (2-back A and B) relative to interleaved rest (Task effects; $ps \leq .05$).

4.2.9 Placebo GLU Modulation (32s Resolution)

The flashing checkerboard minimized GLU fluctuation (mean coefficient of variation percentage = 6.1%) prior to 2-back (vs. rest) modulation.

Placebo 2-back A vs. rest. Overall GLU levels during 2-back A were significantly higher (2.7%; Figure 4.31) than interleaved fixation-cross rest ($F(1,83) = 8.12$, $p < .01$, partial $\eta^2 = 0.09$ [moderate effect size]; 11.59 ± 1.05 vs. 11.29 ± 0.93, respectively; Figure 4.31). Across task blocks, rmANOVA indicated a marginal Task effect ($F(1,16) = 4.01$, $p = .06$, partial $\eta^2 = 0.20$ [moderate-to-large effect size]; Figure 4.33), and non-significant Time ($p = .41$) and Time X Task

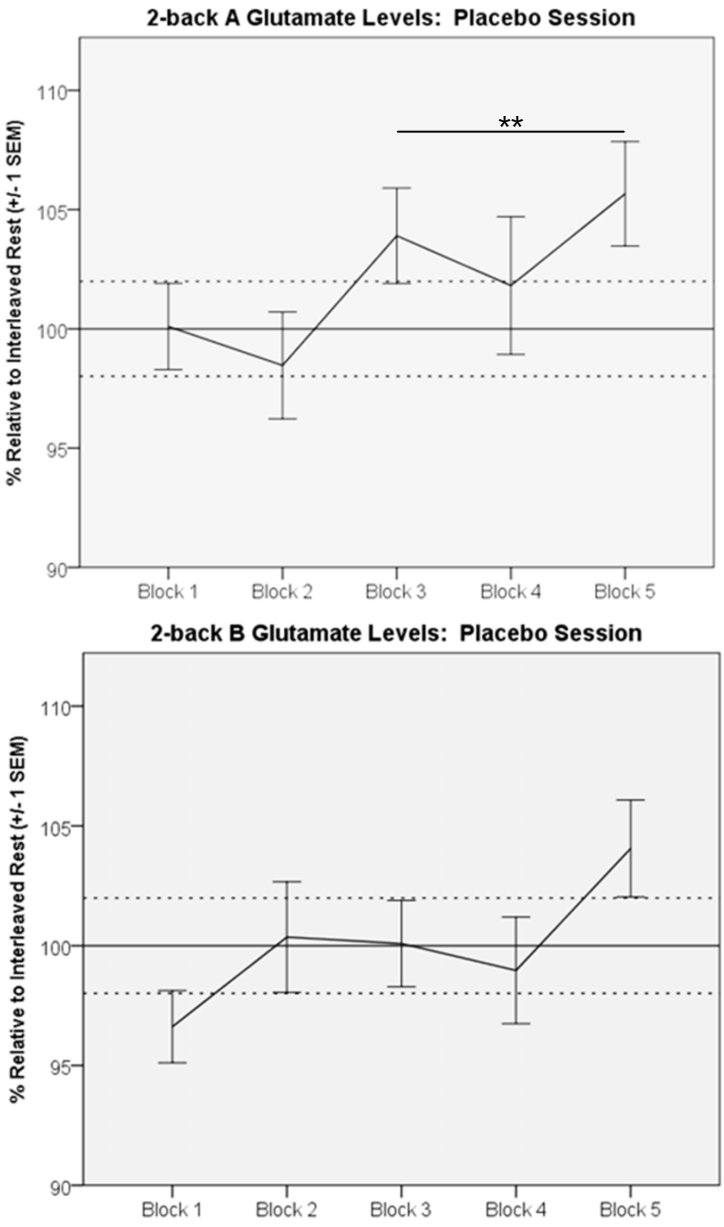

Figure 4.33 & 4.34: Placebo 2-back A & B GLU Levels (32s). Mean (± 1 SEM) 2-back A (upper panel) and B (lower panel) GLU levels (32s; % relative to interleaved fixation cross) during the placebo session are depicted across task blocks.

interaction effects (p = .19). 2-back A GLU levels were higher than interleaved fixation-cross levels (especially in later task blocks).

Placebo 2-back B vs. rest. Overall GLU levels during 2-back B did not differ from interleaved fixation-cross rest (p = .67; 11.25 ± 1.04 vs. 11.29 ± 0.93, respectively; Figure 4.31). Across task blocks, rmANOVA indicated no significant effects: Time (p = .65), Task (p = .71), and Time X Task interaction (p = .17; Figure 4.34).

4.2.10 Stress GLU Modulation (32s Resolution)

The flashing checkerboard minimized GLU fluctuation (mean coefficient of variation percentage = 5.7%) prior to 2-back (vs. rest) modulation.

Stress 2-back A vs. rest. Overall GLU levels during 2-back A were not significantly different from interleaved fixation-cross

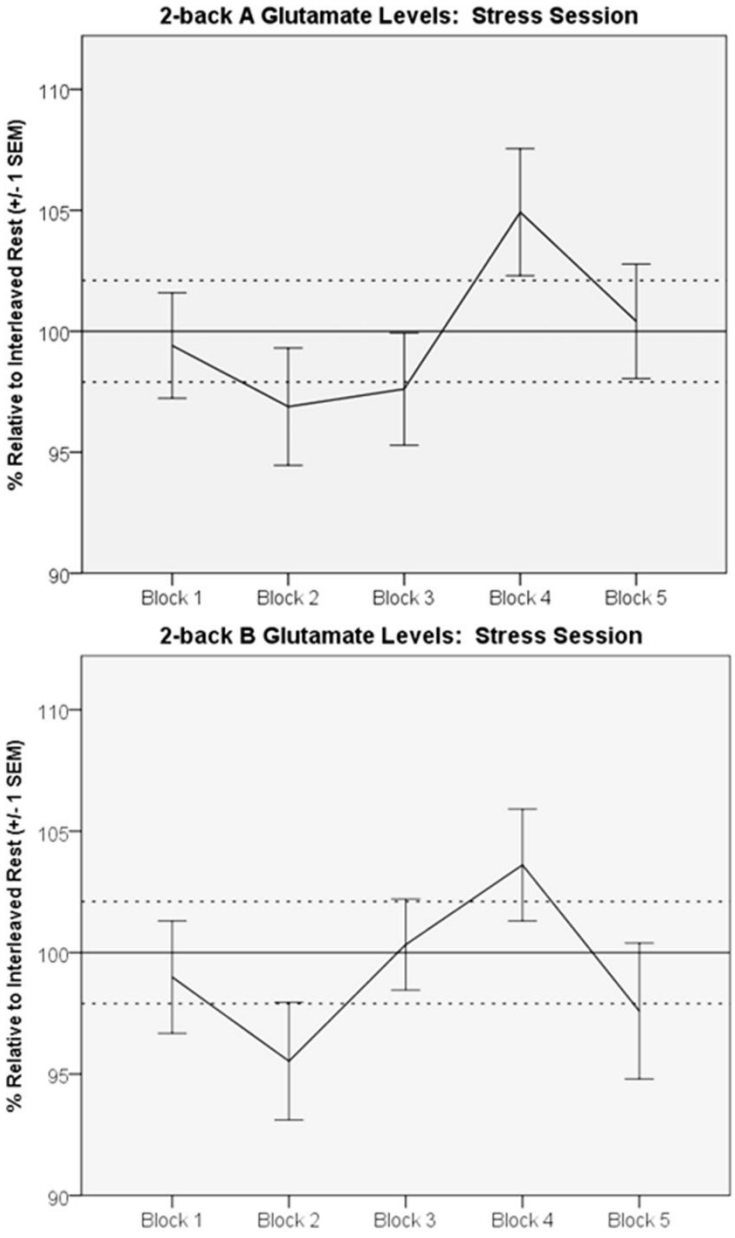

Figure 4.35 & 4.36: Stress 2-back A & B GLU Levels (32s). Mean (± 1 SEM) 2-back A (upper panel) and B (lower panel) GLU levels (32s; % relative to interleaved fixation cross) during the stress session are depicted across task blocks.

rest (p = .58; 11.35 ± 1.03 vs. 11.42 ± 0.98, respectively; Figure 4.32). Across task blocks, rmANOVA indicated no significant effects: Time (p = .45), Task (p = .59), and Time X Task interaction (p = .18; Figure 4.35).

Stress 2-back B vs. rest. Overall GLU levels during 2-back B did not differ from interleaved fixation-cross rest (p = .22; 11.27 ± 0.90 vs. 11.42 ± 0.98, respectively; Figure 4.32). Across task blocks, rmANOVA indicated no significant effects: Time (p = .44), Task (p = .26), and Time X Task interaction (p = .14; Figure 4.36).

4.2.11 BOLD Effect (32s Resolution)

Relative to interleaved fixation-cross rest, rmANOVA indicated spectral linewidth (FWHM) was significantly more narrow for 2-back A during the active stress (Task effect: $F(1,16) = 5.30$, $p < .05$; Time X Task interaction effect: p = .99), but not the placebo session (ps > .05). rmANOVA indicated no effect for task on FWHM for 2-back B for either session (ps > .06).

4.2.12 Neurochemical Specificity (32s Resolution)

During the placebo session, metabolites (PCr+Cr, GPC+PC, Myo-Inositol, and NAA) did not significantly differ as a function of task (2-back A and B vs. interleaved fixation-cross rest; ps ≥ .09).

During the active stress session, Myo-Inositol exhibited significant Task and Time X Task interaction effects ($F(1,16) = 6.18$, $p < .05$ and $F(4,64) = 2.60$, $p < .05$, respectively). Interleaved fixation-cross rest Myo-Inositol levels were higher than 2-back A levels, but tended to converge in later task blocks. GPC+PC exhibited a significant Task effect ($F(1,16) = 9.56$, $p < .01$). GPC+PC levels during rest were generally higher than 2-back A levels across task blocks. NAA and PCr+Cr did not differ as a function of

task (*p*s > .10). LCModel quantification of NAA levels was not biased by the significant BOLD effect (i.e. narrow spectral linewidth did not significantly alter area-under-the-curve quantification).

4.2.13 LCModel Fit Characteristics (64s Resolution)

As anticipated, 64s temporal resolution (16 avgs) was associated with more reliable LCModel fit, relative to 32s (8 avgs) resolution. LCModel fit characteristics described in Table 4.5. Importantly, LCModel fit characteristics did not significantly

Placebo Session				
Fit Characteristic	2-back A	2-back B	Interleaved Rest	Rest vs. Task (*p*)
GLU CRLB %	5.3 ± 0.8	5.4 ± 0.8	5.4 ± 0.6	> .15
GLN CRLB %	24.0 ± 4.7	23.4 ± 3.7	22.9 ± 3.0	> .15
FWHM Hz	4.9 ± 0.9	4.8 ± 0.9	4.9 ± 0.9	> .09
SNR	17.6 ± 3.0	17.8 ± 3.1	17.6 ± 3.0	> .08
Stress Session				
Fit Characteristic	2-back A	2-back B	Interleaved Rest	Rest vs. Task (*p*)
GLU CRLB %	5.3 ± 0.8	5.4 ± 0.7	5.3 ± 0.8	> .19
GLN CRLB %	19.8 ± 4.8	20.1 ± 4.1	20.7 ± 4.1	> .19
FWHM Hz	4.7 ± 0.7	4.7 ± 0.7	4.7 ± 0.8	> .25
SNR	17.4 ± 2.6	17.2 ± 2.6	17.0 ± 2.7	< .01

Table 4.5: LCModel Fit Characteristics (64s). Mean (± 1 SD) LCModel fit characteristics (64s; 16 avgs) are presented by task phase. GLU = glutamate; GLN = glutamine; FWHM = full-width half-maximum; SNR = signal-to-noise; CRLB = Cramer Rao Lower Bound.

differ as a function of task for the placebo session (*p*s > .08). However, consistent with 32s resolution, SNR differed as a function of task during the stress session (2-back A > rest; $p < .01$).

4.2.14 Placebo GLU Modulation (64s Resolution)

Placebo 2-back A vs. rest. Across task blocks, rmANOVA indicated a significant Time X Task interaction ($F(3,48) = 2.80$, $p = .05$, partial $\eta^2 = 0.15$ [moderate-to-large effect size]), but non-significant Time ($p = .44$) and Task effects ($p = .59$). 2-back A GLU

levels were significantly higher than interleaved fixation-cross levels in later task blocks (Figure 4.37).

Placebo 2-back B vs. rest. Across task blocks, rmANOVA indicated no significant effects: Time (p = .51), Task (p = .19), and Time X Task interaction (p = .30) (Figure 4.38).

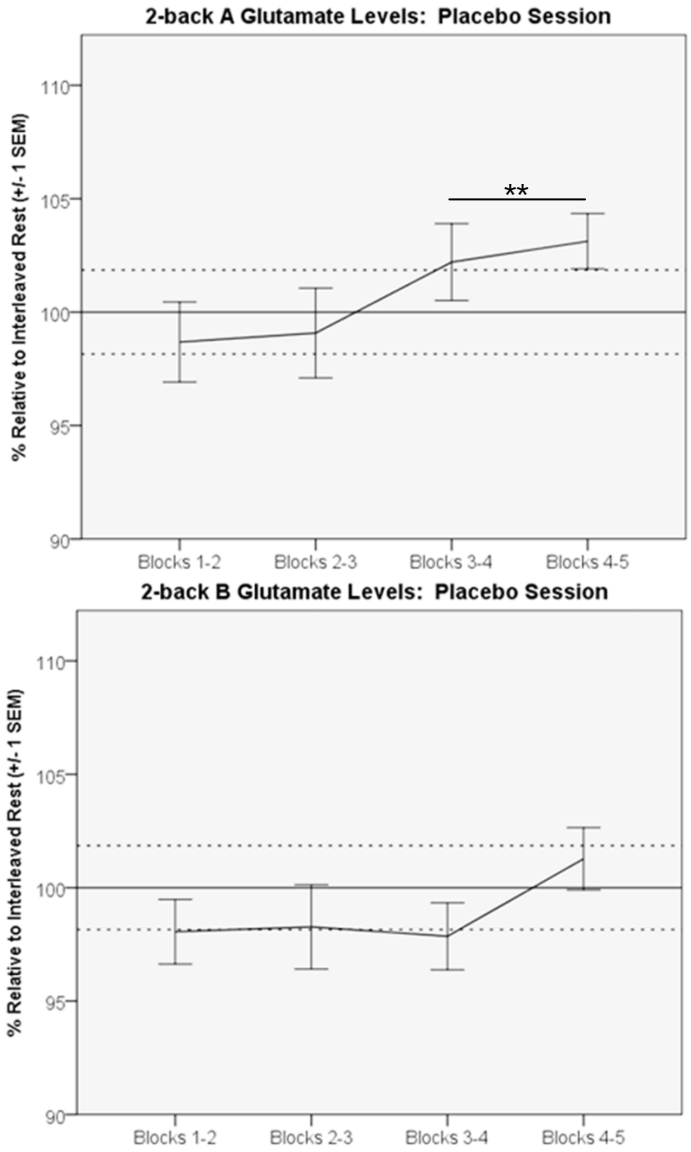

Figure 4.37 & 4.38: Placebo 2-back A & B GLU Levels (64s). Mean (± 1 SEM) 2-back A (upper panel) and B (lower panel) GLU levels (64s; % relative to interleaved fixation cross) during the placebo session are depicted across task blocks.

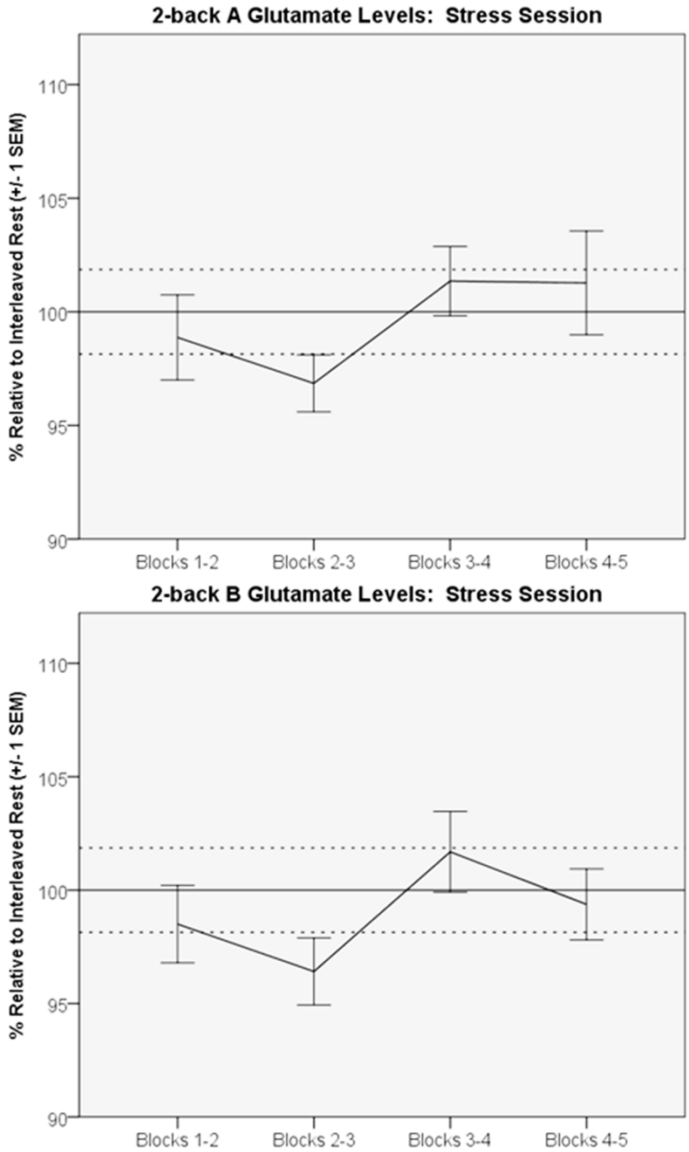

Figure 4.39 & 4.40: Stress 2-back A & B GLU Levels (64s). Mean (± 1 SEM) 2-back A (upper panel) and B (lower panel) GLU levels (64s; % relative to interleaved fixation cross) during the stress session are depicted across task blocks.

4.2.15 Stress GLU Modulation (64s Resolution)

Stress 2-back A vs. rest. Across task blocks, rmANOVA indicated no significant effects: Time (p = .90), Task (p = .54), and Time X Task interaction (p = .18) (Figure 4.39).

Stress 2-back B vs. rest. Across task blocks, rmANOVA indicated no significant effects: Time (p = .99), Task (p = .24), and Time X Task interaction (p = .08) (Figure 4.40).

4.2.16 BOLD Effect (64s Resolution)

rmANOVA indicated spectral linewidth (FWHM) did not significantly differ as a function of task (2-back vs. rest) for the placebo or stress sessions (ps > .20).

4.2.17 Neurochemical Specificity (64s Resolution)

During the placebo session, NAA exhibited a significant Time X Task interaction effect (F(3,48) = 3.24, p < .05), but not a Task effect. NAA levels during interleaved fixation-cross rest were higher than 2-back B, but only in later task blocks. No significant effect for NAA during 2-back A. Consistent with the 32s temporal resolution findings, other metabolites (PCr+Cr, GPC+PC, and Myo-Inositol) did not significantly differ as a function of task (2-back A and B vs. interleaved fixation-cross rest; ps ≥ .10).

Consistent with findings at 32s temporal resolution, Myo-Inositol and GPC+PC differed as a function of task during the active stress session. Myo-Inositol exhibited significant Task and Time X Task interaction effects (F(1,17) = 15.92, p < .001 and F(3,51) = 2.79, p = .05, respectively). Interleaved fixation-cross rest Myo-Inositol levels were higher than 2-back A levels, especially in later task blocks. GPC+PC exhibited significant Task effects for 2-back A and B (F(1,17) = 13.02, p < .01; F(1,17) = 4.57, p <

.05; respectively). GPC+PC levels during rest were higher than 2-back A and B levels across task blocks. NAA and PCr+Cr did not differ as a function of task (*p*s > .10).

4.2.18 Cerebrovascular Reactivity

Second-level contrasts (breath hold > paced breathing) revealed significant clusters (voxel-level; $p < .05$) during both the placebo and active stress sessions (Figure 4.41). Significant clusters were found throughout the cortex (primarily in gray matter) during both sessions. Experimental sessions were contrasted (placebo > stress and stress > placebo) to produce CVR difference maps (Figure 4.42). CVR difference maps identified clusters that significantly differed (voxel-level; $p < .05$) as a function of vascular reactivity between sessions, and thus, may confound between-session contrasts of interest. Therefore, CVR difference maps were subtracted from between-session contrasts of interest to reduce the likelihood of false positives.

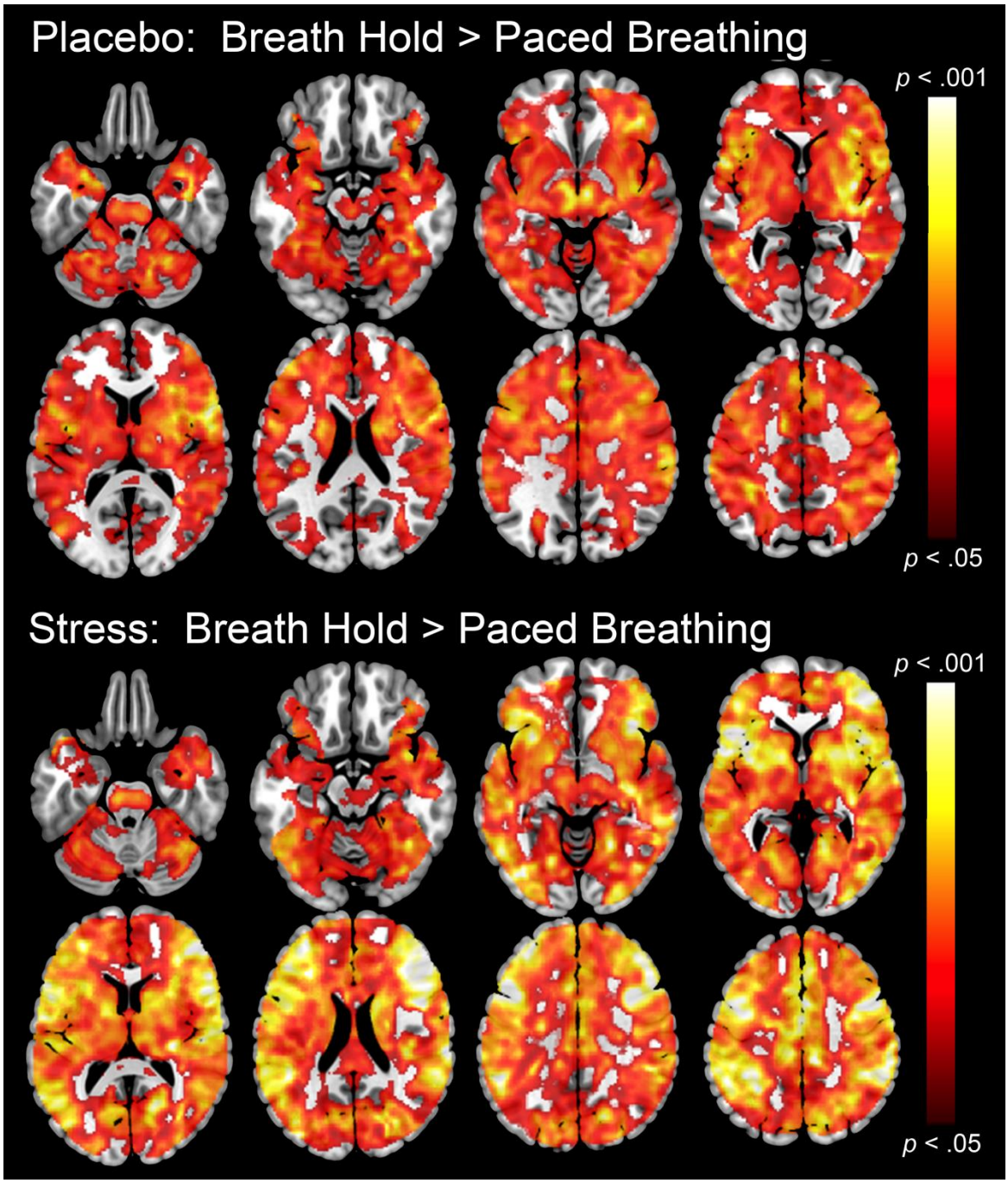

Figure 4.41: Cerebrovascular Reactivity Maps. Cerebrovascular reactivity maps (voxel-wise $p < .05$; breath hold > paced breathing) are depicted on contiguous axial slices for placebo (upper panel) and active stress (lower panel). Lighter color reflects greater cerebrovascular reactivity.

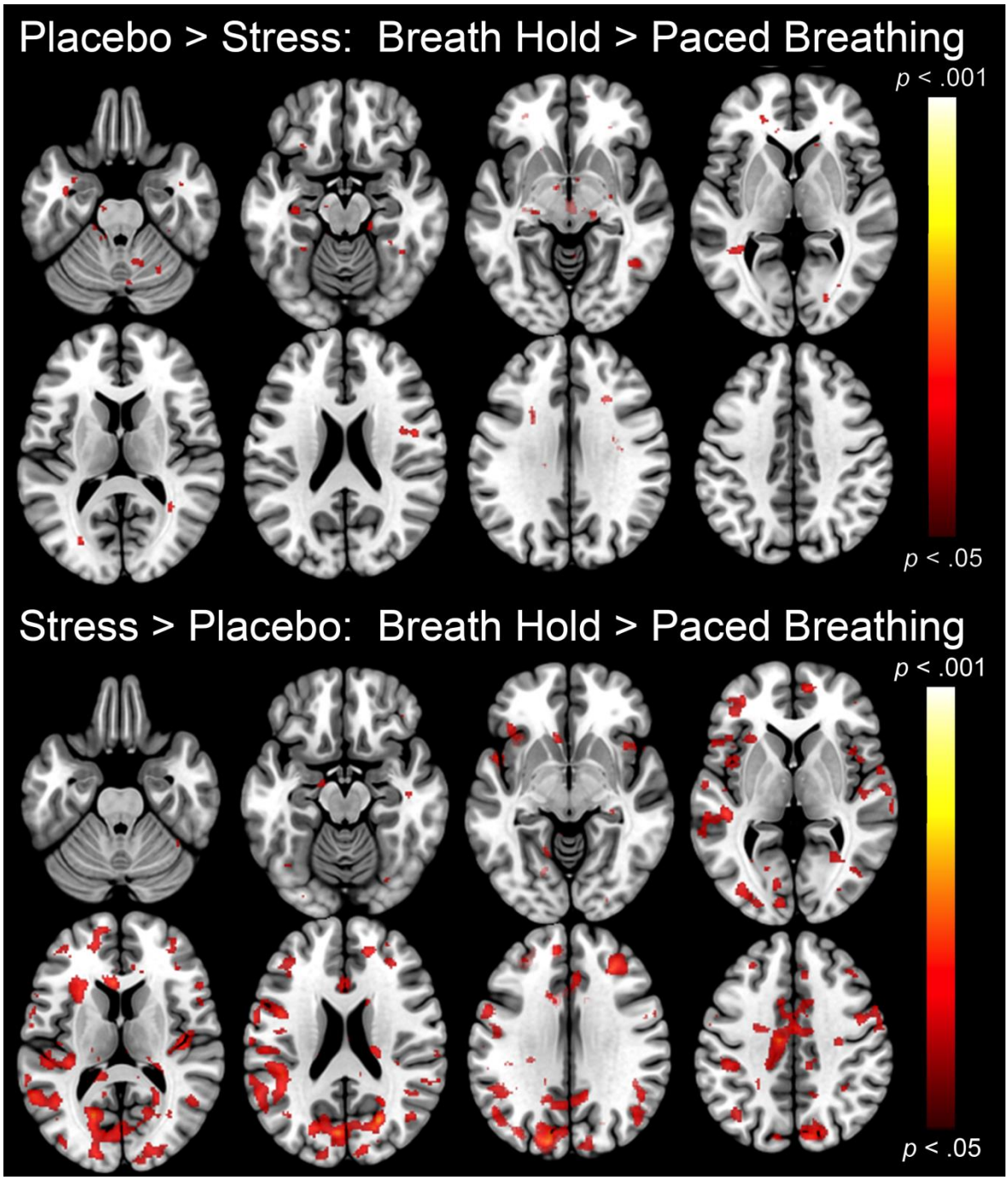

Figure 4.42: Cerebrovascular Reactivity Difference Maps. Cerebrovascular reactivity difference maps (voxel-wise $p < .05$) are depicted on contiguous axial slices contrasting sessions: placebo > stress (upper panel) and stress > placebo (lower panel). Lighter color reflects greater cerebrovascular reactivity.

4.2.19 Letter 2-back fMRI Data

Letter 2-back behavioral data. Behavioral data demonstrated task compliance during the letter 2-back fMRI task. Response accuracy was non-significantly higher during placebo, relative to active stress (p = .11; 89.9 ± 13.9% vs. 84.7 ± 14.9%, respectively).

Letter 2-back > fixation-cross rest. As hypothesized, cluster-level corrected images (p < .05) revealed significant bilateral activation in the dlPFC during 2-back task performance (> fixation-cross rest) during both experimental sessions (Figure 4.43).

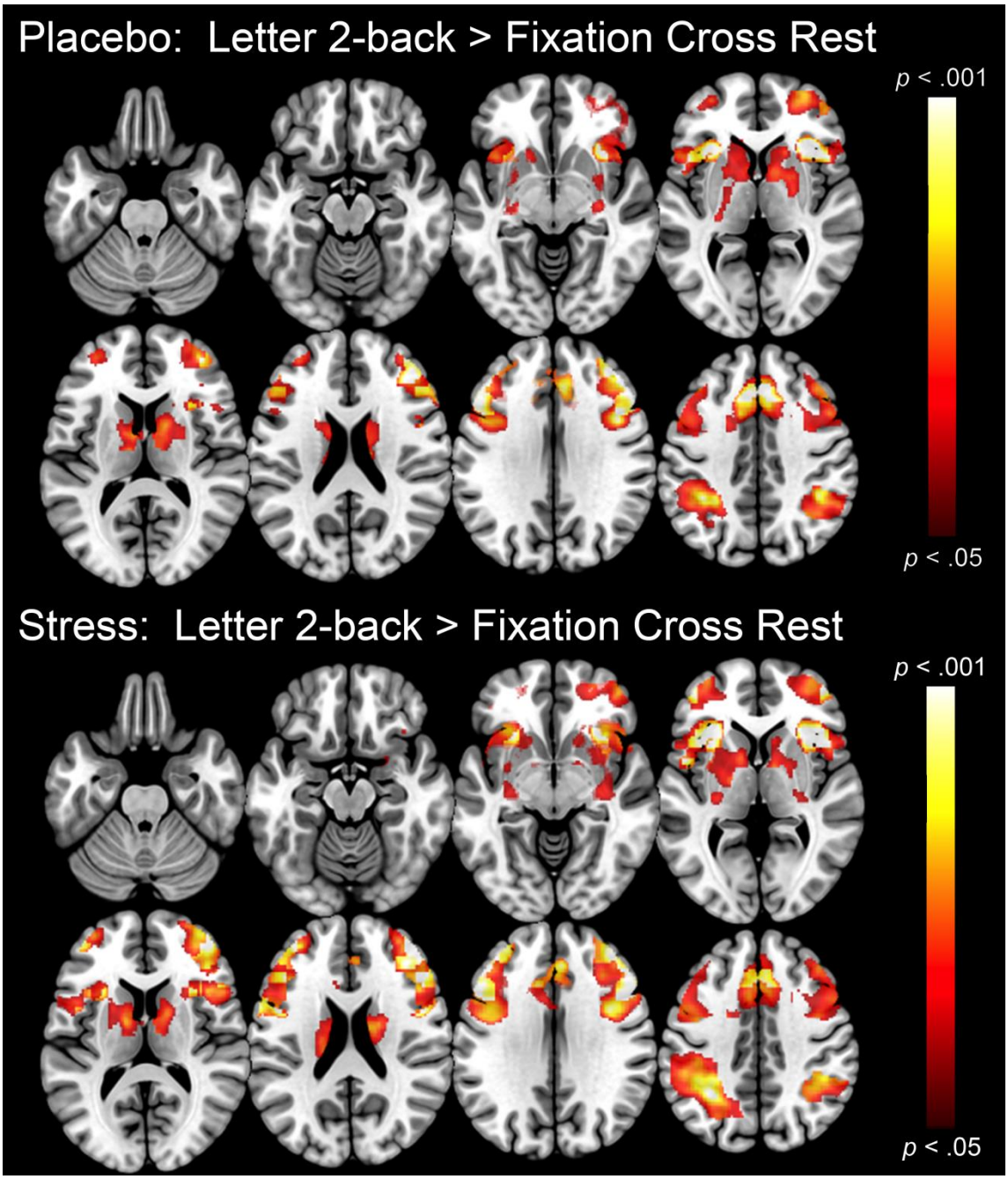

Figure 4.43: Letter 2-back Activation Maps. Cluster-level corrected ($p < .05$) letter 2-back (> fixation cross rest) activation maps are depicted on contiguous axial slices for the placebo (upper panel) and stress session (lower panel). Lighter color reflects more BOLD activation.

Stress > placebo: letter 2-back > rest. Contrary to hypotheses, bilateral dlPFC clusters survived cluster-level and CVR difference map correction for stress > placebo (Figure 4.44). These clusters demonstrated that letter 2-back task performance elicited

greater BOLD activation during active stress, relative to placebo. Significant clusters in the insula suggest participants processed peripheral signals that may be attributed to physiological effects of the stress manipulation (elevated BP, etc.).

Placebo > stress: letter 2-back > rest. The converse comparison revealed one significant cluster (mPFC; Figure 4.44). These results demonstrated that 2-back performance elicited a relatively smaller BOLD response during placebo relative to active stress. Participants exhibited non-significantly higher response accuracy, but smaller dlPFC BOLD response during placebo, relative to active stress.

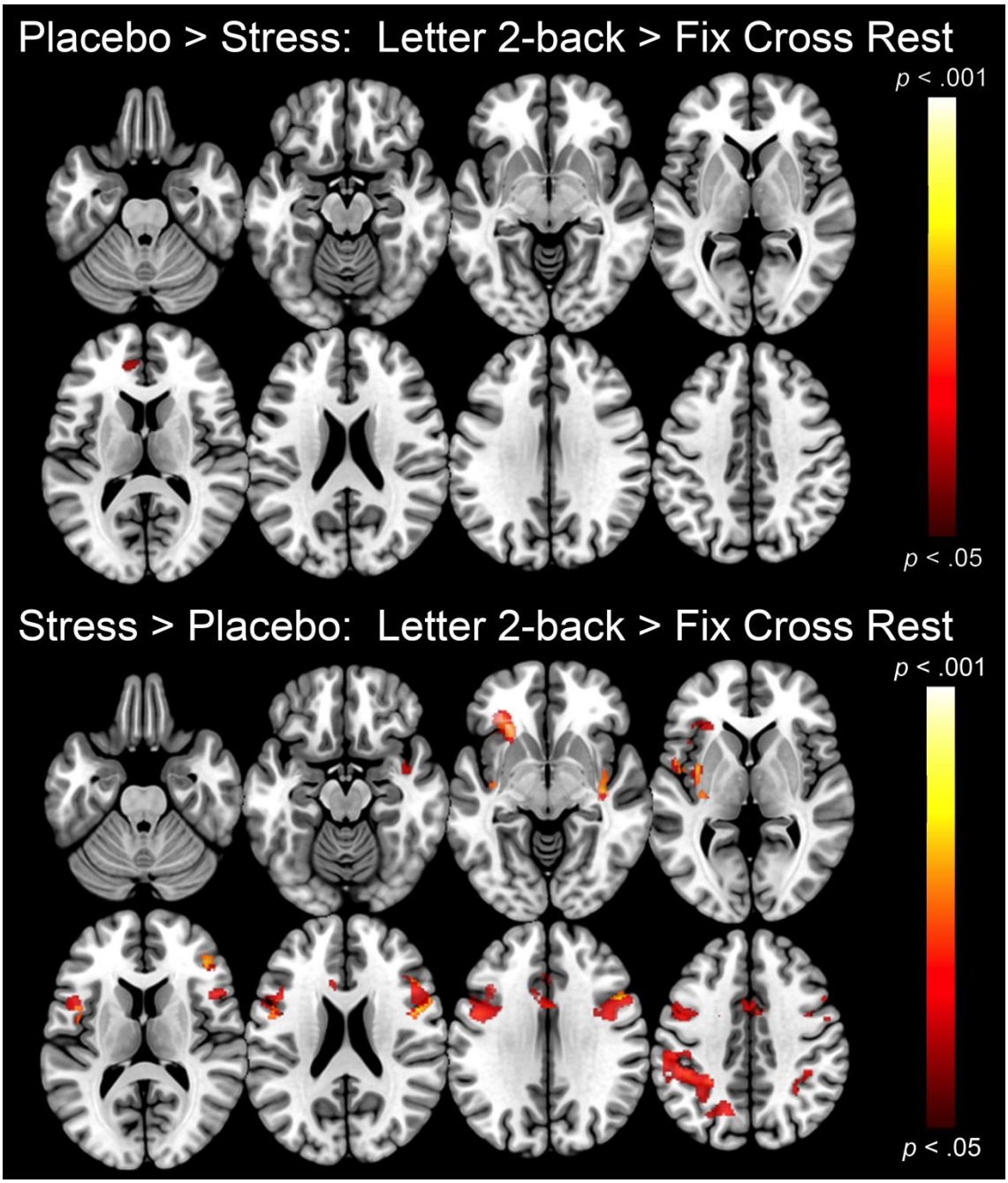

Figure 4.44: Letter 2-back Difference Maps. Cluster-level corrected ($p < .05$) letter 2-back (> fixation cross rest) difference maps are depicted on contiguous axial slices: placebo > stress (upper panel) and stress > placebo (lower panel). Lighter color reflects more BOLD activation.

Letter 2-back > rest: median-split by FTND. Exploratory analyses examined the BOLD response during letter 2-back by splitting the sample into two groups: median-split by FTND. These analyses paralleled the nicotine-seeking and self-administration

data. Less dependent participants exhibited less dlPFC neural engagement (less BOLD activation) during 2-back performance in the stress session (relative to placebo; Figure 4.45). Conversely, more dependent participants engaged their dlPFC more during 2-back performance in the stress session (relative to placebo).

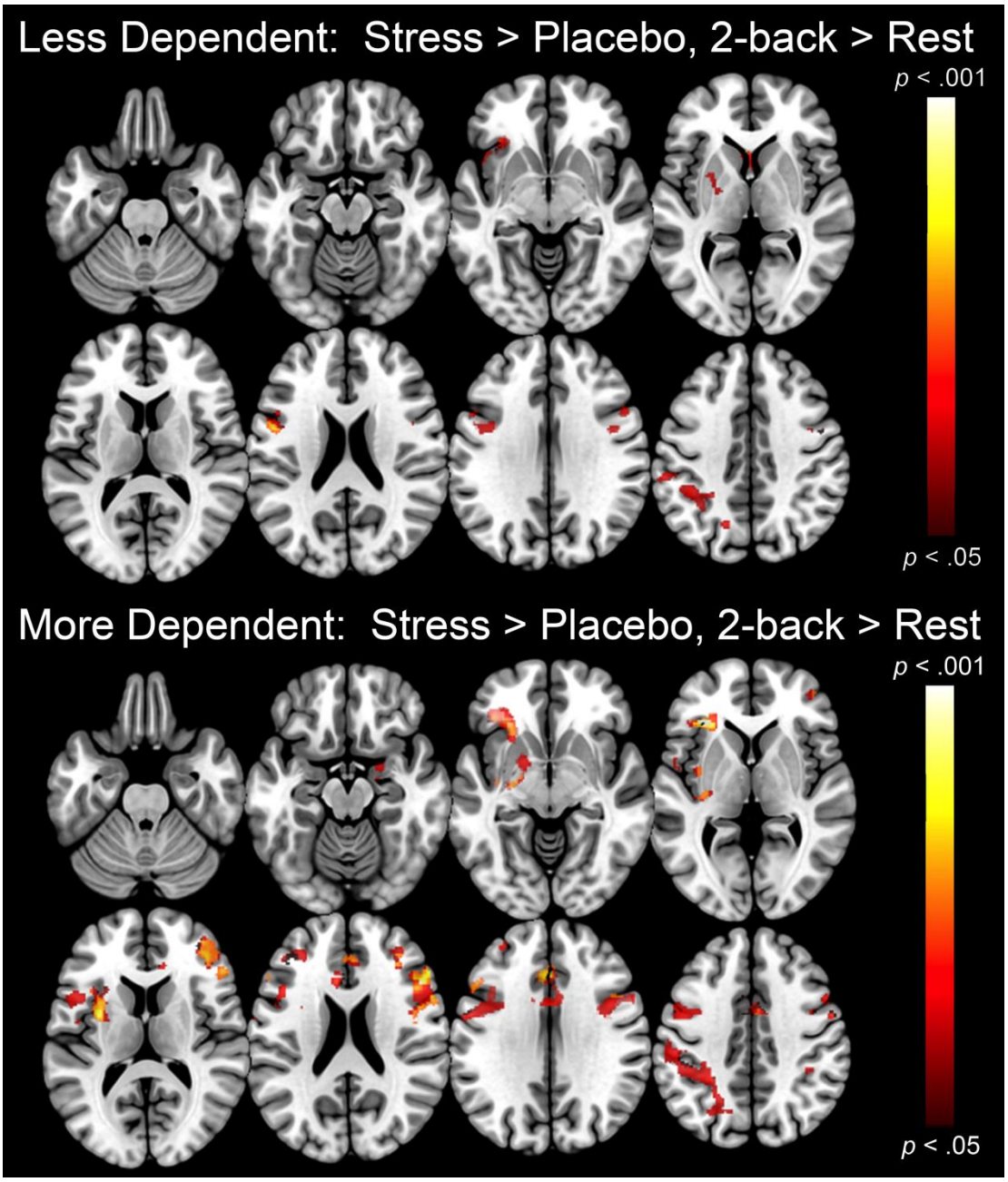

Figure 4.45: Letter 2-back Maps by Nicotine Dependence. Cluster-level corrected (p < .05) letter 2-back (> fixation cross rest) difference maps median split by FTND score are depicted on contiguous axial slices: less (upper panel) and more nicotine dependent (lower panel) stress > placebo. Lighter color reflects more BOLD activation.

4.2.20 Cued N-back Behavioral Data

fMRI behavioral data: smoking vs. neutral cued. Accuracy and response latency were evaluated across N-back levels (0-, 1-, and 2-back) and by image type (smoking vs. neutral) for both experimental sessions.

Neutral images. rmANOVA indicated response accuracy decreased as N-back task difficulty increased (0-back = 94.3 ± 10.9%; 2-back = 64.1 ± 19.5%) for neutral images across experimental sessions (N-back effect: $F(2,26) = 31.57$, $p < .001$; partial $\eta^2 = 0.71$ [very large effect size]; Figure 4.46). There was no effect of experimental session on neutral image response accuracy

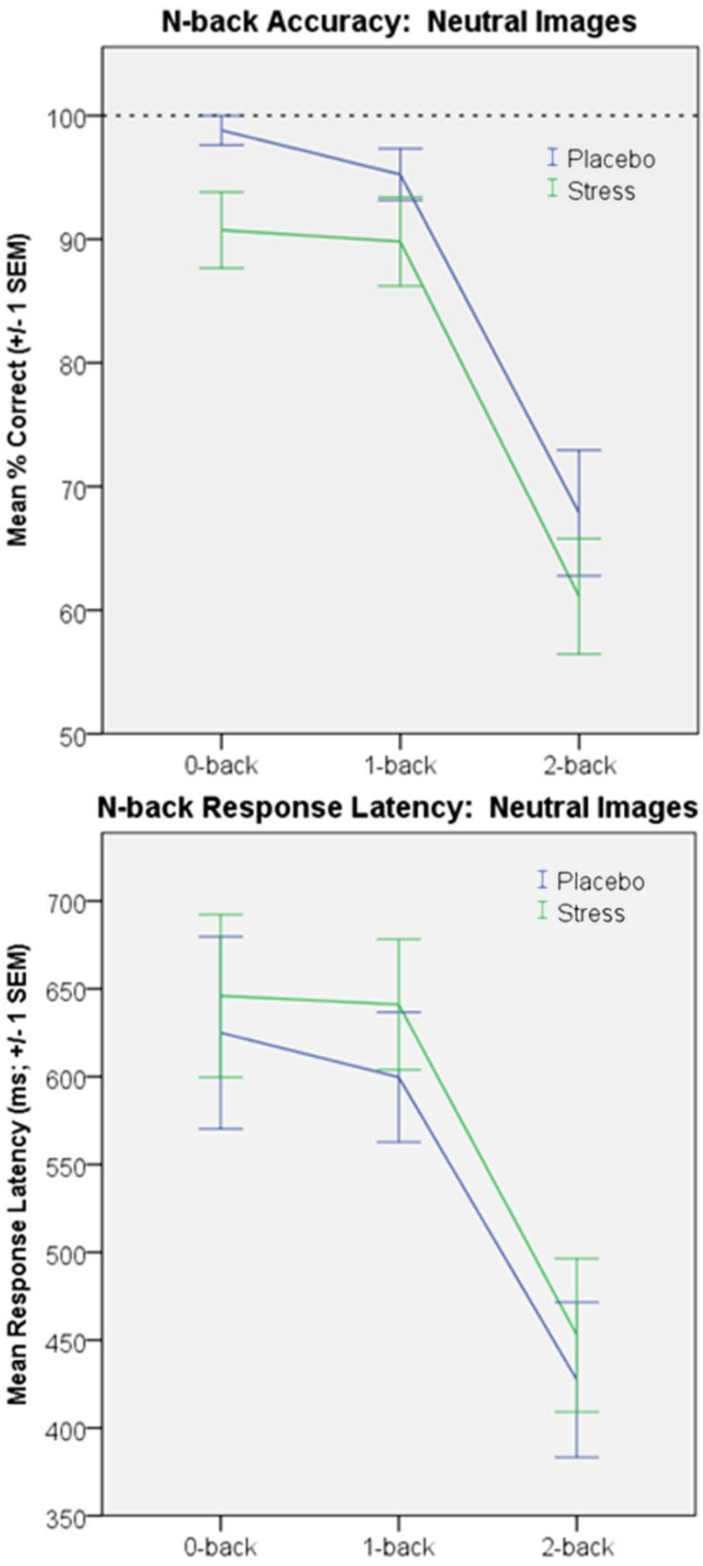

Figure 4.46 & 4.47: Neutral N-back Response Accuracy and Response Latency. Mean (± 1 SEM) response accuracy (% correct; upper panel) and response latency (ms; lower panel) for neutral images during the placebo (blue line) and active stress session (green line) are depicted across N-back levels.

across N-back levels (Dose effect: p = .14; N-back X Dose interaction: p = .82).

For neutral images, response latency decreased as N-back difficulty increased (N-back effect: $F(2,26) = 13.40$, $p < .001$; partial $\eta^2 = 0.51$ [very large effect size]; 0-back = 649.3 ± 231.7ms; 2-back = 449.8 ± 193.8ms; Figure 4.47). Response latency was not differentially affected by experimental session across N-back levels (Dose effect: p = .73; N-back X Dose interaction: p = .69).

Smoking images. rmANOVA indicated response accuracy non-significantly decreased as N-back difficulty increased (0-back = 95.8 ± 10.4%; 2-back = 91.1 ± 13.4%) for smoking images across both experimental sessions (N-back

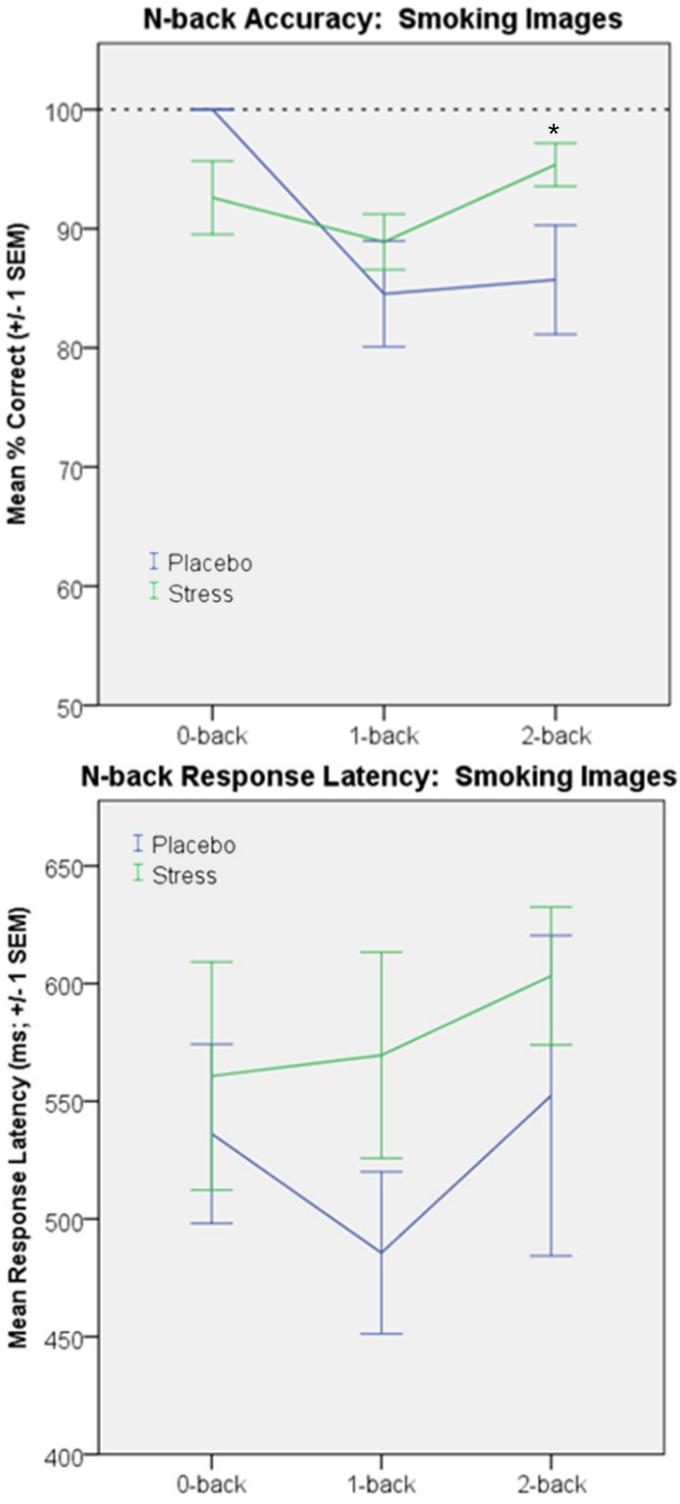

Figure 4.48 & 4.49: Smoking N-back Response Accuracy and Response Latency. Mean (± 1 SEM) response accuracy (% correct; upper panel) and response latency (ms; lower panel) for smoking images during the placebo (blue line) and stress session (green line) are depicted across N-back levels. Paired t-test: *p

effect: $F(2,26) = 3.08$, $p = .06$; partial $\eta^2 = 0.19$ [moderate-to-large effect size]; Figure 4.48). There was no effect of experimental session on smoking image response accuracy across N-back levels (Dose effect: $p = .47$). However, a significant N-back X Dose interaction ($F(2,26) = 8.24$, $p < .01$; partial $\eta^2 = 0.39$ [very large effect size]) indicated response accuracy decreased more as N-back difficulty increased during the placebo session (relative to the stress session).

For smoking images, response latency increased as N-back difficulty increased (N-back effect: $F(2,26) = 3.69$, $p < .05$; partial $\eta^2 = 0.22$ [moderate-to-large effect size]; 0-back = 556.4 ± 191.4ms; 2-back =

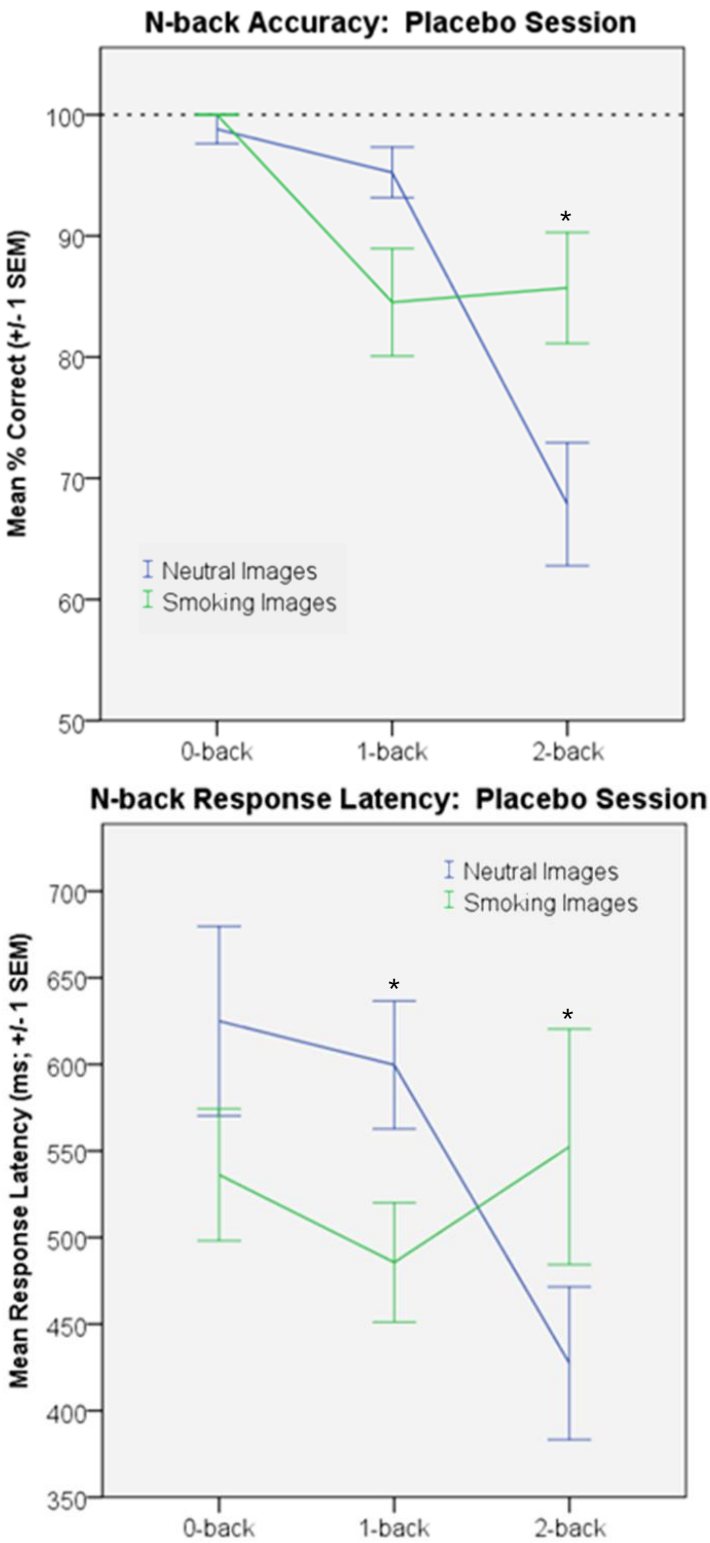

Figure 4.50 & 4.51: Placebo N-back Response Accuracy and Response Latency. Mean (± 1 SEM) response accuracy (% correct; upper panel) and response latency (ms; lower panel) during the placebo session are depicted by image type (neutral: blue line vs. smoking: green line) across N-back levels. Paired t-test: *$p < .05$

602.3 ± 231.7ms; Figure 4.49). Response latency was not differentially affected by experimental session across N-back levels (Dose effect: p = .33; N-back X Dose interaction: p = .46).

Neutral vs. smoking images: placebo session. rmANOVA indicated response accuracy significantly decreased as N-back difficulty increased (0-back = 99.4 ± 3.2%; 2-back = 76.8 ± 20.0%) for both image types (N-back effect: $F(2,26) = 22.05$, $p < .001$; partial $\eta^2 = 0.63$ [very large effect size]; Figure 4.50). There was no effect of image type on response accuracy across N-back levels (Image effect: p = .38). However, a significant N-back X Image interaction ($F(2,26) = 10.98$, $p < .001$; partial $\eta^2 = 0.46$ [very large effect size]) indicated response accuracy decreased less for smoking images as N-back difficulty increased, relative to neutral images.

rmANOVA indicated response latency non-significantly decreased as N-back difficulty increased (N-back effect: $F(2,26) = 2.91$, $p = .07$; partial $\eta^2 = 0.18$ [moderate-to-large effect size]; 0-back = 580.6 ± 178.8ms; 2-back = 489.9 ± 220.1ms; Figure 4.51). Response latency did not differ across N-back levels as a function of image type (Image effect: p = .43). However, a significant N-back X Image interaction ($F(2,26) = 6.43$, $p < .01$; partial $\eta^2 = 0.33$ [very large effect size]) indicated response latency decreased more for neutral images as N-back difficulty increased, relative to smoking images.

Neutral vs. smoking images: stress session. rmANOVA indicated response accuracy significantly decreased as N-back difficulty increased (0-back = 91.7 ± 12.9%; 2-back = 78.2 ± 22.8%) for both image types (N-back effect: $F(2,34) = 16.23$, $p < .001$; partial $\eta^2 = 0.49$ [very large effect size]; Figure 4.52). A main effect of image type across

N-back levels ($F(1,17) = 20.12$, $p < .001$; partial $\eta^2 = 0.54$ [very large effect size]) indicated that participants responded more accurately for smoking vs. neutral images. In addition, a significant N-back X Image interaction ($F(2,34) = 17.18$, $p < .001$; partial $\eta^2 = 0.50$ [very large effect size]) indicated that accuracy decreased less for smoking images (relative to neutral images) as N-back difficulty increased.

rmANOVA indicated response latency significantly decreased as N-back difficulty increased (N-back effect: $F(2,34) = 4.39$, $p < .05$; partial $\eta^2 = 0.21$ [moderate-to-large effect size]; 0-back = 603.4 ± 202.9ms; 2-back = 528.0 ± 173.0ms; Figure 4.53). Response latency did not differ across N-back levels as a function

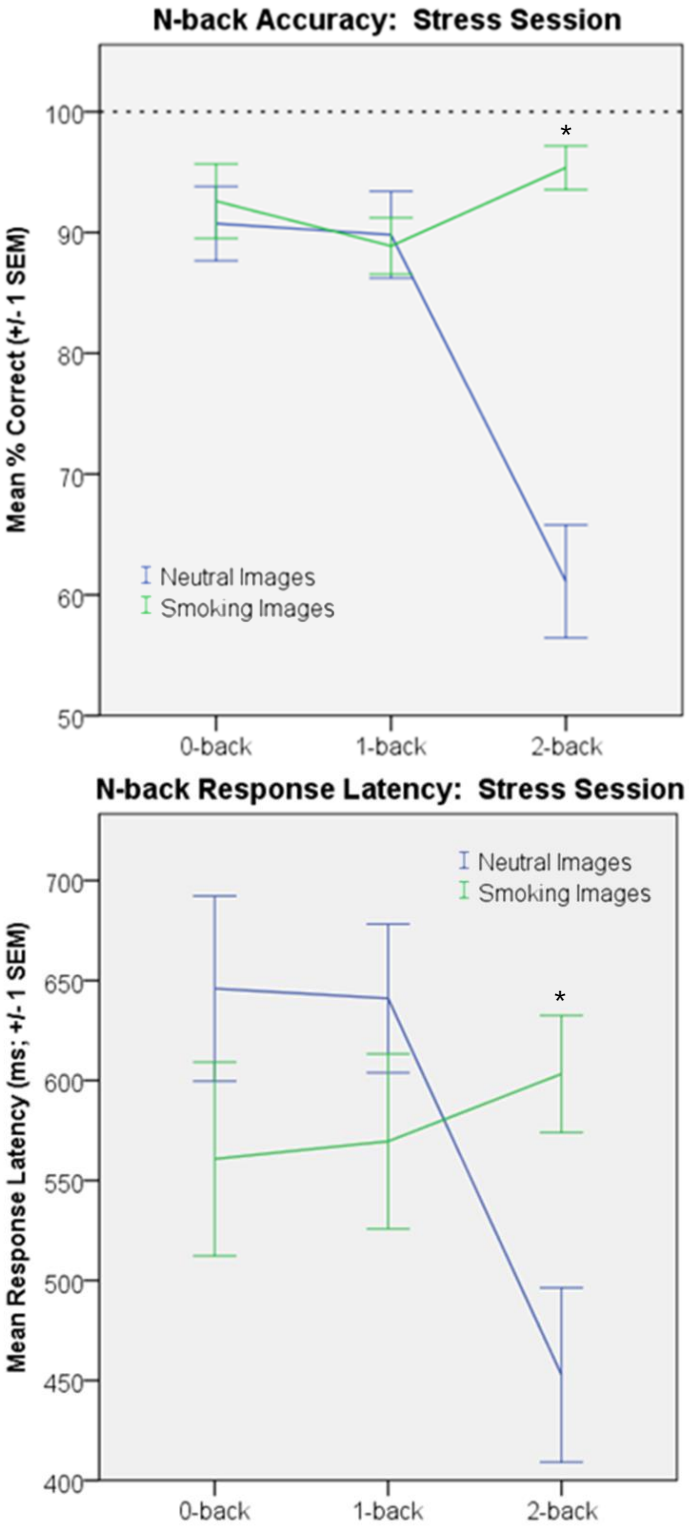

Figure 4.52 & 4.53: Stress N-back Response Accuracy and Response Latency. Mean (± 1 SEM) response accuracy (% correct; upper panel) and response latency (ms; lower panel) during the stress session are depicted by image type (neutral: blue line vs. smoking: green line) across N-back levels. Paired t-test: *$p < .05$

of image type (Image effect: p = .94). However, a significant N-back X Image interaction ($F(2,34) = 11.65$, $p < .001$; partial $\eta^2 = 0.41$ [very large effect size]) indicated that response latency decreased more for neutral images as N-back difficulty increased, relative to smoking images.

4.2.21 Cued N-back fMRI Data

0-back fMRI activation. One subject was excluded from all fMRI BOLD activation analyses that contrasted image type (smoking vs. neutral) because he switched to e-cigarettes and reported paper cigarettes were aversive. BOLD activation analyses focused on the effect of image type (smoking > neutral and neutral > smoking) across N-back levels (0-, 1-, and 2-back; Figure 4.54). During the placebo session, 0-back BOLD response was contrasted by image type. Smoking images elicited greater BOLD response in the amygdala, mPFC, mOFC, and ventral striatum, relative to neutral images. Activation in these regions is often attributed to drug cue salience and/or appetitive motivation. Interestingly, a few clusters in the dlPFC were activated during smoking > neutral cues. The 0-back is an attentional control task and does not substantially engage working memory processes (i.e. dlPFC). Thus, it was plausible that dlPFC activation was associated with network interactions with the mOFC and/or mPFC.

Notably, during the stress session, smoking cues did not elicit the same degree of BOLD response in the mPFC, mOFC, and ventral striatum. A few small clusters in the striatum and one in mOFC/mPFC survived cluster-level correction. These findings were contrary to *a priori* hypotheses.

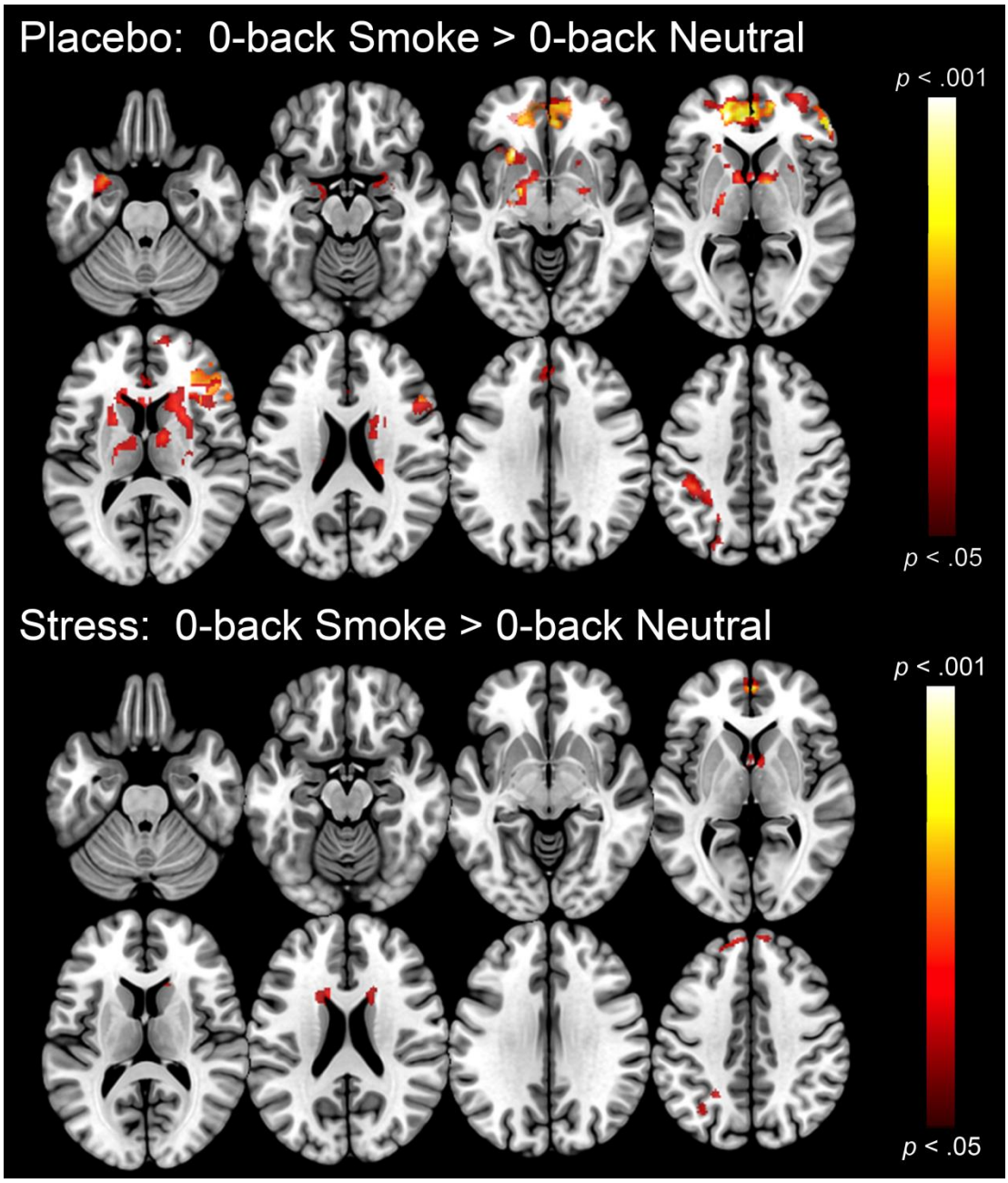

Figure 4.54: Cued 0-back fMRI Activation Maps. Cluster-level corrected ($p < .05$) activation maps during 0-back (smoking > neutral images) are depicted on contiguous axial slices for the placebo (upper panel) and stress session (lower panel). Lighter color reflects more BOLD activation.

1-back fMRI activation. During both experimental sessions, smoking > neutral images elicited robust activation across the network of interest at the 1-back level (Figure 4.55). During placebo, widespread BOLD activation was elicited in the amygdala, mOFC, mPFC, ventral and dorsal striatum, dPFC, dlPFC, dACC, and superior parietal lobule. During the stress session, clusters were found throughout the striatum and PFC, but not in the mOFC or superior parietal lobule. Similar to the 0-back findings, smoking images elicited greater BOLD activation in reward network regions during placebo, relative to the active stress.

2-back fMRI activation. During placebo, subtle BOLD effects were observed in the mOFC, mPFC, and striatum for smoking > neutral images (Figure 4.56). During stress, BOLD activation was limited to three clusters: mOFC, dorsal striatum, and dorsal PFC. Task difficulty (2-back) may have diminished the salience of the smoking images (relative to neutral images). Individuals may have been preoccupied with task performance at the expense of image salience. Notably, smoking images were associated with higher response accuracy (> neutral images) across experimental sessions.

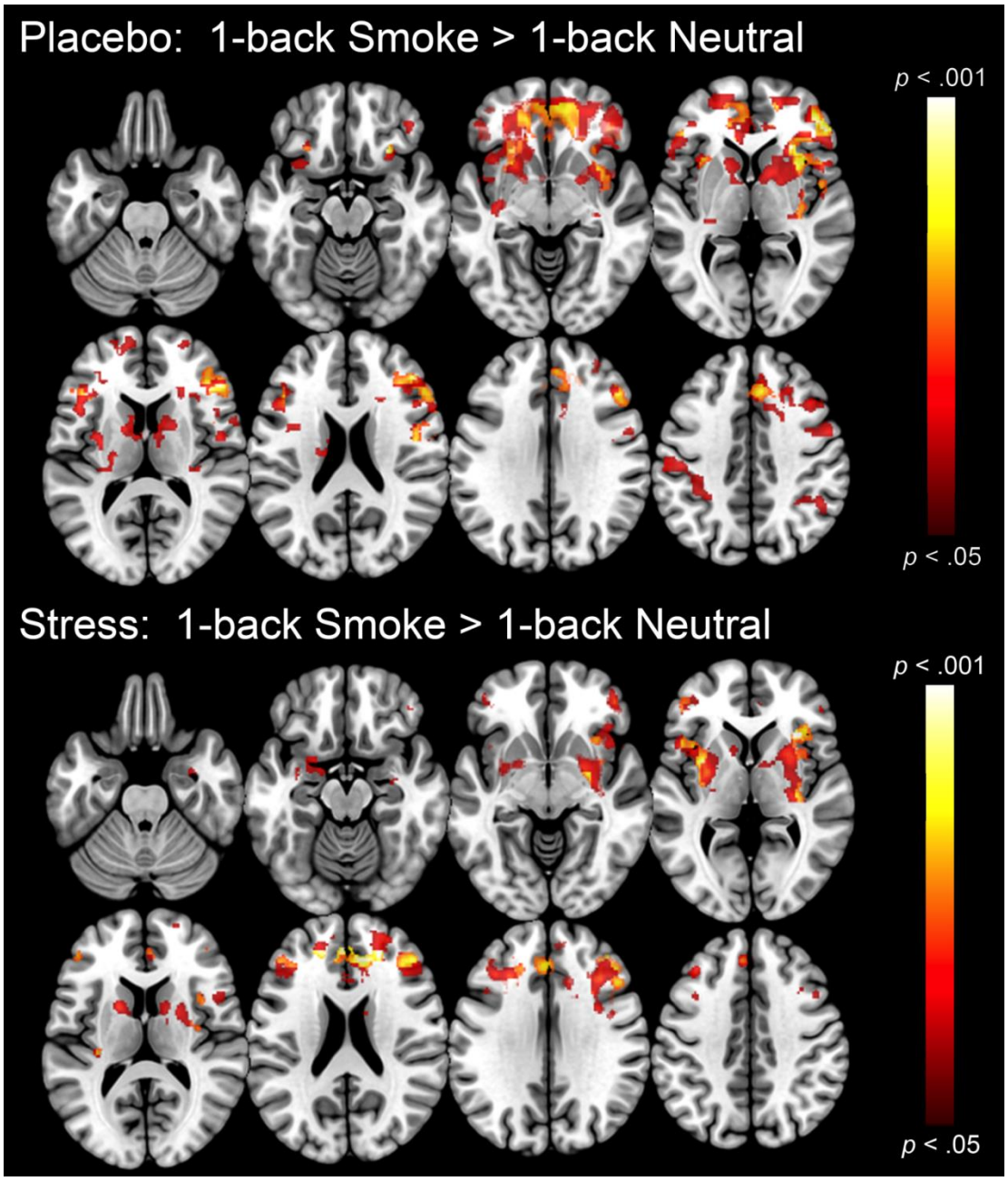

Figure 4.55: Cued 1-back fMRI Activation Maps. Cluster-level corrected ($p < .05$) activation maps during 1-back (smoking > neutral images) are depicted on contiguous axial slices for the placebo (upper panel) and stress session (lower panel). Lighter color reflects more BOLD activation.

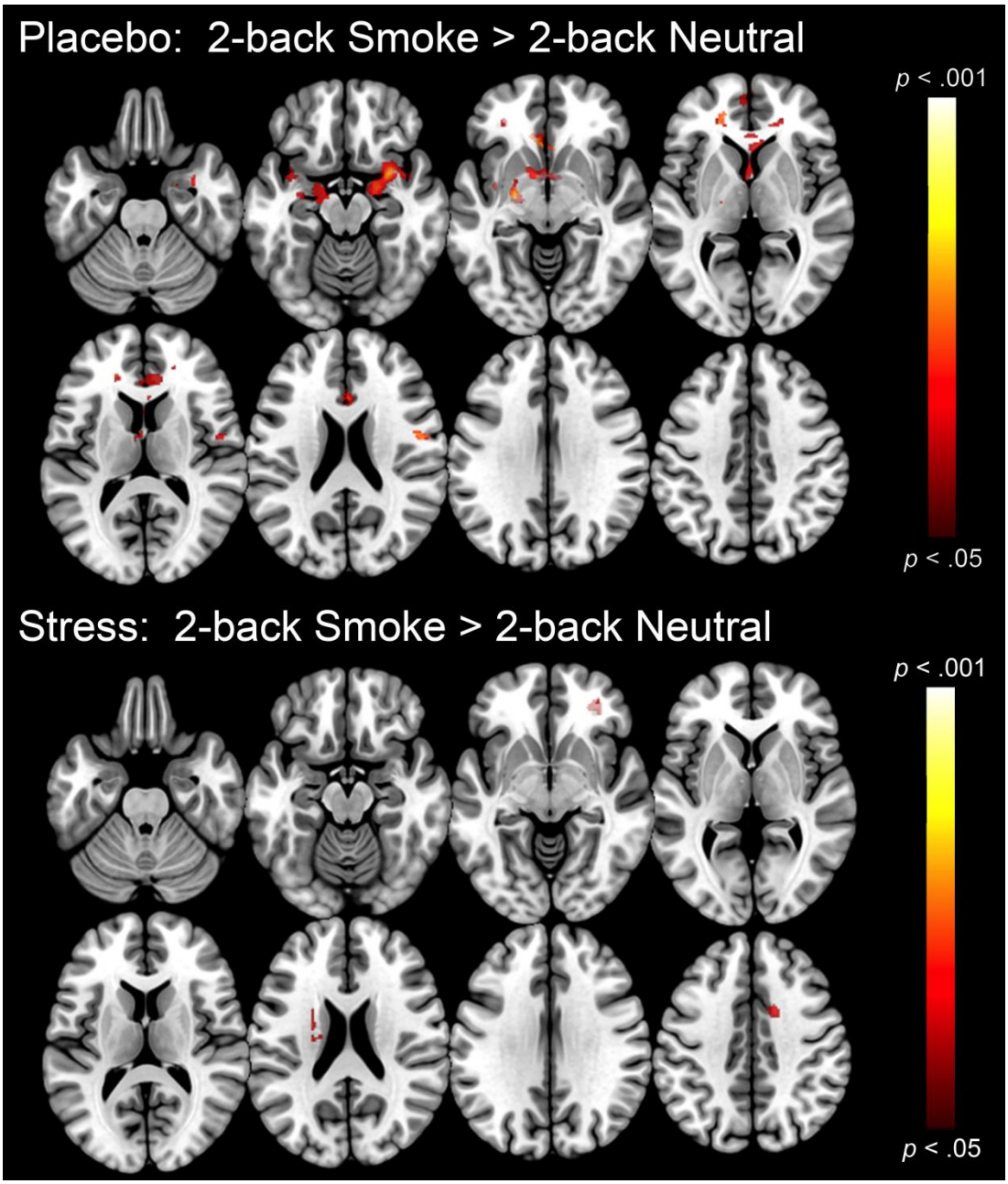

Figure 4.56: Cued 2-back fMRI Activation Maps. Cluster-level corrected ($p < .05$) activation maps during 2-back (smoking > neutral images) are depicted on contiguous axial slices for the placebo (upper panel) and stress session (lower panel). Lighter color reflects more BOLD activation.

Overall fMRI activation. BOLD activation associated with smoking cues (smoking > neutral images) across all N-back levels were contrasted by experimental session (Figure 4.57). For placebo > stress, robust BOLD activation was observed in the ventral

and dorsal striatum, mPFC, mOFC, dlPFC, dPFC, dACC, and superior parietal lobule. Notably, large clusters in the mOFC and mPFC were identified and may be attributed to salience of smoking (> neutral) images, independent of task difficulty. For stress > placebo, one small cluster was observed (mPFC/dACC). Smoking images elicited a more robust BOLD response in the placebo, relative to the stress, session, contrary to *a priori* hypotheses.

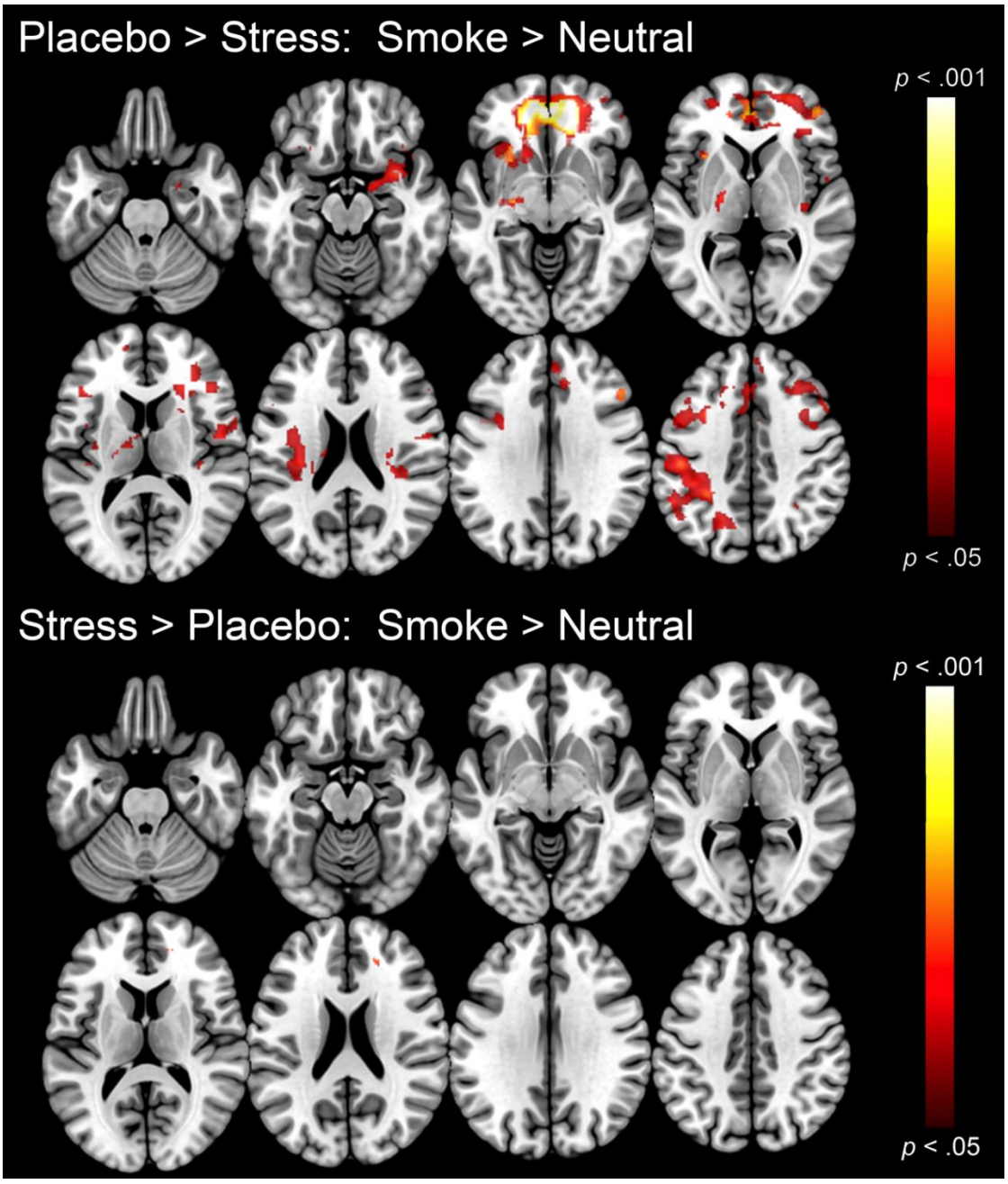

Figure 4.57: Image Effect Difference Maps. Cluster-level corrected ($p < .05$) difference activation maps across N-back levels (smoking > neutral images) are depicted on contiguous axial slices: placebo > stress (upper panel) and stress > placebo (lower panel). Lighter color reflects more BOLD activation.

4.2.22 fMRI vs. ^{1}H fMRS

Exploratory analyses investigated statistical relationships between ^{1}H fMRS GLU levels and BOLD fMRI response during the letter 2-back task. Using each subject's ^{1}H

fMRS voxel as a mask, Z scores (peak activation) and peak cluster extents were extracted from BOLD contrasts (letter 2-back > fixation-cross) at the same temporal resolution (32s; 2-back A and B) as ^{1}H fMRS analyses. This strategy resulted in two correlation matrices: Z scores and cluster extents. Each matrix contained four rows of fMRI metrics (2-back A and B X 2 task repetitions) by eight columns of ^{1}H fMRS GLU levels (first ^{1}H fMRS task block was excluded [practice effect]; 2-back A and B X 4 task repetitions) for a total of 32 matrix cells. Bivariate Pearson correlations were used to examine statistical relationships with a liberal threshold ($p \leq .10$). During the placebo session, 7 of 32 cells (21.9%) were positively correlated for fMRI Z scores and 5 of 32 cells (15.6%) were positively correlated for fMRI cluster extents. During the stress session, 1 cell (3.1%) was negatively correlated for fMRI Z scores and none were correlated for fMRI cluster extents.

CHAPTER 5 DISCUSSION

5.1 ^{1}H fMRS Pilot Study Discussion

5.1.1 ^{1}H fMRS Pilot Study Results Overview

The goals for the pilot study were three-fold: 1) develop and evaluate an automated method for accurate and reliable single voxel placement, 2) develop a working memory ^{1}H fMRS paradigm, and 3) quantify GLU levels during working memory task performance. Our results demonstrated that: automated voxel placement (AVP) method was highly accurate and reliable; the working memory paradigm was feasible; LCModel quantification of metabolite levels at 32s temporal resolution (8 avgs) was reliable; and left dlPFC GLU levels were modulated during working memory task performance. To the best of our knowledge, this was the first study in human subjects that demonstrated dlPFC GLU levels were significantly modulated during working memory task performance. This study validated a novel biomarker of dlPFC cognitive task engagement that is not confounded by vasoactive medications or subject-level differences in cardiovascular health (e.g. aging or chronic substance abuse [cigarette smoking]).

Healthy, medication-free, and well-educated right-hand-dominant college students (N = 16) narrowly selected for age were recruited to participate in a brief pilot study. Participants were instructed to perform two behavioral tasks during continuous *in vivo* single voxel ^{1}H MRS spectra acquisition (Figure 3.1). During the first task (continuous fixation-cross), participants were instructed to focus their visual gaze on a static fixation-cross, relax, and let their thoughts drift. The second task (letter 2-back) included two phases. During phase one, participants were instructed to focus their

visual gaze on a flashing checkerboard (3Hz), relax, and let their thoughts drift. Pilot research in our laboratory demonstrated that flashing checkerboard stabilized GLU levels (minimized variance) more effectively than other stabilization paradigms (unpublished data). During phase two, participants were instructed to complete a letter 2-back task with interleaved blocks of fixation-cross rest. The letter 2-back task is a well-established working memory paradigm. A meta-analysis of letter 2-back fMRI studies demonstrated that task performance was consistently associated with bilateral dlPFC BOLD activation (Owen et al., 2005).

Behavioral data demonstrated that participants were task compliant. Mean letter 2-back response accuracy was high across task blocks (mean accuracy: 94.8% ± 10.7%; mean response latency: 644 ± 171ms). Response accuracy significantly increased across task blocks (from 88.5% in block 1 to 96.9% in block 7; Figure 4.2).

5.1.2 Automated Voxel Placement (AVP)

As part of my graduate training, we developed and evaluated an automated voxel placement (AVP) method to address a frequently over-looked source of error variance in single-voxel magnetic resonance spectroscopy research studies: inconsistent voxel placement. It is well-established that neurochemistry varies by anatomical region and voxel tissue composition (gray vs. white matter) (Erecińska & Silver, 1990; Pouwels & Frahm, 1998). Therefore, inconsistent voxel placement across research subjects (or longitudinally within subjects) increases likelihood of Type I and II error. Three Linux- and Matlab-based scripts were developed: avp_create, avp_coregister, and avp_overlap. Avp_create facilitated creation of a library of voxel locations in template space prior to subject scanning. At the scanner, avp_coregister

automatically coregistered the template voxel to the current research subject based on his/her head position in the scanner (T_1-weighted image; Figure 3.3). At the end of a research study, avp_overlap will extract voxel location information from each subject's .rda file (ASCII file created during MRS spectra acquisition), re-create the voxel in subject space, coregister the voxel to template space, and calculate voxel tissue composition, geometric voxel overlap with the template voxel (i.e. voxel placement accuracy) and geometric voxel overlap across research subjects (i.e. voxel placement reliability). AVP was developed and tested for human brain imaging research on a 3T Siemens Verio system. However, AVP was programmed to be scanner system-, field strength-, anatomy- and subject population-independent.

AVP was used to prescribe voxels for 15 of the 16 ^{1}H fMRS pilot study participants (AVP not used for one subject; experimenter error). Voxel placement accuracy (mean geometric voxel overlap with the template location = 93.2%) and reliability (mean geometric voxel overlap across all participants = 89.9%; Figure 4.1) were excellent. Mean voxel tissue composition was 36.8 ± 3.8% gray and 60.8 ± 4.5% white matter.

5.1.3 GLU Modulation

LCModel fit and metabolite quantification was 100% automated. LCModel fit and GLU quantification at 32s resolution (8 avgs) was reliable (Table 4.1). Importantly, LCModel fit quality did not differ as a function of experimental task. Results from this pilot study demonstrated that GLU levels were modulated during working memory task performance. Relative to continuous fixation-cross rest, left dlPFC GLU levels were significantly higher (3.4%) during the first 32s of letter 2-back task performance (2-back

A) across seven task blocks (Figure 4.5). Similarly, the final 32s of letter 2-back task performance (2-back B) were elevated (2.9%), but non-significantly higher (p = .07) than continuous fixation-cross rest (Figure 4.5). These findings demonstrated, for the first time in human subjects, that working memory task performance increased *in vivo* dlPFC GLU levels.

Relative to interleaved fixation-cross rest, results were more complicated. 2-back A and B exhibited significant Time X Task interactions relative to interleaved fixation-cross rest (Figures 4.7, 4.10, and 4.11). GLU levels were higher during initial task blocks, but lower during middle task blocks. These findings indicate that working memory task performance was associated with elevated GLU levels, but the effect was time-limited. Significant Time effects indicated that GLU levels generally increased across task blocks. We speculated that 2-back task performance became routine and unchallenging for this well-educated sample. Evidence to support this assertion was twofold: 1) response accuracy significantly increased across task blocks (nearly perfect response accuracy after the initial task block), and 2) GLU levels significantly increased across task blocks. A significant increase in GLU levels across task blocks suggested participants engaged their dlPFC during 2-back and during interleaved fixation-cross rest – thus, participants were not truly 'resting.' As participants demonstrated task mastery, their attention may have drifted during the interleaved rest blocks, instead of 'resting.' The dlPFC is involved in numerous cognitive processes – directed attention, rumination, and executive control of lower structures – any of which could have modulated GLU levels. Future studies will investigate an interleaved 0-back attention control task, instead of the interleaved fixation-cross used herein.

The ^{1}H fMRS signal is a direct measurement of *in vivo* GLU molecules from all sources within the voxel. The ^{1}H fMRS signal does not differentiate cell types (pre- vs. post-synaptic neurons or glia) or compartments (intracellular vs. extracellular). Results presented herein demonstrated that GLU concentration (i.e. total number of GLU molecules within the voxel location) was higher during letter 2-back, relative to fixation-cross rest. We interpret these findings as follows: task-related cognitive demand (i.e. increased neural activity) resulted in increased metabolic activity in the dlPFC, which was measured herein as elevated GLU levels. The literature and limitations of the approach provided context for interpretation of these data.

A series of well-controlled studies spanning decades at Yale University demonstrated that neuronal spiking frequency increased in the dlPFC during a spatial working memory task in non-human primates (Goldman-Rakic, 1995). Using the same experimental approach, Arnsten and colleagues demonstrated that spatial working memory was associated with persistent excitatory microcircuits ("delay" cells; primarily mediated via GLU molecules binding NMDA NR2B receptor subunits) in layer III of the cortex (Wang et al., 2013). These microcircuits are thought to maintain memory traces during the delay period (time period between the presentation of stimulus and the target [i.e. blank screen]) such that the primate can respond accurately (Wang et al., 2013). These studies demonstrated that working memory task performance was associated with persistent neural activity, mediated via glutamatergic synapses, in the dlPFC. However, it is unlikely the signal measured in the present study reflected GLU molecules involved in excitatory neurotransmission. Evidence to support this assertion was two-fold: 1) low extracellular GLU concentration and 2) synaptic GLU time scale.

Intracellular GLU concentration is approximately 10 mM (Erecińska & Silver, 1990), whereas extracellular and cerebrospinal GLU concentrations are 0.5-1.0 μM and 1-10 μM, respectively (Schousboe, Bak, Sickmann, Sonnewald, & Waagepetersen, 2007). Thus, the overwhelming majority of the ^{1}H fMRS GLU signal was intracellular (~10^{3} higher concentration than extracellular). Thus, even a 50% increase in synaptic GLU concentration would only increase total ^{1}H fMRS-measured GLU by ~0.0014%. In addition, extracellular GLU molecules are present in the synapse for < 5ms before binding transporters, ion-channels, or G-protein coupled receptors. If the first RF pulse (in the PRESS sequence) excited a GLU molecule traversing the synapse, it is likely the magnetization would be negated when that GLU molecule bound a receptor or transporter before digitization of the signal (TE = 23ms). Therefore, although GLU is the primary excitatory neurotransmitter and previous work found that working memory is mediated via cortical glutamatergic microcircuits in the dlPFC, it is unlikely the signal measured herein reflects GLU molecules involved in neurotransmission. Rather, the overwhelming majority of signal measured in this study was associated with GLU molecules found in pre-synaptic vesicles, circulating as neurochemical intermediates for other neurotransmitters (GABA and glutamine), or as an anaplerotic substrate of the TCA cycle. Fortunately, interpretation of the present data is informed by prior research, which demonstrated GLU concentration scaled with neural activity: increased neural activity was associated with increased GLU levels (Mangia et al., 2006; Schaller et al., 2013; Schaller et al., 2014). Elevated neuronal activity is coupled with elevated glucose extraction and metabolism that should result in elevated GLU levels from all sources measured via ^{1}H fMRS. Extensive ^{13}C MRS research demonstrated GLU-glutamine

neurotransmission cycling rate was tightly coupled with oxidative metabolism in awake and anesthetized rodents (Douglas L Rothman, De Feyter, Graaf, Mason, & Behar, 2011; D. L. Rothman, De Feyter, Maciejewski, & Behar, 2012). A nearly 1:1 relationship indicated that for every molecule of GLU released into the synapse and recycled to the presynaptic neuron as glutamine, approximately one molecule of glucose was metabolized in the TCA cycle (Douglas L Rothman et al., 2011). In other words, elevated spiking activity and excitatory neurotransmission corresponded with elevated metabolic activity to support cellular energy demands (e.g. restoration of ion concentration gradients and metabolic intermediates). Thus, the GLU signal measured in this study likely reflected GLU molecules involved in metabolic events associated with excitatory neurotransmission driven by working memory task performance. Our findings were consistent with previous ^{1}H fMRS studies that demonstrated elevated GLU levels (~2-4%) during neural activity (Mangia et al., 2006; Schaller et al., 2013; Schaller et al., 2014) and a meta-analysis of fMRI studies that found neural activity in the dlPFC was consistently elevated during 2-back task performance (Owen et al., 2005).

5.1.4 Limitations and Alternative Explanations

This pilot study had a number of important limitations. First, as is the case with all single voxel MRS studies, this study was susceptible to partial volume effects. Three factors minimized the influence of partial volume effects on these findings. Voxel placement reliability was excellent (mean geometric voxel overlap across subjects = 89.9%) which minimized partial volume effects. Moreover, tissue voxel composition variability was low across subjects (gray and white matter coefficient of variation percentage was 10.3% and 7.4%, respectively) and included in the calculation of GLU

concentration. Finally, outcome analyses were limited to within-subject comparisons (i.e. GLU levels contrasted by experimental task). Therefore, it was unlikely partial volume effects influenced study findings. Second, we were unable to reliably quantify other relevant neurotransmitters (e.g. GABA and glutamine) due to SNR limitations in the present study. Future studies could use higher field strengths, lower temporal resolution (e.g. more averaging), or other sequences (e.g. MEGA-PRESS) to investigate task-related modulation of GABA and glutamine levels.

There were several alternative explanations for task-related modulation of GLU levels in the dlPFC. First, as reported in other ^{1}H fMRS studies, there was possibility of a BOLD effect (Mangia et al., 2006; Schaller et al., 2013; Schaller et al., 2014). Increased neural activity will increase concentration of oxygenated blood (oversupply of oxygenated hemoglobin relative to oxygen extraction; BOLD effect) which can influence T_2* and spectral linewidth. A BOLD effect would result in narrow metabolite peaks (FWHM). Inconsistent with prior studies, we found no evidence of a significant BOLD effect on FWHM (Task and Time X Task interaction *p*s > .10). Moreover, LCModel should be robust to the influence of spectral linewidth on metabolite level quantification. Indeed, during 2-back A, no metabolites differed as a function of experimental task other than GLU. Second, GLU's transverse relaxation (T_2*) could have changed as a result of task performance. The equation $S = S_0 e^{-TE/T_2}$ describes the relationship between the initial signal (S_0), the measured signal (S), echo time (TE), and transverse magnetization (T_2). To explain the observed effects (task-related GLU levels increased 2.9-3.4% relative to continuous fixation-cross rest), transverse relaxation (T_2*) would need to increase > 30% (GLU T_2 = ~200ms at 3T in the dlPFC (Choi et al., 2006)). Prior

studies indicated T_2* changes alone are unlikely to explain the observed data (Ogawa et al., 1992). Third, Type I error is possible. However, evidence against this explanation was three-fold: 1) results reported herein were consistent with fMRI, fMRS, and electrophysiology literature; 2) the experimental design was carefully selected to mitigate Type I error (e.g. use of a stabilization task [flashing checkerboard], two rest comparison conditions, cognitively-healthy and unmedicated sample, high task compliance, and reliable voxel placement), and 3) moderate effect size (i.e. study was not 'over-powered'). Fourth, LCModel fit quality could have been biased and 'over-fit' GLU levels during 2-back task performance, relative to rest. This was also unlikely. Individual raw spectra were phase- and shift-corrected prior to averaging and LCModel fit (using a 100% automated procedure). Moreover, LCModel fit characteristics (FWHM, SNR, GLU CRLB% and GLN CRLB%) did not differ as a function of experimental task (Table 4.1). Finally, LCModel fit of GLU was reliable (GLU CRLB ~7 ± 1%) across task and rest conditions.

5.1.5 ^{1}H fMRS Pilot Study Results Summary

In summary, this pilot study demonstrated that AVP was an accurate and reliable method of automated voxel placement, LCModel reliably fit ^{1}H fMRS spectra and quantified GLU levels at a cognitive task-relevant time scale (32s; 8 avgs), and letter 2-back task performance modulated GLU levels in the left dlPFC, relative to fixation-cross rest. These data validated an *in vivo* biomarker of cognitive task-related neural engagement. To our knowledge, this was the first demonstration of working memory task-related modulation of GLU levels in humans. However, to date, similar studies using ^{1}H fMRS found cognitive task- or sensory stimulation-related GLU modulation in a

variety of brain regions, including: dlPFC, hippocampus, occipital lobe, and motor cortex. The value of this novel biomarker is twofold: 1) neurochemical specificity and 2) neurovascular coupling independence. ^{1}H fMRS is a direct *in vivo* measure of GLU (and other metabolites). Neurochemical specificity of this approach provides insight not possible using other neuroimaging approaches (e.g. fMRI). While not feasible in the present study, future studies at higher field strength could leverage this approach to examine task-related modulation of glutamine. It is estimated that ~80% of glutamine molecules are directly involved in the GLU-glutamine cycle (i.e. excitatory neurotransmission) (Gruetter, Seaquist, & Ugurbil, 2001; Lebon et al., 2002; Mason, Petersen, De Graaf, Shulman, & Rothman, 2007; D. L. Rothman et al., 2012; Sibson et al., 1997). Second, interpretation of the BOLD fMRI signal (most widely used *in vivo* neuroimaging approach) is complicated by neurovascular coupling. For many research questions, neurovascular coupling is not an insurmountable obstacle. However, interpretation of BOLD signal from research studies that include older populations, compare younger and older subjects, include subjects with cardiovascular confounds (e.g. heart disease or chronic substance use), or use vasoactive pharmacological challenges (e.g. this dissertation study) can be challenging. ^{1}H fMRS is not confounded by neurovascular coupling, and thus, presents an alternative approach to BOLD fMRI for questions of task-related changes in brain function.

5.2 Dissertation Results Discussion

5.2.1 Dissertation Results Overview

The overarching goals for this dissertation project were two-fold: 1) investigate the effects of pharmacological stress manipulation on nicotine-seeking and self-administration, and 2) investigate a plausible neurobiological mechanism by which acute stress may potentiate nicotine-seeking and self-administration. Results demonstrated that the complex experimental design (within-subject, placebo-controlled, double-blind, randomized cross-over design with multi-modal neuroimaging and nicotine self-administration outcome variables) was feasible. Oral pretreatment with pharmacological agents (YOH 54mg + HYD 10mg) significantly increased biomarkers (BP, heart rate, saliva cortisol, and saliva α-amylase) of a physiological stress response, relative to placebo (YOH 0mg + HYD 0mg). Experimental stress significantly increased nicotine-seeking and self-administration (relative to placebo) among non-treatment-seeking cigarette smokers (controlling for nicotine dependence level [FTND]). Multi-modal neuroimaging demonstrated that acute stress impaired dlPFC function and task-related engagement – a plausible neurobiological mechanism of stress-potentiated nicotine self-administration. In the remainder of this dissertation, results will be interpreted, limitations and alternative explanations discussed, and treatment implications described.

5.2.2 Stress and Relapse

As described in the Sections 2.2 and 2.3, ample evidence links experimental stress and substance use relapse (or models of relapse). Preclinical studies reliably demonstrated that pharmacological agents (e.g. YOH) reinstated drug self-administration behavior (model of relapse) across drugs of abuse (Ahmed & Koob,

1997; Buczek et al., 1999; de Jong et al., 2009; Deroche et al., 1997; Erb et al., 2000; Erb et al., 1996; Gass & Olive, 2007; Graf et al., 2013; Mantsch & Katz, 2007; Mantsch et al., 2014; Mantsch et al., 2010; Shepard et al., 2004). Clinical treatment studies indicated that self-reported stress was among the widely cited precipitants to substance use relapse (M. al'Absi, 2006; Heishman, 1999; Hughes, 2009; Hymowitz et al., 1991; Matheny & Weatherman, 1998). Further, individuals who reported high stress levels during abstinence were more likely to relapse (Brewer et al., 1998; S. Cohen & Lichtenstein, 1990). The central question of this dissertation study was simple: how does acute stress influence brain function such that an abstinent individual is more likely to relapse? However, it would be unethical to directly test this research question in treatment-seeking smokers, who are actively attempting to quit. Rather, an approximate ethical approach was used. Nicotine-seeking and self-administration among non-treatment-seeking individuals was measured during two identical experimental sessions: placebo and active stress. Broadly, the literature described three mechanisms through which acute stress may potentiate nicotine self-administration: 1) impair dlPFC function and top-down executive control, 2) intensify aversive internal states (e.g. negative affect, anxiety, etc.) that motivate relief via nicotine use, and 3) increase appetitive motivation, nicotine salience or craving.

5.2.3 Dissertation Sample Characteristics

Self-reported cigarette smokers were recruited locally via Craigslist advertisements. Participants were screened twice for eligibility. Briefly, eligible participants were young (21-35 yrs old), daily cigarette smokers (10+/day; FTND ≥ 4), not currently using other substances (some marijuana and alcohol use was allowed),

and without psychiatric, MRI, or cardiovascular contraindications. The modal participant was 28 years old, male, and African-American. Participants reported smoking ~17 (primarily menthol) cigarettes per day, were moderately dependent (FTND ~ 6), and averaged 13 years of formal education (Table 4.2).

5.2.4 Stress Potentiated Nicotine Self-Administration

Nicotine-seeking and self-administration behavior was measured via a choice progressive ratio task. Participants were able to choose between two options (one puff of their preferred brand of cigarette or money [$0.25]) across 11 choice trials, with escalating response requirements for each successive unit earned. Participants were able to earn any combination of either option, up to a maximum 11 units. Following completion of the 30min task, participants smoked the exact number of cigarette puffs earned on the choice task and inter-puff interval was timed. In this study, the number of puff choices earned (and smoked) defined the extent of nicotine-seeking and self-administration (i.e. direct measure of appetitive nicotine motivation). In addition, inter-puff interval was a direct measure of nicotine self-administration rate (i.e. nicotine consumption rate). Together, nicotine-seeking and self-administration behaviors reflect nicotine motivation, but parsed into appetitive and consumptive phases, respectively.

Nicotine-seeking and self-administration behavior. Results from this study demonstrated that nicotine-seeking and self-administration during the placebo condition were significantly positively correlated with nicotine dependence level (FTND; accounted for 36% of the variance). This was not surprising. More heavily nicotine dependent participants earned and smoked more cigarette puffs than those who were less dependent. In the absence of an experimental manipulation, participants who

smoked more outside of the laboratory chose to smoke more during the research study. Therefore, FTND score was included as a covariate in outcome analyses. Controlling for FTND, active stress significantly increased nicotine-seeking and self-administration (i.e. appetitive nicotine motivation), relative to placebo. During the stress session, nicotine self-administration was not correlated with nicotine dependence level (FTND accounted for 1.1% of the variance). Relative to placebo, less dependent participants (median split by FTND) increased, while more dependent participants decreased, their nicotine-seeking and self-administration (~1.5 puffs and ~1 puff, respectively) during the active stress session.

Nicotine consumption rate. As hypothesized, nicotine consumption rate (mean inter-puff interval [s]) did not significantly differ as a function of active vs. placebo stress. Limited number of observations and highly variable data across subjects may have contributed to this non-significant finding. Nicotine dependence level (FTND) was not related to nicotine consumption rate. Interestingly, our data indicate a differential effect of acute stress on the appetitive and consumptive phases of nicotine motivation which illustrate the specific effects of the stress manipulation.

In summary, relative to placebo, oral pretreatment with 54mg YOH and 10mg HYD potentiated nicotine-seeking and self-administration, controlling for dependence level. These findings were consistent with *a priori* hypotheses and prior research. Further, these data validated this complex experimental model. Future studies can build on this approach and evaluate medications that may blunt the effects of stress on nicotine-seeking and self-administration. The effectiveness of FDA-indicated

medications (e.g. varenicline) for smoking cessation may be enhanced by adjunctive stress-blunting medications (e.g. prazosin).

5.2.5 Subjective and Physiological Effects

Physiological effects. Oral pretreatment with YOH and HYD demonstrated significant physiological effects, consistent with a stress response (Section 4.2.2). Systolic and diastolic BP and HR exhibited significant Time X Dose interaction effects, relative to the placebo session. Peak YOH+HYD effects increased systolic and diastolic BP ~12 and ~7 mmHg and heart rate ~4 bpm relative to the placebo session. YOH and HYD doses were administered such that physiological effects were apparent at the onset of the MRI scan (1pm) and remained elevated throughout experimental procedures (2+ hrs). Saliva cortisol levels exhibited a significant Time X Dose interaction (biomarker of plasma cortisol levels; HYD administration). Saliva α-amylase effects were less obvious and did not exhibit the hypothesized Time X Dose interaction. Saliva α-amylase levels increased throughout the stress session (biomarker of plasma noradrenaline levels; YOH administration), but not the placebo session. FTND score was not related to any physiological effects.

The magnitude of the YOH+HYD-induced stress response was interpreted in the context of other studies. Robust psychosocial stress-induction tasks (public speaking + cognitive tasks) resulted in large effects on saliva cortisol, systolic BP, and HR (Section 4.2.3) (Dickerson & Kemeny, 2004; Ginty et al., 2014). Effect sizes from those studies were comparable to those observed in this study. In summary, oral pretreatment with YOH 54mg and HYD 10mg elicited a significant physiological stress response that lasted 2+ hours (relative to placebo), comparable in magnitude to a robust psychosocial

stressor. Physiological effects supported *a priori* hypotheses (less saliva α-amylase). These data provided additional support that YOH+HYD is a valuable experimental approach with methodological advantages compared to psychosocial stress-induction techniques (reliable physiological stress response, placebo-control, double-blind administration, dose-control, and sustained stress response [2+ hr]). Importantly, the doses used herein were medically-safe and no adverse events occurred. Yet, despite these methodological advantages, few human studies outside Dr. Greenwald's laboratory have investigated their effects in substance use disorders.

Subjective effects. Participants completed a battery of self-reported measures periodically throughout each experimental session. The measures assessed general internal states (anxiety and positive and negative affect) and nicotine-specific internal states (withdrawal symptoms and relief-motivated and appetitive craving).

Nicotine-specific subjective effects. Self-reported nicotine withdrawal symptoms were measured via the Minnesota Nicotine Withdrawal Scale (MNWS). Individuals reported a significant increase in nicotine withdrawal across time within each session, but withdrawal did not differ as a function of experimental session (active vs. placebo stress). This was consistent with *a priori* hypotheses. Participants reported greater nicotine withdrawal severity the longer they were unable to smoke (i.e. positive control), but YOH+HYD did not modulate this effect. Similarly, appetitive and relief-motivated craving (Brief Questionnaire of Smoking Urges; QSU) scores increased across time within each session, but did not differ as a function of active vs. placebo stress. Individuals craved cigarettes more the longer they abstained from smoking (i.e. positive control of response consistency). We hypothesized that relief-motivated craving, but not

appetitive craving, would increase more during the active stress session, relative to placebo. In summary, there was no evidence from these subjective effects measures that YOH+HYD enhanced nicotine withdrawal symptoms, appetitive craving, or relief-motivated craving, relative to placebo.

These findings are relevant for substance use treatment. All three FDA-indicated pharmacotherapies for smoking cessation (varenicline, bupropion, and nicotine replacement products) target nicotine withdrawal and craving. However, as described in Section 1.2, these medications (despite their effective attenuation of nicotine withdrawal symptoms and craving) are associated with dismal long-term abstinence rates. Findings presented herein indicate that acute stress does not potentiate nicotine-seeking and self-administration via enhanced nicotine withdrawal or craving. Therefore, it is unlikely that varenicline, bupropion, or nicotine replacement products would successfully attenuate the effects of acute stress. Indeed, prior research demonstrated that varenicline blocked smoking cue-induced craving, but not stress- *plus* cue-induced craving (Ray et al., 2013). Bupropion increased physiological indices of stress reactivity during acute smoking abstinence (Kotlyar et al., 2006). In addition, long term nicotine use is associated with elevated circulating stress hormones and dysregulated stress reactivity (Kreek & Koob, 1998; Wilkins et al., 1982). In summary, varenicline, bupropion, and nicotine replacement products effectively attenuate nicotine withdrawal and craving, but do not attenuate (rather, may enhance) an individual's physiological response to stress. Data presented herein suggested that acute stress does not act via withdrawal or craving to potentiate nicotine-seeking and self-administration behavior.

The effectiveness of FDA-indicated pharmacotherapies for smoking cessation may be enhanced by adjunctive medications that blunt an individual's stress response.

Alternative explanations. One alternative explanation is that participants did not respond accurately or thoughtfully on these measures. Participant fatigue or disinterest is possible as experimental sessions were long and repetitive. However, this is unlikely because significant Time effects were found across experimental sessions. Results demonstrated that participant withdrawal and craving increased as function of time since last cigarette, as hypothesized (i.e. positive control). Moreover, this study was powered to detect moderate effect sizes (not likely a statistical power issue).

General subjective effects. Self-reported anxiety (STAI; state version) decreased throughout each experimental session, but did not differ as a function of active vs. placebo stress (Section 4.2.4). While significant, anxiety decreased an average of ~5% from baseline levels. We attributed this effect to participant's becoming more comfortable as time elapsed during experimental sessions. Individuals may have been slightly apprehensive about participation in a medical research study (especially one that involved pharmacological dosing and an MRI scan). Self-reported affect (both positive and negative) was measured via the Positive and Negative Affect scale (PANAS). Participants reported a significant increase in negative affect throughout each experimental session, but no effect of experimental session. Controlling for FTND, positive affect decreased throughout each experimental session, but did not differ as a function of active vs. placebo stress. FTND was not significantly related to anxiety or negative affect. In summary, there is no evidence from this study that YOH+HYD intensified aversive internal states, relative to placebo. These findings suggested that

acute stress probably does not act via aversive internal states to potentiate nicotine-seeking and self-administration.

Alternative explanations. As described above, this study was not under-powered to detect effects. Participant apathy or boredom may have influenced these data (possible with any subjective measure). However, participant responding was consistent across experimental sessions (conducted at least 48 hrs apart) and within each session. Finally, variable distributions approximated normality (or were corrected) at each time point prior to statistical analyses. Thus, our observations do not suggest that a few apathetic participants skewed these findings.

5.2.6 Neurochemistry Results

Voxel placement. The AVP method was in-development when this project launched subject recruitment. AVP was not used during the first six scans (14.3%; manual placement), which resulted in poor geometric voxel overlap with the template voxel (~62%; Figure 4.28 and Table 4.3). Voxel placement was assisted by AVP (e.g. coordinate location was accurate, but rotation angles were incorrect or vice versa) in the next 11 scans (~26%), which were associated with moderate accuracy (~75% overlap with the template voxel). Finally, AVP prescribed the voxel location and rotation angles for the remaining 25 scans (~60%) which had excellent accuracy (96% overlap with the template voxel). Across all scans, mean voxel placement accuracy was very good for this study (~86% overlap with the template voxel).

However, it is important to remember that ^{1}H fMRS analyses were limited to within-subject and within-session comparisons: GLU levels during 2-back were contrasted with rest separately for placebo and active stress. No between-subject or

between-session comparisons were analyzed. Therefore, voxel placement variability across experimental sessions was more meaningful than voxel placement variability across subjects. Mean between-session overlap within each subject (i.e. voxel placement consistency across sessions) was very good (87% geometric overlap). To provide context, 87% geometric voxel overlap is associated with ~1mm voxel placement error during one scan. Mean voxel tissue composition for all scans was approximately two-thirds white (~66%) and one-third gray (~32%) matter. In summary, AVP resulted in excellent voxel placement accuracy and reliability. Overall, both between-subject and between-session voxel overlap accuracy was very good (~86% and ~87%, respectively).

Behavioral data. Behavioral data demonstrated task compliance for both experimental sessions (Section 4.2.7). Response accuracy during the letter 2-back increased across task blocks during both experimental sessions (Time effect), but accuracy improved more during the placebo session (Time X Dose interaction). On average, participants responded significantly more accurately during placebo (~87%) than active stress (~78%; Task effect). Response latency decreased across task blocks for both sessions (i.e. task proficiency improved with repetition), but did not differ as a function of active vs. placebo stress. In summary, response accuracy increased across task blocks in both sessions (indicative of practice effects). As hypothesized, YOH+HYD impaired 2-back response accuracy (relative to placebo), consistent with prior research using a robust psychosocial stressor (Qin et al., 2009).

GLU modulation (32s resolution). LCModel fit and metabolite quantification was 100% automated. As described above, individual raw spectra were phase- and shift-corrected prior to averaging and LCModel fit.

During the placebo session, GLU quantification at 32s resolution (8 avgs) was reliable (Table 4.4) and importantly, LCModel fit characteristics did not differ as a function of experimental task. GLU levels were significantly higher (2.7%) during 2-back A relative to interleaved fixation-cross. Across task blocks, GLU levels were marginally higher during 2-back A vs. rest (Task effect: p = .06). 2-back A GLU levels increased (relative to rest) in later task blocks. GLU levels during 2-back B did not differ from interleaved fixation-cross levels (p = .67). In general, GLU modulation (during 2-back A) corresponded with 2-back response accuracy across task blocks (with the exception of task block 2). The behavioral data demonstrated that participants performed poorly during the first task block, but significantly improved with task repetition. During the first task block, poor response accuracy was associated with virtually no GLU modulation (i.e. limited dlPFC task engagement). Was poor task performance the cause of, or the result of, limited dlPFC task engagement? Unfortunately, the answer is unknowable from the present findings. Poor task accuracy and dlPFC engagement in the first task block may have resulted from task complexity (resolved in later blocks; i.e. practice effects) or the novel and distracting MRI environment (to which, participants habituated). From task blocks 3 to 5, GLU modulation was apparent and steadily increased which paralleled response accuracy. In summary, letter 2-back task performance modulated GLU levels in the left dlPFC during the first 32s (2-back A), but the effect was time-limited and not consistently found in the final 32s (2-back B) of task

performance. Moreover, GLU modulation generally paralleled response accuracy across task blocks. Findings during the placebo session in this study were consistent with ^{1}H fMRS pilot study results in healthy control subjects.

During the stress session, GLU levels did not differ as a function of task performance (2-back A or B vs. interleaved fixation-cross rest; *p*s > .10). Moreover, two LCModel fit characteristics differed as a function of experimental task (2-back vs. interleaved fixation-cross rest): FWHM and SNR. SNR was higher and FWHM was lower (more narrow spectral linewidth) during 2-back > rest. Importantly, these differences did not translate into biased LCModel GLU fit uncertainty (GLU and glutamine CRLB% did not differ as a function of experimental task). However, we cannot rule out the possibility that these biases did not influence or confound GLU quantification (Type II error is possible). Therefore a second analysis strategy was used: 64s (16 avgs) moving average.

GLU modulation (64s resolution). Spectra from the 32s analyses were averaged across task blocks: task block 1 data for 2-back A was averaged with task block 2 data for 2-back A, and so on. This strategy was repeated for all task blocks and experimental phases (2-back B and rest). This resulted in 4 time points for 2-back A, B, and rest. As expected, 64s (16 avgs) resolution was associated with higher SNR and more reliable LCModel fit. Relative to 32s resolution, SNR was ~5 points higher and GLU CRLB% was at least 1% lower (with less variability).

During the placebo session, LCModel fit characteristics did not differ as a function of experimental task for the placebo session (Table 4.5). A significant Time X Task interaction indicated that GLU levels were higher during 2-back A relative to

interleaved fixation-cross rest, but only in later task blocks. These results were similar to the 32s resolution findings. Again, consistent with 32s resolution GLU findings, 2-back B didn't differ as a function of experimental task. Across four analytic strategies (and two samples), findings presented herein repeatedly demonstrated that dlPFC GLU levels were modulated during the first 32s of letter 2-back task performance (i.e. 2-back A), but the effect was inconsistent and blunted during the final 32s of task performance. There are two plausible explanations for these findings: 1) cognitive task switching or directed attention modulated dlPFC GLU levels (and that effect was time-limited) or 2) working memory performance modulated dlPFC GLU levels temporarily, but new steady state levels were not established (i.e. habituation). Unfortunately, there was not sufficient temporal resolution to disentangle these explanations. It should be noted that this effect was contrary to *a priori* hypotheses. We hypothesized 2-back performance would increase dlPFC GLU levels throughout the entire task block (i.e. establish new steady state levels).

During the stress session, GLU levels were not modulated as a function of experimental task (non-significant Task and Time X Task interaction effects). Further, GLU levels during 2-back were generally lower than fixation-cross rest. Only one LCModel fit characteristic differed as a function of experimental task for the 64s resolution (SNR was higher during 2-back A than rest). However, a small difference in SNR did not bias the certainty in the LCModel quantification of GLU or glutamine across task phases (*p*s > .19).

In summary, this second analysis strategy corroborated initial findings at 32s resolution and demonstrated, with more reliable LCModel fit, that 2-back performance

modulated dlPFC GLU levels (relative to fixation-cross rest) during placebo, but not active stress.

As described in Section 5.1.3 above, the ^{1}H fMRS signal is a direct measurement of *in vivo* GLU molecules from all possible sources within the voxel. Thus, results during the placebo session demonstrated that the number of GLU molecules within the voxel location was higher during letter 2-back A relative to fixation-cross rest. We interpreted these findings to indicate task-related cognitive demand during 2-back increased neural and metabolic activity (and thus, GLU levels) in the left dlPFC. These findings were consistent with the electrophysiology, ^{1}H fMRS, fMRI BOLD literature, and findings in the ^{1}H fMRS pilot study.

Limitations and alternative explanations. All of the same limitations from the ^{1}H fMRS pilot study apply here. First, partial volume effects were possible. However, partial volume effects were unlikely because the analysis strategy focused on within-subject comparisons (GLU levels during task vs. rest) and voxel tissue composition variability was low across experimental sessions (gray and white matter coefficient of variation percentage was 10.5% and 7.2%, respectively). Second, AVP was associated with accurate and reliable voxel placement. Voxel placement accuracy between-subjects for this study was high (~86%). More importantly, within-subject voxel replacement reliability (from the first to the second experimental session) was very good (~87%). Third, due to SNR limitations, we were unable to reliably quantify other relevant neurotransmitters (e.g. GABA and glutamine). Future studies could use higher field strengths or different MRS sequences (e.g. MEGA-PRESS) to investigate task-related modulation of GABA and glutamine levels.

There are several alternative explanations for task-related GLU modulation. First, the BOLD effect (i.e. FWHM) was nearly significant during the placebo session (p = .06) and was significant during the stress session (p < .05). The BOLD effect may have influenced metabolite quantification and T_2*. However, LCModel should be immune to the influence of linewidth on metabolite level quantification. Indeed, we found that NAA levels did not differ as a function of task during either experimental session, which suggested the BOLD effect did not bias NAA quantification. During the placebo session, no metabolites differed as a function of experimental task other than GLU. However, during stress, GPC+PC and Myo-Inositol did differ as a function of experimental task, contrary to *a priori* hypotheses. Second, GLU's transverse relaxation (T_2*) could have changed as a result of task performance. However, as described above, transverse relaxation alone was unlikely to explain the observed increase in GLU signal during placebo (Ogawa et al., 1992). Third, Type I error was possible for the placebo session. However, evidence against this explanation was four-fold: 1) results were consistent with the pilot study and the literature; 2) the experimental paradigm was designed to minimize the possibility of Type I error (e.g. the use of a stabilization task [flashing checkerboard], comparison to an interleaved fixation-cross rest condition, and reliable voxel placement); 3) observed moderate effect size (i.e. study was not over-powered); and 4) LCModel fit characteristics and metabolite levels (other than GLU) didn't differ as a function of experimental task. Fourth, Type II error was possible for the stress session. LCModel fit characteristics (FWHM and SNR) significantly differed as a function of experimental task during the stress session. However, these differences did not influence uncertainty of LCModel GLU fit (GLU and glutamine CRLB% did not differ

between 2-back vs. rest; ^{1}H MRS glutamine peaks overlap with GLU at 3T). Moreover, LCModel fit of GLU was reliable (GLU CRLB <7 ± <1%) across task and rest conditions. Further, the FWHM bias (BOLD effect) did not influence the quantification of NAA (which didn't differ as a function of experimental task). Finally, overall GLU levels during 2-back tended to be lower (not higher) than interleaved fixation-cross levels.

Neurochemistry results summary. In summary, our findings indicated that letter 2-back task performance modulated GLU levels in the left dlPFC (relative to interleaved fixation-cross rest) during the placebo, but not the active stress condition (consistent with *a priori* hypotheses*)*. These findings were consistent with the ^{1}H fMRS pilot study. As described in detail above, we interpreted task-related dlPFC GLU modulation to reflect increased neural and metabolic activity associated with excitatory neurotransmission driven by working memory task performance. We believe GLU modulation is an *in vivo* biomarker of dlPFC engagement during working memory performance. Importantly, ^{1}H fMRS GLU levels, as a biomarker, are not confounded by neurovascular coupling.

Extensive research at Yale University demonstrated that working memory task performance in non-human primates was associated with increased neuronal spiking frequency in the dlPFC (Goldman-Rakic, 1995). As described in Sections 2.4.3 and 2.5.1, persistent excitatory microcircuits (glutamatergic) in cortical layer III are thought to

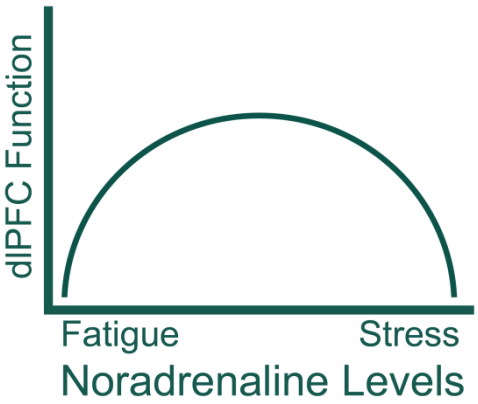

Figure 5.1: Noradrenaline Levels and dlPFC Function. The inverted 'U' relationship between noradrenaline levels and dlPFC function is depicted.

maintain working memory traces during the 'delay' period (necessary for accurate responding) (Wang et al., 2013). Using the same task paradigm and selective pharmacological challenges, Arnsten and colleagues demonstrated that working memory task performance and dlPFC neural spiking frequency exhibited an inverted 'U'-shaped relationship with noradrenaline levels (Figure 5.1) (A. F. Arnsten, 2009). Inadequate α_2-noradrenergic receptor stimulation (i.e. fatigue) or excessive noradrenergic stimulation (i.e. stress) impaired working memory in non-human primates (A. F. Arnsten, 2009). Synaptic noradrenaline has the highest binding affinity for α_2-noradrenergic receptors and lower affinity for α_1- and β_1-noradrenergic receptors (A. F. Arnsten, 2009). Thus, in the presence of excessive noradrenaline levels (i.e. stress), noradrenaline molecules will 'spill over' and bind lower affinity α_1- or β_1-noradrenergic receptors, disrupt persistent excitatory microcircuits that maintain working memory traces during the 'delay' period, and impair response accuracy (A. F. Arnsten, 2009). YOH is a pre-synaptic α_2-noradrenegeric antagonist that disinhibits presynaptic noradrenergic release. The dose used in this study (oral pretreatment with 54mg of YOH) significantly increased two biomarkers of a physiological stress response (BP and saliva α-amylase; sympathetic ANS), relative to placebo. It is speculative, but plausible, that YOH significantly elevated noradrenergic levels (stimulating lower affinity α_1- and/or β_1-noradrenergic receptors), which disrupted excitatory microcircuits in the dlPFC and impaired 2-back task accuracy (shifting individuals to the right side of the downward slope on the inverted 'U' in Figure 5.1). ^{1}H fMRS data support this hypothesis. During placebo, noradrenaline levels were 'normal' and response accuracy was high. 2-back task performance significantly modulated GLU levels indicative of dlPFC engagement

(consistent with non-human primate studies) (A. F. Arnsten, 2009). However, during the active stress session, YOH+HYD significantly elevated BP and saliva α-amylase, which was associated with attenuated GLU modulation (i.e. impaired dlPFC engagement) and impaired response accuracy. These data support the hypothesis that acute stress potentiates drug-seeking behavior via impaired top-down (specifically dlPFC) executive function. Further, the present findings, in combination with the literature, provided support that noradrenaline levels may be the culprit. Medications (e.g. prazosin [α_1-adrenoreceptor antagonist] and propranolol [β_1- and β_2-adrenoreceptor antagonist]) that block noradrenergic stimulation of lower affinity α_1 and β_1 receptors may rescue dlPFC function. As described in Section 2.4.3, dlPFC function is associated with a host of cognitive processes (e.g. delayed gratification, self-control, decision making, and goal-directed action) necessary for prolonged abstinence. Acute stress-compromised dlPFC function could predispose an individual to habit-directed behavior (i.e. stimulus-response; cigarette cue induced smoking relapse) or ill-prepared to adequately suppress cigarette craving/withdrawal symptoms. Future studies should examine the effects of prazosin and/or propranolol on dlPFC function and drug-seeking behavior during acute experimental stress challenge.

The present dlPFC GLU modulation findings were buttressed by the rigorous experimental design used: within-subject, double-blind placebo-controlled, and randomized cross-over design. All research subjects completed both experimental sessions (which were identical) and typically within 7 days of one another (76% of subjects). Further, all outcome analyses examined within-subject comparisons; thus, each subject served as his/her own control.

5.2.7 BOLD fMRI Results

Cerebrovascular reactivity (CVR). In the present study, neurovascular coupling was a potential problem due to the use of a pharmacological challenge with known vasoconstrictive properties. Thus, the breath-hold challenge task was implemented to control for CVR differences. Briefly, participants were instructed (visually) to change their breathing throughout the task across three phases: uncontrolled ('normal') breathing, paced breathing (3s in and 3s out), and breath hold (11s). Prior research demonstrated a robust BOLD response during breath hold (relative to paced breathing) (Bright & Murphy, 2013; Lipp et al., 2015; Magon et al., 2009; Murphy et al., 2011; Sousa et al., 2014). Significant activation on this task reflected vascular effects (i.e. non-neuronal) due to breath hold. As part of our fMRI analysis strategy, all between-session (placebo vs. active stress) comparisons were CVR-corrected to reduce the possibility of false positives due to the vascular effects of YOH+HYD.

Letter 2-back vs. fixation-cross rest. Behavioral data demonstrated task compliance. Contrary to ^{1}H fMRS behavioral data, response accuracy was non-significantly higher during placebo vs. active stress (p = .11; 90% vs. 85%, respectively). Data collection errors resulted in a substantial missing data (24%) for this outcome variable and may have resulted in this comparison being under-powered. As hypothesized, 2-back performance was associated with robust bilateral PFC activation, relative to fixation-cross rest, during both experimental sessions (Figure 4.43; (Owen et al., 2005)). However, contrary to *a priori* hypotheses, between-session comparisons (CVR-corrected) revealed significantly more PFC activation during task performance (2-back > rest) in the stress, relative to placebo, session (Figure 4.44). Even with the CVR-

correction, we cannot rule out the possibility of YOH confounding these results. YOH has robust vasoconstrictive effects that make interpretation of this finding challenging. Within-session, task-evoked BOLD responses (i.e. 2-back > rest) are less confounded and associated with a more straightforward interpretation.

Few studies have examined the effect of YOH on task-evoked BOLD responses in human subjects. However, a number of studies have investigated the effects of caffeine (another vasoconstrictive agent) on BOLD response. Unfortunately, these studies provided little clarity for the unexpected BOLD findings in this study. In a well-controlled study among infrequent caffeine users, visual stimulation and finger-tapping tasks evoked attenuated BOLD responses in the visual and motor cortices (respectively) during caffeine (250mg oral dose), relative to placebo (Diukova et al., 2012). Conversely, during visual and motor stimulation tasks, BOLD responses (in another study) in visual and motor cortices (respectively) were amplified during intravenous caffeine injection (2.5mg/kg), relative to saline (Chen & Parrish, 2009b). Further, there was evidence that caffeine altered cerebral blood flow and cerebral metabolic rate of oxygen in the visual cortex during visual stimulation, relative to placebo (Chen & Parrish, 2009a; Griffeth, Perthen, & Buxton, 2011). Therefore, in addition to the conflicting BOLD activation findings in the literature, the neurobiological underpinnings of the BOLD signal may be altered by acute administration of a vasoconstrictive agent. The present study did not measure other physiological indices (e.g. cerebral blood flow, cerebral blood volume, oxygen metabolism) that may have provided greater insight into these unexpected BOLD findings.

The effects of caffeine on BOLD response in the PFC are more consistent, but may be confounded by the cognitive-enhancing effects of caffeine. During an auditory oddball task, caffeine was associated with greater task-evoked BOLD response in the PFC, relative to placebo (Diukova et al., 2012). Similarly, during working memory task performance, caffeine (100mg oral dose) amplified BOLD response in the PFC, relative to placebo (Klaassen et al., 2013; Koppelstaetter et al., 2008). These findings were consistent with the unexpected results observed herein during the letter 2-back paradigm: amplified task-evoked BOLD response in the PFC during YOH+HYD. It is possible that task-induced BOLD response exhibited regional differences due to heterogeneous vasoconstrictive effects (vessel diameter or vascularization differences in the PFC vs. visual/motor cortices). However, caffeine has known cognitive-enhancing properties, while YOH+HYD tended to impair task performance, which further complicated interpretation. Indeed, auditory oddball task performance was enhanced during caffeine, relative to placebo (Diukova et al., 2012). In the working memory studies, caffeine mostly did not alter working memory task performance (letter 2-back and 3-, 4-, and 5-letter Sternberg accuracy were unaffected; 6-letter Sternberg accuracy was impaired), relative to placebo (Klaassen et al., 2013; Koppelstaetter et al., 2008). In summary, between-session interpretation of BOLD response data is complicated by the vasoconstrictive properties of YOH. Interpretation of task-evoked BOLD within each experimental session is more straightforward and provides greater clarity for neural activation across brain regions during task performance.

Letter 2-back exploratory analyses. Exploratory analyses examined task-induced activation median split by nicotine dependence level (FTND). These analyses

paralleled the significant Dose X FTND interaction effects on nicotine-seeking and self-administration (Figure 4.45). Less nicotine dependent participants exhibited smaller task-evoked BOLD response in the dlPFC in the stress (relative to placebo) session. Conversely, more nicotine dependent individuals exhibited larger task-evoked BOLD response in the dlPFC. These findings were consistent with the central tenet of this research study: stress potentiated nicotine self-administration via impaired dlPFC task-engagement.

fMRI N-back smoking vs. neutral cued. Accuracy and response latency were evaluated across levels of task difficulty (0-, 1-, and 2-back) and by image type (smoking vs. neutral) for both experimental sessions.

Stress effects. Neutral images were associated with an N-back effect for both the placebo and active stress sessions (as task difficulty increased, response accuracy decreased; Figure 4.46). Interestingly, a similar effect was found for response latency: across both sessions response latency decreased, as task difficulty increased (Figure 4.47). Smoking images were associated with an N-back X Dose interaction effect: response accuracy decreased more as a function of task difficulty during placebo vs. active stress. This effect may reflect that acute stress amplified smoking image salience, which buoyed response accuracy. Similar to the findings with neutral images, response latency decreased as task difficulty increased for smoking images (across both experimental sessions).

Image effects. During both experimental sessions, significant N-back effects demonstrated that response accuracy decreased as task difficulty increased for both image types (Figure 4.50 and 4.52). Response accuracy differed as a function of image

type during the stress session (smoking > neutral images), but not the placebo session. N-back X Image interaction indicated response accuracy decreased more for neutral images than smoking images, as task difficulty increased. Response latency (for both image types) decreased as task difficulty increased during the stress session, but not the placebo session (p = .07; Figures 4.51 and 4.53). During both experimental sessions, response latency decreased across N-back levels more for neutral images, relative to smoking images. Main effects of image type were non-significant during placebo and active stress.

Activation results. Following repeated substance use, drug-paired visual cues become conditioned stimuli and elicit dopamine release in the nucleus accumbens (without substance administration), consistent with anticipatory appetitive craving (N. Volkow et al., 2009; N. D. Volkow et al., 2006, 2008). In fMRI studies of visual drug cues, BOLD activation was often robust, but patterns varied across studies. Consistently activated regions during drug cue exposure fMRI studies were: amygdala, mOFC/mPFC, dlPFC, and ventral and dorsal striatum (Chase et al., 2011; Engelmann et al., 2012; Kühn & Gallinat, 2011; Wilson et al., 2004). Methodological factors, such as *treatment status* (out-of-treatment individuals show more robust activation), *time since last cigarette* (acute abstinence enhanced cue reactivity), and *temporal delay until next smoking opportunity* (immediate smoking opportunities were associated with more robust activation) influence BOLD fMRI results (Jasinska et al., 2014; Wilson et al., 2005). These factors were considered in the design of the present study. Non-treatment-seeking smokers, in acute abstinence at the time of fMRI BOLD data collection (~2hr since paced puff procedure), were reminded they would have an

opportunity to smoke following the MRI scan. fMRI activation analyses focused on the effect of image type (smoking > neutral) across N-back levels (0-, 1-, and 2-back) and compared the relative task-evoked BOLD response between experimental sessions. Across N-back levels, smoking (> neutral) images elicited greater BOLD response in 'reward'-associated brain regions during placebo, compared to active stress. These findings were contrary to *a priori* hypotheses. During 0- and 1-back (while response accuracy was high and didn't differ by image type), greater BOLD activation was observed in the ventral and dorsal striatum, mPFC, mOFC, and amygdala during placebo, relative to stress.

Activation in the ventral striatum is associated with drug craving, appetitive motivation, and encompasses the 'final common pathway' of addictive behaviors (Rita Z Goldstein & Volkow, 2002; R. Z. Goldstein & Volkow, 2011; Peter W Kalivas & Volkow, 2005; G. F. Koob & Volkow, 2010; N. Volkow et al., 2009). Amygdala activation is associated with the emotional salience of drug cue (Chase et al., 2011; Engelmann et al., 2012; Kühn & Gallinat, 2011; Wilson et al., 2004). Activation in the dorsal striatum may indicate mental rehearsal of habitual or 'over-learned' behaviors (e.g. smoking) (L. Schwabe, Joels, et al., 2012; L. Schwabe et al., 2010; L. Schwabe & Wolf, 2011). mOFC and mPFC activation may reflect reward appraisal, anticipation, or drug cue salience (Chase et al., 2011; Hayashi et al., 2013; Wilson et al., 2004).

At the 2-back level, response accuracy differed as a function of image type (smoking > neutral) and experimental session (stress > placebo). Behavioral proficiency differences complicated interpretation of the BOLD activation patterns. Generally, activation was diminished during 2-back task performance during both experimental

sessions. This was not unexpected; 2-back task performance demanded greater attentional focus, which may have minimized the salience of smoking images. Sporadic clusters were observed in the amygdala, ventral striatum, mOFC, and vlPFC during the placebo session. During stress, three clusters were found: mOFC, dorsal striatum, and dorsal PFC. Direct comparisons of experimental sessions (CVR-corrected; stress vs. placebo) across all N-back levels revealed robust BOLD activation differences. As described above, the vasoconstrictive properties of YOH may confound interpretation of direct between-session comparisons, but are presented here for continuity and transparency. 'Reward'-region activation was much greater during placebo, relative to active stress. Large clusters were found in the amygdala, ventral and dorsal striatum, mOFC, mPFC, dACC, vlPFC, superior parietal lobule, and dlPFC during placebo (> stress). These findings may reflect enhanced cue salience and appetitive motivation during placebo. Conversely, only one cluster was found in the mOFC for stress (> placebo). These neural activation patterns suggest that stress attenuated smoking cue-evoked BOLD activation, relative to placebo. These findings were contrary to *a priori* hypotheses and inconsistent with subjective effects (nicotine withdrawal and craving) as well as, nicotine-seeking and self-administration results. These findings do not support the idea that stress potentiated nicotine-seeking and self-administration via amplified 'bottom-up' signaling (e.g. enhanced smoking cue salience or appetitive motivation).

5.2.8 fMRI vs. ^{1}H fMRS

Exploratory analyses examined the statistical relationship between BOLD fMRI response and ^{1}H fMRS GLU levels during letter 2-back (> fixation-cross rest). These tasks were performed sequentially (^{1}H fMRS always preceded fMRI), but task parameters were identical. The ^{1}H fMRS voxel for each subject was used as a mask for

fMRI contrasts, from which Z scores (peak activation) and peak cluster extents were extracted, for the initial 32s and final 32s of task performance (2-back A and B, respectively). The first fMRS task block was ignored (allow response accuracy to stabilize; practice effects). Thus, the analysis space consisted of two bivariate correlation matrices (Z score and cluster extents) with 32 cells (four rows of fMRI metrics [2-back A and B X 2 task repetitions] by 8 columns of fMRS metrics [2-back A and B X 4 task repetitions]) for the placebo and active stress sessions. Seven of 32 cells (21.9%) were positively correlated for fMRI Z scores and 5 of 32 cells (15.6%) were positively correlated for fMRI cluster extents during the placebo session. During the stress session, 1 cell (3.1%) was negatively correlated for fMRI Z scores and none were correlated for fMRI cluster extents. Thus, letter 2-back task performance was associated with moderate statistical coherence within subjects across neuroimaging metrics (fMRI BOLD and ^{1}H fMRS GLU) during the placebo session, and virtually no coherence during the active stress session. These exploratory findings emphasized the discrepant effects of stress on neuroimaging biomarkers of dlPFC task-engagement (YOH+HYD amplified BOLD activation, but attenuated GLU modulation during letter 2-back), and highlighted the importance of considering YOH's vasoconstrictive effects on BOLD response.

5.3 Overall Summary

The three primary goals of the ^{1}H fMRS pilot study were to: 1) develop and evaluate the AVP method for voxel placement, 2) develop a working memory ^{1}H fMRS paradigm, and 3) quantify dlPFC GLU modulation during working memory task performance. Results from the pilot study demonstrated that the AVP method was

feasible, reliable, and accurate. This novel method for automated voxel placement is publicly available (free-of-charge) for download. AVP was developed to be flexible such that it can be used across single voxel neuroimaging studies, regardless of: subject population, anatomical region, MRI scanner system, and field strength. Results from the ^{1}H fMRS pilot study (N = 16) demonstrated that 2-back task performance modulated dlPFC GLU levels relative to continuous and interleaved fixation-cross rest. 2-back A GLU levels were ~3% higher than rest. Importantly, LCModel fit characteristics did not differ as a function of experimental task and metabolites other than GLU were not modulated during 2-back A performance. Results during 2-back B were mixed and complicated by significant task-related modulation of Myo-Inositol and NAA. Working memory task-related GLU modulation in the dlPFC likely reflected increased metabolic activity driven by cognitive task engagement. In summary, the ^{1}H fMRS pilot study validated a novel *in vivo* biomarker of dlPFC task-engagement that is <u>not</u> confounded by vascular effects.

The two primary goals for the dissertation study were to: 1) investigate the effects of pharmacological stress manipulation on nicotine-seeking and self-administration and 2) investigate a neurobiological mechanism through which acute stress may potentiate nicotine self-administration. Self-reported cigarette smokers were screened for psychiatric, cognitive, MRI and cardiovascular contraindications. Participants (N = 21) completed two identical oral-dosing experimental sessions: active (YOH 54mg + HYD 10mg) and placebo stress (YOH 0mg + HYD 0mg). A rigorous experimental design was used: within-subject, placebo-controlled, double-blind, and randomized cross-over design. Active pharmacological stress increased biomarkers of

a physiological stress response (BP, HR, saliva cortisol and α-amylase) throughout experimental procedures (2+ hrs), relative to placebo. Active stress (relative to placebo) potentiated nicotine-seeking and self-administration (controlling for nicotine dependence level [FTND]) on an 11-trial choice progressive ratio task (30min). Stress did not alter nicotine consumption rate (inter-puff interval). These findings were consistent with *a priori* hypotheses and validated the experimental model used herein. Nicotine withdrawal, cigarette craving, and negative affect increased throughout each session (as length of experimental abstinence increased), but were not altered as a function of active vs. placebo stress (contrary to *a priori* hypotheses). Similarly, anxiety and positive affect decreased throughout each experimental session, but were not differentially affected by active vs. placebo stress. Consistent with the ^{1}H fMRS pilot study, working memory task performance modulated GLU levels in the left dlPFC during the placebo session. GLU levels were 2.7% higher during the first 32s of letter 2-back task performance relative to interleaved fixation-cross rest. During the stress session, GLU levels did not differ as a function of 2-back performance. Behavioral data demonstrated that participants' responded significantly more accurately during placebo, relative to active stress. These results were consistent with *a priori* hypotheses and extensive non-human primate research. During both placebo and active stress, letter 2-back performance evoked significant bilateral BOLD response. Inconsistent with *a priori* hypotheses, BOLD response in the dlPFC was greater during stress, relative to placebo. However, YOH is vasoconstrictive, which may have confounded between-session BOLD comparisons. Smoking-related and neutral images were yoked with letter N-back to investigate smoking cue-evoked BOLD response. Results

demonstrated that smoking-related (> neutral) images elicited greater BOLD response in 'reward'-associated brain regions during placebo, relative to active stress. Across N-back levels, activation was consistently observed in the mOFC, mPFC, ventral striatum, amygdala, and PFC during placebo, but not active stress. Activation in 'reward'-associated brain regions may reflect the salience of visual smoking cues or cue-elicited appetitive motivation.

Taken together, results from this study suggest that acute experimental stress (relative to placebo) elicited a robust physiological stress response, potentiated nicotine-seeking and self-administration, impaired dlPFC function, attenuated dlPFC task-related engagement, and suppressed 'reward' region BOLD response to visual smoking cues among non-treatment-seeking cigarette smokers. These findings provide empirical support for a plausible neurobiological mechanism. Acute stress may have potentiated nicotine-seeking and self-administration via impaired dlPFC function and attenuated task-related engagement. It is speculative, but plausible, that excessive noradrenergic stimulation mediated the effect of stress on dlPFC function. In summary, data presented herein support the theory that acute stress may act via a 'top-down' mechanism to precipitate substance use relapse. There was no evidence from this study that acute stress amplified 'bottom-up' signals (withdrawal, craving, aversive internal state, or visual smoking cue salience) to increase nicotine-seeking and self-administration. Future studies will investigate dose-response relationships and pharmacological agents (e.g. prazosin and propranolol) that may blunt the effects of acute stress on dlPFC function and nicotine-seeking and self-administration.

REFERENCES

Abercrombie, E. D., Keefe, K. A., DiFrischia, D. S., & Zigmond, M. J. (1989). Differential effect of stress on in vivo dopamine release in striatum, nucleus accumbens, and medial frontal cortex. *J Neurochem, 52*(5), 1655-1658.

Ahmed, S. H., & Koob, G. F. (1997). Cocaine-but not food-seeking behavior is reinstated by stress after extinction. *Psychopharmacology (Berl), 132*(3), 289-295.

al'Absi, M. (2006). Hypothalamic-pituitary-adrenocortical responses to psychological stress and risk for smoking relapse. *Int J Psychophysiol, 59*(3), 218-227. doi:10.1016/j.ijpsycho.2005.10.010

al'Absi, M. (2006). Hypothalamic–pituitary–adrenocortical responses to psychological stress and risk for smoking relapse. *International Journal of Psychophysiology, 59*(3), 218-227.

al'Absi, M., Hatsukami, D., & Davis, G. L. (2005). Attenuated adrenocorticotropic responses to psychological stress are associated with early smoking relapse. *Psychopharmacology (Berl), 181*(1), 107-117. doi:10.1007/s00213-005-2225-3

Andersson, K., Eneroth, P., Fuxe, K., Mascagni, F., & Agnati, L. F. (1985). Effects of chronic exposure to cigarette smoke on amine levels and turnover in various hypothalamic catecholamine nerve terminal systems and on the secretion of pituitary hormones in the male rat. *Neuroendocrinology, 41*(6), 462-466.

Arnsten, A., & Goldman-Rakic, P. S. (1985). Alpha 2-adrenergic mechanisms in prefrontal cortex associated with cognitive decline in aged nonhuman primates. *Science, 230*(4731), 1273-1276.

Arnsten, A. F. (2009). Stress signalling pathways that impair prefrontal cortex structure and function. *Nature Reviews Neuroscience, 10*(6), 410-422.

Arnsten, A. F., Mathew, R., Ubriani, R., Taylor, J. R., & Li, B.-M. (1999). α-1 noradrenergic receptor stimulation impairs prefrontal cortical cognitive function. *Biol Psychiatry, 45*(1), 26-31.

Arnsten, A. F., Wang, M. J., & Paspalas, C. D. (2012). Neuromodulation of thought: flexibilities and vulnerabilities in prefrontal cortical network synapses. *Neuron, 76*(1), 223-239.

Aron, A. R., & Poldrack, R. A. (2006). Cortical and subcortical contributions to stop signal response inhibition: role of the subthalamic nucleus. *Journal of Neuroscience, 26*(9), 2424-2433.

Balleine, B. W., & Dickinson, A. (1998). Goal-directed instrumental action: contingency and incentive learning and their cortical substrates. *Neuropharmacology, 37*(4), 407-419.

Balleine, B. W., & O'Doherty, J. P. (2010). Human and rodent homologies in action control: corticostriatal determinants of goal-directed and habitual action. *Neuropsychopharmacology, 35*(1), 48-69. doi:10.1038/npp.2009.131

Banich, M. T. (2009). Executive Function: The Search for an Integrated Account. *Current Directions in Psychological Science, 18*(2), 89-94. doi:10.1111/j.1467-8721.2009.01615.x

Bechara, A. (2005). Decision making, impulse control and loss of willpower to resist drugs: a neurocognitive perspective. *Nat Neurosci, 8*(11), 1458-1463.

Birnbaum, S., Gobeske, K. T., Auerbach, J., Taylor, J. R., & Arnsten, A. F. (1999). A role for norepinephrine in stress-induced cognitive deficits: α-1-adrenoceptor mediation in the prefrontal cortex. *Biol Psychiatry, 46*(9), 1266-1274.

Birnbaum, S. G., Yuan, P., Wang, M., Vijayraghavan, S., Bloom, A., Davis, D., . . . Arnsten, A. (2004). Protein kinase C overactivity impairs prefrontal cortical regulation of working memory. *Science, 306*(5697), 882-884.

Brazell, M., Mitchell, S., & Gray, J. (1991). Effect of acute administration of nicotine on in vivo release of noradrenaline in the hippocampus of freely moving rats: a dose-response and antagonist study. *Neuropharmacology, 30*(8), 823-833.

Brewer, D. D., Catalano, R. F., Haggerty, K., Gainey, R. R., & Fleming, C. B. (1998). RESEARCH REPORT A meta-analysis of predictors of continued drug use during and after treatment for opiate addiction. *Addiction, 93*(1), 73-92.

Bright, M. G., & Murphy, K. (2013). Reliable quantification of BOLD fMRI cerebrovascular reactivity despite poor breath-hold performance. *Neuroimage, 83*, 559-568.

Brody, A. L., Mandelkern, M. A., Jarvik, M. E., Lee, G. S., Smith, E. C., Huang, J. C., . . . London, E. D. (2004). Differences between smokers and nonsmokers in regional gray matter volumes and densities. *Biol Psychiatry, 55*(1), 77-84.

Buczek, Y., Le, A., Wang, A., Stewart, J., & Shaham, Y. (1999). Stress reinstates nicotine-seeking but not sucrose solution seeking in rats. *Psychopharmacology (Berl), 144*(2), 183-188.

Charney, D. S., Heninger, G. R., & Redmond Jr, D. E. (1983). Yohimbine induced anxiety and increased noradrenergic function in humans: effects of diazepam and clonidine. *Life Sciences, 33*(1), 19-29.

Charney, D. S., Woods, S., Krystal, J. H., Nagy, L., & Heninger, G. (1992). Noradrenergic neuronal dysregulation in panic disorder: the effects of intravenous yohimbine and clonidine in panic disorder patients. *Acta psychiatrica scandinavica, 86*(4), 273-282.

Chase, H. W., Eickhoff, S. B., Laird, A. R., & Hogarth, L. (2011). The neural basis of drug stimulus processing and craving: an activation likelihood estimation meta-analysis. *Biol Psychiatry, 70*(8), 785-793.

Chen, Y., & Parrish, T. B. (2009a). Caffeine's effects on cerebrovascular reactivity and coupling between cerebral blood flow and oxygen metabolism. *Neuroimage, 44*(3), 647-652.

Chen, Y., & Parrish, T. B. (2009b). Caffeine dose effect on activation-induced BOLD and CBF responses. *Neuroimage, 46*(3), 577-583.

Chikazoe, J., Jimura, K., Hirose, S., Yamashita, K.-i., Miyashita, Y., & Konishi, S. (2009). Preparation to inhibit a response complements response inhibition during performance of a stop-signal task. *Journal of Neuroscience, 29*(50), 15870-15877.

Childs, E., & De Wit, H. (2009). Hormonal, cardiovascular, and subjective responses to acute stress in smokers. *Psychopharmacology (Berl), 203*(1), 1.

Choi, C., Coupland, N. J., Bhardwaj, P. P., Kalra, S., Casault, C. A., Reid, K., & Allen, P. S. (2006). T2 measurement and quantification of glutamate in human brain in vivo. *Magnetic resonance in medicine, 56*(5), 971-977.

Cohen, J. (1992). A power primer. *Psychol Bull, 112*(1), 155.

Cohen, S., & Lichtenstein, E. (1990). Perceived stress, quitting smoking, and smoking relapse. *Health Psychology, 9*(4), 466.

Corbit, L. H., & Balleine, B. W. (2003). The role of prelimbic cortex in instrumental conditioning. *Behav Brain Res, 146*(1), 145-157.

Cox, L. S., Tiffany, S. T., & Christen, A. G. (2001). Evaluation of the brief questionnaire of smoking urges (QSU-brief) in laboratory and clinical settings. *Nicotine & Tobacco Research, 3*(1), 7-16.

Crum, A. J., Salovey, P., & Achor, S. (2013). Rethinking stress: the role of mindsets in determining the stress response. *J Pers Soc Psychol, 104*(4), 716-733. doi:10.1037/a0031201

Cryer, P. E., Haymond, M. W., Santiago, J. V., & Shah, S. D. (1976). Norepinephrine and epinephrine release and adrenergic mediation of smoking-associated hemodynamic and metabolic events. *New England Journal of Medicine, 295*(11), 573-577.

Dagher, A., Tannenbaum, B., Hayashi, T., Pruessner, J. C., & McBride, D. (2009). An acute psychosocial stress enhances the neural response to smoking cues. *Brain Res, 1293*, 40-48. doi:10.1016/j.brainres.2009.07.048

Dale, A., Fischl, B., & Sereno, M. (1999). Cortical surface-based analysis. I. Segmentation and surface reconstruction. *Neuroimage, 9*(2), 179-194. doi:10.1006/nimg.1998.0395

de Jong, I. E., Steenbergen, P. J., & de Kloet, E. R. (2009). Behavioral sensitization to cocaine: cooperation between glucocorticoids and epinephrine. *Psychopharmacology (Berl), 204*(4), 693-703.

Dedovic, K., D'Aguiar, C., & Pruessner, J. C. (2009). What stress does to your brain: a review of neuroimaging studies. *Canadian journal of psychiatry. Revue canadienne de psychiatrie, 54*(1), 6-15.

Deroche, V., Marinelli, M., Le Moal, M., & Piazza, P. V. (1997). Glucocorticoids and behavioral effects of psychostimulants. II: cocaine intravenous self-administration and reinstatement depend on glucocorticoid levels. *Journal of Pharmacology and Experimental Therapeutics, 281*(3), 1401-1407.

Di Chiara, G., & Imperato, A. (1988). Drugs abused by humans preferentially increase synaptic dopamine concentrations in the mesolimbic system of freely moving rats. *Proceedings of the National Academy of Sciences, 85*(14), 5274-5278.

Dickerson, S. S., & Kemeny, M. E. (2004). Acute stressors and cortisol responses: a theoretical integration and synthesis of laboratory research. *Psychol Bull, 130*(3), 355-391. doi:10.1037/0033-2909.130.3.355

Diukova, A., Ware, J., Smith, J. E., Evans, C. J., Murphy, K., Rogers, P. J., & Wise, R. G. (2012). Separating neural and vascular effects of caffeine using simultaneous EEG-FMRI: differential effects of caffeine on cognitive and sensorimotor brain responses. *Neuroimage, 62*(1), 239-249. doi:10.1016/j.neuroimage.2012.04.041

Doxey, J., Lane, A., Roach, A., & Virdce, N. (1984). Comparison of the α-adrenoceptor antagonist profiles of idazoxan (RX 781094), yohimbine, rauwolscine and corynanthine. *Naunyn-Schmiedeberg's archives of pharmacology, 325*(2), 136-144.

Ehlert, U., Erni, K., Hebisch, G., & Nater, U. (2006). Salivary α-amylase levels after yohimbine challenge in healthy men. *The Journal of Clinical Endocrinology & Metabolism, 91*(12), 5130-5133.

Eisenberg, M. J., Filion, K. B., Yavin, D., Bélisle, P., Mottillo, S., Joseph, L., . . . Rinfret, S. (2008). Pharmacotherapies for smoking cessation: a meta-analysis of randomized controlled trials. *Canadian Medical Association Journal, 179*(2), 135-144.

Engelmann, J. M., Versace, F., Robinson, J. D., Minnix, J. A., Lam, C. Y., Cui, Y., . . . Cinciripini, P. M. (2012). Neural substrates of smoking cue reactivity: a meta-analysis of fMRI studies. *Neuroimage, 60*(1), 252-262.

Epstein, D. H., Preston, K. L., Stewart, J., & Shaham, Y. (2006). Toward a model of drug relapse: an assessment of the validity of the reinstatement procedure. *Psychopharmacology (Berl), 189*(1), 1-16.

Erb, S., Hitchcott, P. K., Rajabi, H., Mueller, D., Shaham, Y., & Stewart, J. (2000). Alpha-2 adrenergic receptor agonists block stress-induced reinstatement of cocaine seeking. *Neuropsychopharmacology, 23*(2), 138-150.

Erb, S., Shaham, Y., & Stewart, J. (1996). Stress reinstates cocaine-seeking behavior after prolonged extinction and a drug-free period. *Psychopharmacology (Berl), 128*(4), 408-412.

Erecińska, M., & Silver, I. A. (1990). Metabolism and role of glutamate in mammalian brain. *Progress in neurobiology, 35*(4), 245-296.

Etter, J. F., & Stapleton, J. A. (2006). Nicotine replacement therapy for long-term smoking cessation: a meta-analysis. *Tob Control, 15*(4), 280-285. doi:10.1136/tc.2005.015487

Feltenstein, M. W., Ghee, S. M., & See, R. E. (2012). Nicotine self-administration and reinstatement of nicotine-seeking in male and female rats. *Drug Alcohol Depend, 121*(3), 240-246.

Figner, B., Knoch, D., Johnson, E. J., Krosch, A. R., Lisanby, S. H., Fehr, E., & Weber, E. U. (2010). Lateral prefrontal cortex and self-control in intertemporal choice. *Nat Neurosci, 13*(5), 538-539.

Fox, H. C., Anderson, G. M., Tuit, K., Hansen, J., Kimmerling, A., Siedlarz, K. M., . . . Sinha, R. (2012). Prazosin effects on stress-and cue-induced craving and stress response in alcohol-dependent individuals: preliminary findings. *Alcoholism: Clinical and Experimental Research, 36*(2), 351-360.

Fox, H. C., Seo, D., Tuit, K., Hansen, J., Kimmerling, A., Morgan, P. T., & Sinha, R. (2012). Guanfacine effects on stress, drug craving and prefrontal activation in cocaine dependent individuals: preliminary findings. *J Psychopharmacol, 26*(7), 958-972. doi:10.1177/0269881111430746

Gass, J. T., & Olive, M. F. (2007). Reinstatement of Ethanol-Seeking Behavior Following Intravenous Self-Administration in Wistar Rats. *Alcoholism: Clinical and Experimental Research, 31*(9), 1441-1445.

Ginty, A. T., Jones, A., Carroll, D., Roseboom, T. J., Phillips, A. C., Painter, R., & de Rooij, S. R. (2014). Neuroendocrine and cardiovascular reactions to acute psychological stress are attenuated in smokers. *Psychoneuroendocrinology, 48*, 87-97.

Goldberg, M., & Robertson, D. (1983). Yohimbine: a pharmacological probe for study of the alpha 2-adrenoreceptor. *Pharmacol Rev, 35*(3), 143-180.

Goldman-Rakic, P. (1995). Cellular basis of working memory. *Neuron, 14*(3), 477-485.

Goldstein, R. Z., & Volkow, N. D. (2002). Drug addiction and its underlying neurobiological basis: neuroimaging evidence for the involvement of the frontal cortex. *American Journal of Psychiatry, 159*(10), 1642-1652.

Goldstein, R. Z., & Volkow, N. D. (2011). Dysfunction of the prefrontal cortex in addiction: neuroimaging findings and clinical implications. *Nat Rev Neurosci, 12*(11), 652-669. doi:10.1038/nrn3119

Gonzales, D., Rennard, S. I., Nides, M., Oncken, C., Azoulay, S., Billing, C. B., . . . Reeves, K. R. (2006). Varenicline, an α4β2 nicotinic acetylcholine receptor partial agonist, vs sustained-release bupropion and placebo for smoking cessation: a randomized controlled trial. *Jama, 296*(1), 47-55.

Graf, E. N., Wheeler, R. A., Baker, D. A., Ebben, A. L., Hill, J. E., McReynolds, J. R., . . . Gasser, P. J. (2013). Corticosterone acts in the nucleus accumbens to enhance dopamine signaling and potentiate reinstatement of cocaine seeking. *J Neurosci, 33*(29), 11800-11810. doi:10.1523/JNEUROSCI.1969-13.2013

Greenwald, M. K., Lundahl, L. H., & Steinmiller, C. L. (2013). Yohimbine increases opioid-seeking behavior in heroin-dependent, buprenorphine-maintained individuals. *Psychopharmacology (Berl), 225*(4), 811-824.

Griffeth, V. E., Perthen, J. E., & Buxton, R. B. (2011). Prospects for quantitative fMRI: investigating the effects of caffeine on baseline oxygen metabolism and the response to a visual stimulus in humans. *Neuroimage, 57*(3), 809-816.

Gruetter, R., Seaquist, E. R., & Ugurbil, K. (2001). A mathematical model of compartmentalized neurotransmitter metabolism in the human brain. *American Journal of Physiology-Endocrinology And Metabolism, 281*(1), E100-E112.

Hare, T. A., Camerer, C. F., & Rangel, A. (2009). Self-control in decision-making involves modulation of the vmPFC valuation system. *Science, 324*(5927), 646-648.

Hare, T. A., Hakimi, S., & Rangel, A. (2014). Activity in dlPFC and its effective connectivity to vmPFC are associated with temporal discounting. *Front Neurosci, 8*.

Hayashi, T., Ko, J. H., Strafella, A. P., & Dagher, A. (2013). Dorsolateral prefrontal and orbitofrontal cortex interactions during self-control of cigarette craving. *Proceedings of the National Academy of Sciences, 110*(11), 4422-4427.

Heatherton, T. F., Kozlowski, L. T., Frecker, R. C., & Fagerstrom, K. O. (1991). The Fagerström test for nicotine dependence: a revision of the Fagerstrom Tolerance Questionnaire. *British journal of addiction, 86*(9), 1119-1127.

Heishman, S. J. (1999). Behavioral and cognitive effects of smoking: relationship to nicotine addiction. *Nicotine & Tobacco Research, 1*(Suppl 2), S143-S147.

Honey, R. A., Honey, G. D., O'loughlin, C., Sharar, S. R., Kumaran, D., Bullmore, E. T., . . . Bisbrown-Chippendale, R. (2004). Acute ketamine administration alters the brain responses to executive demands in a verbal working memory task: an FMRI study. *Neuropsychopharmacology: official publication of the American College of Neuropsychopharmacology, 29*(6).

Hughes, J. R. (1992). Tobacco withdrawal in self-quitters. *Journal of consulting and clinical psychology, 60*(5), 689.

Hughes, J. R. (2009). Smokers' beliefs about the inability to stop smoking. *Addict Behav, 34*(12), 1005-1009.

Hughes, J. R., Gust, S. W., Skoog, K., Keenan, R. M., & Fenwick, J. W. (1991). Symptoms of tobacco withdrawal: a replication and extension. *Arch Gen Psychiatry, 48*(1), 52.

Hughes, J. R., & Hatsukami, D. (1986). Signs and symptoms of tobacco withdrawal. *Arch Gen Psychiatry, 43*(3), 289-294.

Hymowitz, N., Sexton, M., Ockene, J., & Grandits, G. (1991). Baseline factors associated with smoking cessation and relapse. *Preventive Medicine, 20*(5), 590-601.

Imperato, A., Angelucci, L., Casolini, P., Zocchi, A., & Puglisi-Allegra, S. (1992). Repeated stressful experiences differently affect limbic dopamine release during and following stress. *Brain Res, 577*(2), 194-199.

Jasinska, A. J., Stein, E. A., Kaiser, J., Naumer, M. J., & Yalachkov, Y. (2014). Factors modulating neural reactivity to drug cues in addiction: a survey of human neuroimaging studies. *Neuroscience & Biobehavioral Reviews, 38*, 1-16.

Jorenby, D. E., Leischow, S. J., Nides, M. A., Rennard, S. I., Johnston, J. A., Hughes, A. R., . . . Doan, K. (1999). A controlled trial of sustained-release bupropion, a nicotine patch, or both for smoking cessation. *New England Journal of Medicine, 340*(9), 685-691.

Kahn, J.-P., Rubinow, D. R., Davis, C. L., Kling, M., & Post, R. M. (1988). Salivary cortisol: a practical method for evaluation of adrenal function. *Biol Psychiatry, 23*(4), 335-349.

Kalivas, P. W., Volkow, N., & Seamans, J. (2005). Unmanageable motivation in addiction: a pathology in prefrontal-accumbens glutamate transmission. *Neuron, 45*(5), 647-650. doi:10.1016/j.neuron.2005.02.005

Kalivas, P. W., & Volkow, N. D. (2005). The neural basis of addiction: a pathology of motivation and choice. *American Journal of Psychiatry, 162*(8), 1403-1413.

Kalman, D. (2002). The subjective effects of nicotine: methodological issues, a review of experimental studies, and recommendations for future research. *Nicotine & Tobacco Research, 4*(1), 25-70.

Kirschbaum, C., Kudielka, B. M., Gaab, J., Schommer, N. C., & Hellhammer, D. H. (1999). Impact of gender, menstrual cycle phase, and oral contraceptives on the activity of the hypothalamus-pituitary-adrenal axis. *Psychosomatic medicine, 61*(2), 154-162.

Kirschbaum, C., Wüst, S., & Strasburger, C. (1992). 'Normal'cigarette smoking increases free cortisol in habitual smokers. *Life Sciences, 50*(6), 435-442.

Klaassen, E. B., de Groot, R. H., Evers, E. A., Snel, J., Veerman, E. C., Ligtenberg, A. J., . . . Veltman, D. J. (2013). The effect of caffeine on working memory load-related brain activation in middle-aged males. *Neuropharmacology, 64*, 160-167.

Klose, U. (1990). In vivo proton spectroscopy in presence of eddy currents. *Magnetic Resonance in Medicine, 14*(1), 26-30.

Koob, G. F. (2008). A role for brain stress systems in addiction. *Neuron, 59*(1), 11-34. doi:10.1016/j.neuron.2008.06.012

Koob, G. F. (2009). Dynamics of neuronal circuits in addiction: reward, antireward, and emotional memory. *Pharmacopsychiatry, 42 Suppl 1*, S32-41. doi:10.1055/s-0029-1216356

Koob, G. F. (2010). The role of CRF and CRF-related peptides in the dark side of addiction. *Brain Res, 1314*, 3-14. doi:10.1016/j.brainres.2009.11.008

Koob, G. F., & Le Moal, M. (1997). Drug abuse: hedonic homeostatic dysregulation. *Science, 278*(5335), 52-58.

Koob, G. F., & Moal, M. L. (1997). Drug Abuse: Hedonic Homeostatic Dysregulation. *Science, 278*(5335), 52-58. doi:10.1126/science.278.5335.52

Koob, G. F., & Volkow, N. D. (2010). Neurocircuitry of addiction. *Neuropsychopharmacology, 35*(1), 217-238. doi:10.1038/npp.2009.110

Koppelstaetter, F., Poeppel, T. D., Siedentopf, C. M., Ischebeck, A., Verius, M., Haala, I., . . . Gotwald, T. (2008). Does caffeine modulate verbal working memory processes? An fMRI study. *Neuroimage, 39*(1), 492-499.

Kotlyar, M., Brauer, L. H., al'Absi, M., Adson, D. E., Robiner, W., Thuras, P., . . . Candell, S. (2006). Effect of bupropion on physiological measures of stress in smokers during nicotine withdrawal. *Pharmacology Biochemistry and Behavior, 83*(3), 370-379.

Kreek, M. J., & Koob, G. F. (1998). Drug dependence: stress and dysregulation of brain reward pathways. *Drug Alcohol Depend, 51*(1), 23-47.

Krystal, J. H., Abi-Saab, W., Perry, E., D'Souza, D. C., Liu, N., Gueorguieva, R., . . . Levine, L. (2005). Preliminary evidence of attenuation of the disruptive effects of the NMDA glutamate receptor

antagonist, ketamine, on working memory by pretreatment with the group II metabotropic glutamate receptor agonist, LY354740, in healthy human subjects. *Psychopharmacology (Berl), 179*(1), 303-309.

Kühn, S., & Gallinat, J. (2011). Common biology of craving across legal and illegal drugs–a quantitative meta-analysis of cue-reactivity brain response. *European Journal of Neuroscience, 33*(7), 1318-1326.

Kumsta, R., Entringer, S., Hellhammer, D. H., & Wüst, S. (2007). Cortisol and ACTH responses to psychosocial stress are modulated by corticosteroid binding globulin levels. *Psychoneuroendocrinology, 32*(8), 1153-1157.

Lancaster, T., Stead, L., Silagy, C., & Sowden, A. (2000). Regular review: Effectiveness of interventions to help people stop smoking: findings from the Cochrane Library. *BMJ: British Medical Journal, 321*(7257), 355.

Le, A., Funk, D., Juzytsch, W., Coen, K., Navarre, B. M., Cifani, C., & Shaham, Y. (2011). Effect of prazosin and guanfacine on stress-induced reinstatement of alcohol and food seeking in rats. *Psychopharmacology (Berl), 218*(1), 89-99.

Le, A., Harding, S., Juzytsch, W., Funk, D., & Shaham, Y. (2005). Role of alpha-2 adrenoceptors in stress-induced reinstatement of alcohol seeking and alcohol self-administration in rats. *Psychopharmacology (Berl), 179*(2), 366-373.

Le, A. D., Funk, D., Juzytsch, W., Coen, K., Navarre, B. M., Cifani, C., & Shaham, Y. (2011). Effect of prazosin and guanfacine on stress-induced reinstatement of alcohol and food seeking in rats. *Psychopharmacology (Berl), 218*(1), 89-99. doi:10.1007/s00213-011-2178-7

Lebon, V., Petersen, K. F., Cline, G. W., Shen, J., Mason, G. F., Dufour, S., . . . Rothman, D. L. (2002). Astroglial contribution to brain energy metabolism in humans revealed by 13C nuclear magnetic resonance spectroscopy: elucidation of the dominant pathway for neurotransmitter glutamate

repletion and measurement of astrocytic oxidative metabolism. *The Journal of Neuroscience, 22*(5), 1523-1531.

Leo, R. J., & Latif, T. (2007). Repetitive transcranial magnetic stimulation (rTMS) in experimentally induced and chronic neuropathic pain: a review. *The Journal of Pain, 8*(6), 453-459.

Li, B.-M., Mao, Z.-M., Wang, M., & Mei, Z.-T. (1999). Alpha-2 adrenergic modulation of prefrontal cortical neuronal activity related to spatial working memory in monkeys. *Neuropsychopharmacology, 21*(5), 601-610.

Li, B.-M., & Mei, Z.-T. (1994). Delayed-response deficit induced by local injection of the α_2-adrenergic antagonist yohimbine into the dorsolateral prefrontal cortex in young adult monkeys. *Behavioral and neural biology, 62*(2), 134-139.

Lipp, I., Murphy, K., Caseras, X., & Wise, R. G. (2015). Agreement and repeatability of vascular reactivity estimates based on a breath-hold task and a resting state scan. *Neuroimage, 113*, 387-396.

Luijten, M., Littel, M., & Franken, I. H. (2011). Deficits in inhibitory control in smokers during a Go/NoGo task: an investigation using event-related brain potentials. *PLoS One, 6*(4), e18898.

Luo, S., Ainslie, G., Pollini, D., Giragosian, L., & Monterosso, J. R. (2012). Moderators of the association between brain activation and farsighted choice. *Neuroimage, 59*(2), 1469-1477.

Magon, S., Basso, G., Farace, P., Ricciardi, G. K., Beltramello, A., & Sbarbati, A. (2009). Reproducibility of BOLD signal change induced by breath holding. *Neuroimage, 45*(3), 702-712.

Mangia, S., Tkáč, I., Gruetter, R., Van de Moortele, P.-F., Maraviglia, B., & Uğurbil, K. (2006). Sustained neuronal activation raises oxidative metabolism to a new steady-state level: evidence from 1H NMR spectroscopy in the human visual cortex. *Journal of Cerebral Blood Flow & Metabolism, 27*(5), 1055-1063.

Mantsch, J. R., & Katz, E. S. (2007). Elevation of glucocorticoids is necessary but not sufficient for the escalation of cocaine self-administration by chronic electric footshock stress in rats. *Neuropsychopharmacology, 32*(2), 367-376. doi:10.1038/sj.npp.1301077

Mantsch, J. R., Vranjkovic, O., Twining, R. C., Gasser, P. J., McReynolds, J. R., & Blacktop, J. M. (2014). Neurobiological mechanisms that contribute to stress-related cocaine use. *Neuropharmacology, 76 Pt B*, 383-394. doi:10.1016/j.neuropharm.2013.07.021

Mantsch, J. R., Weyer, A., Vranjkovic, O., Beyer, C. E., Baker, D. A., & Caretta, H. (2010). Involvement of noradrenergic neurotransmission in the stress- but not cocaine-induced reinstatement of extinguished cocaine-induced conditioned place preference in mice: role for beta-2 adrenergic receptors. *Neuropsychopharmacology, 35*(11), 2165-2178. doi:10.1038/npp.2010.86

Mason, G. F., Petersen, K. F., De Graaf, R. A., Shulman, G. I., & Rothman, D. L. (2007). Measurements of the anaplerotic rate in the human cerebral cortex using 13C magnetic resonance spectroscopy and [1-13C] and [2-13C] glucose. *J Neurochem, 100*(1), 73-86.

Matheny, K. B., & Weatherman, K. E. (1998). Predictors of smoking cessation and maintenance. *J Clin Psychol, 54*(2), 223-235.

Mattila, M., Seppala, T., & Mattila, M. (1988). Anxiogenic effect of yohimbine in healthy subjects: comparison with caffeine and antagonism by clonidine and diazepam. *International clinical psychopharmacology, 3*(3), 215-229.

McClure, S. M., Ericson, K. M., Laibson, D. I., Loewenstein, G., & Cohen, J. D. (2007). Time discounting for primary rewards. *The Journal of Neuroscience, 27*(21), 5796-5804.

McClure, S. M., Laibson, D. I., Loewenstein, G., & Cohen, J. D. (2004). Separate neural systems value immediate and delayed monetary rewards. *Science, 306*(5695), 503-507.

Meikle, A. W., & Tyler, F. H. (1977). Potency and duration of action of glucocorticoids: effects of hydrocortisone, prednisone and dexamethasone on human pituitary-adrenal function. *The American journal of medicine, 63*(2), 200-207.

Mills, E. J., Wu, P., Lockhart, I., Thorlund, K., Puhan, M., & Ebbert, J. O. (2012). Comparisons of high-dose and combination nicotine replacement therapy, varenicline, and bupropion for smoking cessation: a systematic review and multiple treatment meta-analysis. *Ann Med, 44*(6), 588-597. doi:10.3109/07853890.2012.705016

Murburg, M. M., Villacres, E. C., Ko, G. N., & Veith, R. C. (1991). Effects of yohimbine on human sympathetic nervous system function. *The Journal of Clinical Endocrinology & Metabolism, 73*(4), 861-865.

Murphy, K., Harris, A. D., & Wise, R. G. (2011). Robustly measuring vascular reactivity differences with breath-hold: normalising stimulus-evoked and resting state BOLD fMRI data. *Neuroimage, 54*(1), 369-379.

Nater, U., & Rohleder, N. (2009). Salivary alpha-amylase as a non-invasive biomarker for the sympathetic nervous system: current state of research. *Psychoneuroendocrinology, 34*(4), 486-496.

Nestor, L., McCabe, E., Jones, J., Clancy, L., & Garavan, H. (2011). Differences in “bottom-up” and “top-down” neural activity in current and former cigarette smokers: evidence for neural substrates which may promote nicotine abstinence through increased cognitive control. *Neuroimage, 56*(4), 2258-2275.

Nides, M., Glover, E. D., Reus, V. I., Christen, A. G., Make, B. J., Billing, C. B., & Williams, K. E. (2008). Varenicline versus bupropion SR or placebo for smoking cessation: a pooled analysis. *American journal of health behavior, 32*(6), 664-675.

Ogawa, S., Tank, D. W., Menon, R., Ellermann, J. M., Kim, S. G., Merkle, H., & Ugurbil, K. (1992). Intrinsic signal changes accompanying sensory stimulation: functional brain mapping with magnetic resonance imaging. *Proceedings of the National Academy of Sciences, 89*(13), 5951-5955.

Owen, A. M., McMillan, K. M., Laird, A. R., & Bullmore, E. (2005). N-back working memory paradigm: A meta-analysis of normative functional neuroimaging studies. *Hum Brain Mapp, 25*(1), 46-59.

Patton, J. H., & Stanford, M. S. (1995). Factor structure of the Barratt impulsiveness scale. *J Clin Psychol, 51*(6), 768-774.

Pellow, S., Johnston, A. L., & File, S. E. (1987). Selective agonists and antagonists for 5-hydroxytryptamine receptor subtypes, and interactions with yohimbine and FG 7142 using the elevated plus-maze test in the rat. *Journal of pharmacy and pharmacology, 39*(11), 917-928.

Perkins, K. A., Epstein, L. H., Jennings, J. R., & Stiller, R. (1986). The cardiovascular effects of nicotine during stress. *Psychopharmacology (Berl), 90*(3), 373-378.

Picciotto, M. R., Brunzell, D. H., & Caldarone, B. J. (2002). Effect of nicotine and nicotinic receptors on anxiety and depression. *Neuroreport, 13*(9), 1097-1106.

Pocock, G., Richards, C. D., & Richards, D. (2013). *Human physiology*: Oxford university press.

Potenza, M. N., Hong, K. I., Lacadie, C. M., Fulbright, R. K., Tuit, K. L., & Sinha, R. (2012). Neural correlates of stress-induced and cue-induced drug craving: influences of sex and cocaine dependence. *Am J Psychiatry, 169*(4), 406-414. doi:10.1176/appi.ajp.2011.11020289

Pouwels, P. J., & Frahm, J. (1998). Regional metabolite concentrations in human brain as determined by quantitative localized proton MRS. *Magnetic resonance in medicine, 39*(1), 53-60.

Powell, J., Dawkins, L., & Davis, R. E. (2002). Smoking, reward responsiveness, and response inhibition: tests of an incentive motivational model. *Biol Psychiatry, 51*(2), 151-163.

Provencher, S. (2008). LCModel: Version.

Pruessner, J. C., Champagne, F., Meaney, M. J., & Dagher, A. (2004). Dopamine release in response to a psychological stress in humans and its relationship to early life maternal care: a positron emission tomography study using [11C] raclopride. *The Journal of Neuroscience, 24*(11), 2825-2831.

Qin, S., Hermans, E. J., van Marle, H. J., Luo, J., & Fernández, G. (2009). Acute psychological stress reduces working memory-related activity in the dorsolateral prefrontal cortex. *Biol Psychiatry, 66*(1), 25-32.

Ramos, B. P., Colgan, L., Nou, E., Ovadia, S., Wilson, S. R., & Arnsten, A. F. (2005). The beta-1 adrenergic antagonist, betaxolol, improves working memory performance in rats and monkeys. *Biol Psychiatry, 58*(11), 894-900.

Rangel, A., Camerer, C., & Montague, P. R. (2008). A framework for studying the neurobiology of value-based decision making. *Nature Reviews Neuroscience, 9*(7), 545-556.

Ray, L. A., Lunny, K., Bujarski, S., Moallem, N., Krull, J. L., & Miotto, K. (2013). The effects of varenicline on stress-induced and cue-induced craving for cigarettes. *Drug Alcohol Depend, 131*(1), 136-142.

Rohleder, N., & Kirschbaum, C. (2006). The hypothalamic–pituitary–adrenal (HPA) axis in habitual smokers. *International Journal of Psychophysiology, 59*(3), 236-243.

Rothman, D. L., De Feyter, H. M., Graaf, R. A., Mason, G. F., & Behar, K. L. (2011). 13C MRS studies of neuroenergetics and neurotransmitter cycling in humans. *NMR in Biomedicine, 24*(8), 943-957.

Rothman, D. L., De Feyter, H. M., Maciejewski, P. K., & Behar, K. L. (2012). Is there in vivo evidence for amino acid shuttles carrying ammonia from neurons to astrocytes? *Neurochem Res, 37*(11), 2597-2612. doi:10.1007/s11064-012-0898-7

Rougé-Pont, F., Piazza, P. V., Kharouby, M., Le Moal, M., & Simon, H. (1993). Higher and longer stress-induced increase in dopamine concentrations in the nucleus accumbens of animals predisposed to amphetamine self-administration. A microdialysis study. *Brain Res, 602*(1), 169-174.

SAMHSA. (2011). Results from the 2011 National Survey on Drug Use and Health Summary of National Findings. *NSDUH Series H-44*(HHS Publication No. (SMA) 12-4713), 1-174.

Schaller, B., Mekle, R., Xin, L., Kunz, N., & Gruetter, R. (2013). Net increase of lactate and glutamate concentration in activated human visual cortex detected with magnetic resonance spectroscopy at 7 tesla. *J Neurosci Res, 91*(8), 1076-1083.

Schaller, B., Xin, L., O'Brien, K., Magill, A. W., & Gruetter, R. (2014). Are glutamate and lactate increases ubiquitous to physiological activation? A ^{1}H functional MR spectroscopy study during motor activation in human brain at 7Tesla. *Neuroimage, 93*, 138-145.

Schousboe, A., Bak, L. K., Sickmann, H. M., Sonnewald, U., & Waagepetersen, H. S. (2007). Energy substrates to support glutamatergic and GABAergic synaptic function: role of glycogen, glucose and lactate. *Neurotoxicity research, 12*(4), 263-268.

Schwabe, L., Joels, M., Roozendaal, B., Wolf, O. T., & Oitzl, M. S. (2012). Stress effects on memory: an update and integration. *Neurosci Biobehav Rev, 36*(7), 1740-1749. doi:10.1016/j.neubiorev.2011.07.002

Schwabe, L., Tegenthoff, M., Hoffken, O., & Wolf, O. T. (2010). Concurrent glucocorticoid and noradrenergic activity shifts instrumental behavior from goal-directed to habitual control. *J Neurosci, 30*(24), 8190-8196. doi:10.1523/JNEUROSCI.0734-10.2010

Schwabe, L., Tegenthoff, M., Hoffken, O., & Wolf, O. T. (2012). Simultaneous glucocorticoid and noradrenergic activity disrupts the neural basis of goal-directed action in the human brain. *J Neurosci, 32*(30), 10146-10155. doi:10.1523/JNEUROSCI.1304-12.2012

Schwabe, L., & Wolf, O. T. (2011). Stress-induced modulation of instrumental behavior: from goal-directed to habitual control of action. *Behav Brain Res, 219*(2), 321-328. doi:10.1016/j.bbr.2010.12.038

Schwabe, L., & Wolf, O. T. (2013). Stress and multiple memory systems: from 'thinking'to 'doing'. *Trends in Cognitive Sciences, 17*(2), 60-68.

Selye, H. (1936). A syndrome produced by diverse nocuous agents. *Nature, 138*(3479), 32.

Selye, H. (1973). The Evolution of the Stress Concept: The originator of the concept traces its development from the discovery in 1936 of the alarm reaction to modern therapeutic applications of syntoxic and catatoxic hormones. *American scientist, 61*(6), 692-699.

U.S. Department of Health and Human Services (2014). The health consequences of smoking—50 years of progress: A report of the surgeon general. *Atlanta, GA: US Department of Health and Human Services, Centers for Disease Control and Prevention, National Center for Chronic Disease Prevention and Health Promotion, Office on Smoking and Health, 17*.

Shaham, Y., Erb, S., & Stewart, J. (2000). Stress-induced relapse to heroin and cocaine seeking in rats: a review. *Brain Research Reviews, 33*(1), 13-33.

Shaham, Y., Shalev, U., Lu, L., de Wit, H., & Stewart, J. (2003). The reinstatement model of drug relapse: history, methodology and major findings. *Psychopharmacology (Berl), 168*(1-2), 3-20.

Shaham, Y., & Stewart, J. (1995). Stress reinstates heroin-seeking in drug-free animals: an effect mimicking heroin, not withdrawal. *Psychopharmacology (Berl), 119*(3), 334-341.

Shepard, J. D., Bossert, J. M., Liu, S. Y., & Shaham, Y. (2004). The anxiogenic drug yohimbine reinstates methamphetamine seeking in a rat model of drug relapse. *Biol Psychiatry, 55*(11), 1082-1089.

Shiffman, S., West, R. J., & Gilbert, D. G. (2004). Recommendation for the assessment of tobacco craving and withdrawal in smoking cessation trials. *Nicotine & Tobacco Research, 6*(4), 599-614.

Sibson, N., Dhankhar, A., Mason, G., Behar, K., Rothman, D., & Shulman, R. (1997). In vivo 13C NMR measurements of cerebral glutamine synthesis as evidence for glutamate–glutamine cycling. *Proceedings of the National Academy of Sciences, 94*(6), 2699-2704.

Silagy, C., Lancaster, T., Stead, L., Mant, D., & Fowler, G. (2005). Nicotine replacement therapy for smoking cessation (Review).

Simons, J. S., & Gaher, R. M. (2005). The Distress Tolerance Scale: Development and validation of a self-report measure. *Motivation and Emotion, 29*(2), 83-102.

Sinha, R. (2001). How does stress increase risk of drug abuse and relapse? *Psychopharmacology (Berl), 158*(4), 343-359.

Sinha, R. (2009). Modeling stress and drug craving in the laboratory: implications for addiction treatment development. *Addict Biol, 14*(1), 84-98. doi:10.1111/j.1369-1600.2008.00134.x

Sinha, R., Garcia, M., Paliwal, P., Kreek, M. J., & Rounsaville, B. J. (2006). Stress-induced cocaine craving and hypothalamic-pituitary-adrenal responses are predictive of cocaine relapse outcomes. *Arch Gen Psychiatry, 63*(3), 324-331.

Sinha, R., Lacadie, C., Skudlarski, P., Fulbright, R. K., Rounsaville, B. J., Kosten, T. R., & Wexler, B. E. (2005). Neural activity associated with stress-induced cocaine craving: a functional magnetic resonance imaging study. *Psychopharmacology (Berl), 183*(2), 171-180.

Sinha, R., & Li, C. S. (2007). Imaging stress- and cue-induced drug and alcohol craving: association with relapse and clinical implications. *Drug Alcohol Rev, 26*(1), 25-31. doi:10.1080/09595230601036960

Smith, S., Jenkinson, M., Woolrich, M., Beckmann, C., Behrens, T., Johansen-Berg, H., . . . Matthews, P. (2004). Advances in functional and structural MR image analysis and implementation as FSL. *Neuroimage, 23 Suppl 1*, S208-219. doi:10.1016/j.neuroimage.2004.07.051

Sousa, I., Vilela, P., & Figueiredo, P. (2014). Reproducibility of hypocapnic cerebrovascular reactivity measurements using BOLD fMRI in combination with a paced deep breathing task. *Neuroimage, 98*, 31-41.

Spielberger, C. D. (1983). Manual for the State-Trait Anxiety Inventory STAI (form Y)(" self-evaluation questionnaire").

Spielberger, C. D. (2010). *State-Trait Anxiety Inventory*: Wiley Online Library.

Stanford, M. S., Mathias, C. W., Dougherty, D. M., Lake, S. L., Anderson, N. E., & Patton, J. H. (2009). Fifty years of the Barratt Impulsiveness Scale: An update and review. *Personality and Individual Differences, 47*(5), 385-395. doi:10.1016/j.paid.2009.04.008

Stanley, J. A., Burgess, A., Khatib, D., Ramaseshan, K., Arshad, M., Wu, H., & Diwadkar, V. A. (2017). Functional dynamics of hippocampal glutamate during associative learning assessed with in vivo ^{1}H functional magnetic resonance spectroscopy. *Neuroimage*.

Stanley, J. A., Drost, D. J., Williamson, P. C., & Thompson, R. T. (1995). The use of a priori knowledge to quantify short echo *in vivo* ^{1}H MR spectra. *Magnetic Resonance in Medicine, 34*(1), 17-24.

Stine, S. M., Southwick, S. M., Petrakis, I. L., Kosten, T. R., Charney, D. S., & Krystal, J. H. (2002). Yohimbine-induced withdrawal and anxiety symptoms in opioid-dependent patients. *Biol Psychiatry, 51*(8), 642-651.

Swan, G. E., Ward, M. M., & Jack, L. M. (1996). Abstinence effects as predictors of 28-day relapse in smokers. *Addict Behav, 21*(4), 481-490.

Tidey, J. W., Higgins, S. T., Bickel, W. K., & Steingard, S. (1999). Effects of response requirement and the availability of an alternative reinforcer on cigarette smoking by schizophrenics. *Psychopharmacology (Berl), 145*(1), 52-60.

Tricomi, E., Balleine, B. W., & O'Doherty, J. P. (2009). A specific role for posterior dorsolateral striatum in human habit learning. *European Journal of Neuroscience, 29*(11), 2225-2232.

Tsuda, A., Steptoe, A., West, R., Fieldman, G., & Kirschbaum, C. (1996). Cigarette smoking and psychophysiological stress responsiveness: effects of recent smoking and temporary abstinence. *Psychopharmacology (Berl), 126*(3), 226-233.

Ucar, E. Y., Araz, O., Yilmaz, N., Akgun, M., Meral, M., Kaynar, H., & Saglam, L. (2014). Effectiveness of pharmacologic therapies on smoking cessation success: three years results of a smoking cessation clinic. *interventions, 4*, 5.

Valentin, V. V., Dickinson, A., & O'Doherty, J. P. (2007). Determining the neural substrates of goal-directed learning in the human brain. *Journal of Neuroscience, 27*(15), 4019-4026.

van Stegeren, A. H., Roozendaal, B., Kindt, M., Wolf, O. T., & Joëls, M. (2010). Interacting noradrenergic and corticosteroid systems shift human brain activation patterns during encoding. *Neurobiol Learn Mem, 93*(1), 56-65.

Volkow, N., Fowler, J., Wang, G., Baler, R., & Telang, F. (2009). Imaging dopamine's role in drug abuse and addiction. *Neuropharmacology, 56*, 3-8.

Volkow, N. D., Wang, G.-J., Telang, F., Fowler, J. S., Logan, J., Childress, A.-R., . . . Wong, C. (2006). Cocaine cues and dopamine in dorsal striatum: mechanism of craving in cocaine addiction. *The Journal of Neuroscience, 26*(24), 6583-6588.

Volkow, N. D., Wang, G.-J., Telang, F., Fowler, J. S., Logan, J., Childress, A.-R., . . . Wong, C. (2008). Dopamine increases in striatum do not elicit craving in cocaine abusers unless they are coupled with cocaine cues. *Neuroimage, 39*(3), 1266-1273.

Wang, M., Ramos, B. P., Paspalas, C. D., Shu, Y., Simen, A., Duque, A., . . . Nou, E. (2007). α2A-adrenoceptors strengthen working memory networks by inhibiting cAMP-HCN channel signaling in prefrontal cortex. *Cell, 129*(2), 397-410.

Wang, M., Yang, Y., Wang, C.-J., Gamo, N. J., Jin, L. E., Mazer, J. A., . . . Arnsten, A. F. (2013). NMDA receptors subserve persistent neuronal firing during working memory in dorsolateral prefrontal cortex. *Neuron, 77*(4), 736-749.

Watson, D., Clark, L. A., & Tellegen, A. (1988). Development and validation of brief measures of positive and negative affect: the PANAS scales. *J Pers Soc Psychol, 54*(6), 1063.

West, S. G., Finch, J. F., & Curran, P. J. (1995). Structural equation models with nonnormal variables: Problems and remedies.

Wilkins, J., Carlson, H., Van Vunakis, H., Hill, M., Gritz, E., & Jarvik, M. (1982). Nicotine from cigarette smoking increases circulating levels of cortisol, growth hormone, and prolactin in male chronic smokers. *Psychopharmacology (Berl), 78*(4), 305-308.

Wilson, S. J., Sayette, M. A., Delgado, M. R., & Fiez, J. A. (2005). Instructed smoking expectancy modulates cue-elicited neural activity: a preliminary study. *Nicotine & Tobacco Research, 7*(4), 637-645.

Wilson, S. J., Sayette, M. A., & Fiez, J. A. (2004). Prefrontal responses to drug cues: a neurocognitive analysis. *Nat Neurosci, 7*(3), 211-214.

Woodcock, E. A., Arshad, M., Khatib, D., & Stanley, J. A. (2017). *Automated Voxel Placement: A Linux-based Suite of Tools for Accurate and Reliable Single Voxel Coregistration*. in preparation.

Yin, H. H., & Knowlton, B. J. (2006). The role of the basal ganglia in habit formation. *Nature Reviews Neuroscience, 7*(6), 464-476.

Yin, H. H., Knowlton, B. J., & Balleine, B. W. (2004). Lesions of dorsolateral striatum preserve outcome expectancy but disrupt habit formation in instrumental learning. *European Journal of Neuroscience, 19*(1), 181-189.

Yin, H. H., Ostlund, S. B., Knowlton, B. J., & Balleine, B. W. (2005). The role of the dorsomedial striatum in instrumental conditioning. *European Journal of Neuroscience, 22*(2), 513-523.

Zachary, R. A. (1991). *Shipley institute of living scale*: WPS, Western Psychological Services.

ABSTRACT

NEUROPHARMACOLOGICAL INVESTIGATION OF STRESS AND NICOTINE SELF-ADMINISTRATION AMONG CURRENT CIGARETTE SMOKERS

by

ERIC ANDREW WOODCOCK

August 2017

Advisor: Dr. Mark K. Greenwald

Major: Neuroscience (Translational)

Degree: Doctor of Philosophy

Nicotine use, especially cigarette smoking, is a significant public health problem. Existing pharmacotherapies attenuate nicotine craving and withdrawal symptoms. However, the majority of patients relapse within the first year of treatment. Treatment studies indicate a commonly cited precipitant to smoking relapse is stress. Pharmacotherapies do not attenuate, and may exacerbate, the effects of acute stress. Experimental studies (preclinical and clinical) indicate that acute stress potentiates drug-seeking behavior across drugs of abuse. Despite a robust literature linking acute stress and substance use, neurobiological mechanisms remain poorly understood. A more complete understanding of the neurobiological effects of acute stress on brain function may facilitate development of novel interventions. Adjunctive stress-blunting medications may improve the effectiveness of existing pharmacotherapies.

The present study investigated the effects of pharmacological stress-induction among cigarette smokers. Non-treatment-seeking cigarette smokers were recruited locally and screened for psychiatric, medical, and neuroimaging contraindications. Using a double-blind, placebo-controlled within-subject random cross-over design,

participants (N = 21) completed two oral-dosing experimental sessions: active (yohimbine [YOH] 54mg + hydrocortisone [HYD] 10mg) and placebo (YOH 0mg + HYD 0mg) stress. Prior research indicated that YOH+HYD is a robust pharmacological stress-induction technique that stimulates the Autonomic Nervous System (ANS) and Hypothalamic-Pituitary-Adrenal (HPA) axis systems, increases circulating levels of noradrenaline and cortisol (two primary stress hormones), and potentiates drug-seeking behavior. Throughout each experimental session, subjective and physiological effects were measured. In addition, participants completed a 60min magnetic resonance imaging (MRI) scan which consisted of three task paradigms: 1) letter 2-back, 2) smoking cued letter N-back, and 3) breath-hold challenge. Participants completed a working memory paradigm (letter 2-back) during proton functional magnetic resonance spectroscopy (^{1}H fMRS). Left dorsolateral prefrontal cortex (dlPFC) neurochemistry was evaluated during letter 2-back task performance. Next, participants completed a cued N-back paradigm that consisted of images (cigarette smoking or neutral) centered behind capitalized letters across three levels of N-back task difficulty: 0-, 1-, and 2-back. Finally, participants were instructed (visually) to control their breathing across three phases: 'normal' breathing, paced breathing (3s in/3s out), and breath-hold challenge (11s). After the MRI scan, participants completed a choice progressive ratio task. Across 11 independent choice trials, participants could earn one cigarette puff (preferred brand) or money ($0.25) via behavioral responding. Each successive unit earned (puffs or money, independently) was associated with a higher response requirement (progressive ratio schedule). At the end of the 30min task, participants smoked the exact number of cigarette puffs earned and/or were provided the amount of

money earned. Number of puffs earned and smoked was a direct measure of nicotine-seeking and self-administration behavior (nicotine motivation). Participants were compensated for their time.

Results indicated that oral pretreatment with YOH+HYD increased biomarkers of a physiological stress response: systolic and diastolic blood pressure, heart rate, saliva cortisol and α-amylase (indirect biomarker of noradrenaline levels), relative to placebo. YOH+HYD potentiated nicotine-seeking and self-administration behavior (controlling for nicotine dependence level), relative to placebo. Appetitive and relief-motivated cigarette craving, nicotine withdrawal symptoms, negative affect, and anxiety levels increased throughout each session, but did not differ by experimental session (active vs. placebo stress). Similarly, positive affect decreased throughout each session, but did not as a function of stress. ^{1}H fMRS indicated that letter 2-back performance increased left dlPFC glutamate (GLU) levels relative to interleaved fixation cross rest (indicative of task engagement) during the placebo, but not active stress, session. Further, YOH+HYD impaired letter 2-back response accuracy, relative to placebo. Across N-back levels (0-, 1-, and 2-back), fMRI indicated more robust neural activation across 'reward'-associated brain regions in response to smoking images (> neutral images) during placebo, relative to active stress.

Results demonstrated YOH+HYD induced a sustained physiological stress response (ANS and HPA axis) and potentiated nicotine-seeking and self-administration. YOH+HYD attenuated dlPFC task engagement and impaired response accuracy during a well-established working memory task. These findings provide experimental support for a plausible neurobiological mechanism through which acute stress may potentiate

nicotine self-administration. Acute stress-impaired dlPFC function may potentiate nicotine self-administration and, among abstinence-motivated individuals, precipitate smoking relapse. Prior research demonstrated dlPFC function is associated with a host of cognitive processes (e.g. delayed gratification, self-control, decision making, etc.) associated with prolonged smoking abstinence. Future studies are needed to confirm this hypothesis, investigate dose-response relationships, and evaluate the efficacy of stress-blunting medications in combination with existing pharmacotherapies for smoking cessation.

AUTOBIOGRAPHICAL STATEMENT

“If we knew what we were doing, it would not be called research, would it?”

-Albert Einstein